

ATOMIC ENERGY AUTHORITY  
CAIRO, EGYPT

INTERNATIONAL ATOMIC  
ENERGY AGENCY  
VIENNA, AUSTRIA

REGIONAL (AFRA IV - 11), (RAF/4/O12)  
TRAINING COURSE  
ON  
"RESEARCH REACTOR OPERATIONAL PERSONNEL"  
(15 -26) MARCH, 1997  
CAIRO, EGYPT  
ORGANIZED  
BY  
IAEA - EAEA

COURSE DIRECTOR  
PROF. M.K. SHAAT  
AFRA PROJECT CO-ORDINATOR

SUPERVISED  
BY  
PROF. H. F. ALY  
PRESIDENT OF EAEA  
AFRA NATIONAL CO-ORDINATOR

VOLUME (3)

## Contents

### Course objectives

#### A. Theoretical Part:

- 1- Basic Nuclear Physics
- 2- Reactor Physics
- 3- Reactor kinetics
- 4- Heat Transfer and Fluid Flow
- 5- Reactor Instrumentation
  - 5.1 Detectors
  - 5.2 ET-RR-1 Instrumentation
  - 5.3 Computers in Measurement and Data processing
- 6- Radiation Detection and Dosimetry
  - 6.1 R.D. Measurements
  - 6.2 Calibration of Radiation detectors
  - 6.3 Dosimetry
- 7- Radiation protection Biological Effects
  - 7.1 Biological Effects of Ionizing Radiation
  - 7.2 Safe Transport of Radioisotopes
- 8- Spent Fuel and Waste Management
- 9- Reactor operation Principles
- 10- Reactor Experiments
  - 10-1 Review of Experiments for Research Reactors
  - 10-2 Description of Experiments
    - 1) Silicon Doping
    - 2) Control Rod Calibration
    - 3) Temperature Coefficient of Reactivity
    - 4) Criticality Experiment
    - 5) Neutron and gamma Flux Mapping
- 11- Reactor Management
- 12- Reactor Safety
- 13- Emergency Plan
- 14- In-Core Fuel Management
- 15- Shielding Calculations
- 16- Water Chemistry
- 17- Safeguards Requirements
- 18- Re-furbishing and Upgrading of Research reactors (ET-RR-1)
- 19- Description of the ET-RR-1 Reactor

B. Practical Part:

- 1- Visit to the ET-RR-1 Reactor systems and Experimental Facilities.
- 2- Operation Procedure of ET-RR-1
- 3- Carrying out Experiments:
  - Criticality at different power Levels
  - Power Calibration
  - Control Rod Calibration
  - Temperature Coefficient of Reactivity
  - Neutron and gamma flux Mapping
  - Scram due to loss of Flow
  - Decay Heat Measurement by Data Acquisition System

REGIONAL ARIKA TRAINING COURSE FOR REACTOR OPERATIONAL PERSONNEL  
CAIRO - EGYPT

(15 - 26) MARCH 1997

Week 1

TIME	SATURDAY 15 MARCH 97	SUNDAY 16 MARCH 97	MONDAY 17 MARCH 97	TUESDAY 18 MARCH 97	WEDNESDAY 19 MARCH 97
9:30 - 10:20	Course Opening	Basic Nuclear Physics	Heat Transfer and fluid flow	Radiation detection measurements (GM count. Sci.) w/ A.Z.2	Spent Fuel and Waste Management
		<i>M. Mekhael</i>	<i>M. Khattab</i>		<i>R. El-Serogy</i>
10:30 - 11:20	Course objectives, review of the course programme	Reactor Physics	Heat transfer and fluid flow	Dosimetry (TLD, materials, read not systems)	Handling of Radioisotopes
	<i>IAEA, DIMIC</i>	<i>M. Mekhael</i>	<i>A. Abdalla</i>	<i>S. Youssef</i>	<i>R. El-Shenawi</i>
11:20 - 11:40	COFFEE BREAK				
11:40 - 12:30	Reports of participants	Reactor physics	Reactor Instrumentation (detectors)	Radiation Protection at R.R.	Review of Experiments for Research Reactor
		<i>M. Mekhael</i>	<i>M. Shaat</i>	<i>M. Gomaa</i>	<i>A. Hassan</i>
12:40 - 13:30	Reports of participants	Reactor Kinetics	ET-RR-1 Instrumentation	Biological Effects of Ionizing Radiation	Silicon Doping
		<i>M. Shaat</i>	<i>M. Shaat</i>	<i>A. El-Maghrabi</i>	<i>M. Sultan</i>
13:40 - 14:30	Reports of participants	Reactor Kinetics	ET-RR-1 Instrumentation	Reactor operation principles	Emergency plan
		<i>M. Shaat</i>	<i>M. Shaat</i>	<i>M. Shaat</i>	<i>M. Gomaa</i>
14:30	LUNCH				



Week 2

TIME	SATURDAY 22 MARCH 97	SUNDAY 23 MARCH 97	MONDAY 24 MARCH 97	TUESDAY 25 MARCH 97	WEDNESDAY 26 MARCH 97
9:30 - 10:20	Reactor Safety	Incove Fuel Management	Re furnishing and upgrading of Research reactors	Calibration of radiation detectors	Shielding Calculations
	H. Bock, IAEA	M. Melkhael	M. Khattab	W. Aziz	M. Nagy
10:30 - 11:20	Reactor Management	Description of the ET-RR-1 reactor	Operation of ET-RR-1 (practical)	Water Chemistry	Safe guards requirements
	H. Bock, IAEA	M. Khattab		M. Marawan	M. Sultan
11:20 - 11:40	COFFEE BREAK				
11:40 - 12:30	Computers in measurement and data processing	Visit to the ET-RR-1 reactor.	Criticality, Power Calibration (practical)	Temp. Coefficient measurement (practical)	
	M. Shaat	A. El-kafas	S. Sheibl	A. El-Kafas	
12:40 - 13:30	Description of experiments	Visit to the ET-RR-1 Experimental Facilities	Control rod Calibration (practical)	Decay heat After ET-RR-1 shut down (practical)	Course Evaluation
	E. Saad	A. El-kafas	S. Sheibl	A. El-Kafas	H. Bock, M. Sultan M. Shaat
13:40 - 14:30	Description of experiments	Neutron and gamma flux mapping	Control rod Calibration (practical)	Decay heat measurement (practical)	-----
	W. Aziz	H. Bock, IAEA	S. Sheibl	A. El-Kafas	
14:30	LUNCH				

A Lecture Submitted to:

Regional (AFRA) Training Course for Reactor Operational Personnel, Cairo - Egypt (15 - 20 March 1997).

**A REVIEW ON THE EXPERIMENTAL RESEARCH  
ACTIVITIES IN PHYSICS  
USING THE FIRST EGYPTIAN RESEARCH REACTOR**

**A. M. HASSAN**

*Reactor and Neutron physics Departement, Nuclear research centre  
Atomic Energy Authority, Cairo, Egypt.*

**ABSTRACT**

This lecture is devoted to review the most important experimental research activities in reactor and neutron physics using the facilities of the first Egyptian Research Reactor (ET-RR-1). A short report on the experiments including some measurements are given. Neutron cross-sections, neutron flux, neutron capture  $\gamma$ -rays and neutron activation analysis, neutron diffraction and radiation shielding experiments are presented. Special attention has been paid on the description of the Reverse Time of Flight (RTOF) multipurpose diffractometer and the computerized tomography by neutron and  $\gamma$ -ray systems, which are recently installed at horizontal neutron beams of the (ET-RR-1).

**INTRODUCTION**

In general, the nuclear research reactor is considered as an intense source of neutrons. It is prepared for research in the fields of reactor and neutron physics, in addition to its uses for isotopes production. The beams of neutrons at the reactor sites and reactor core are used for such purposes. Nowadays, there are several hundreds of nuclear research reactors of different types in operation all over the world. In the mean time, a huge number of publications are appeared every year dealing with the problems of reactor and neutron physics and their related topics. This was performed by means of the neutron beam facilities. Also, it could be noticed that the majority of the experiments apply the most advanced and highly developed techniques in the last few decades.

The ET-RR-1 which made critical in (1961), has a maximum neutron flux of  $(2 \times 10^{13} \text{ n / cm}^2 \cdot \text{s})$  and an average thermal neutron flux of  $(10^{13} \text{ n / cm}^2 \cdot \text{s})$  at the maximum power of (2MW). This reactor is provided with 9 horizontal channels, 9 vertical channels, sliding graphite thermal column and 3 special channels for biological research. The maximum intensity of the neutron flux at the outer end of each radial channel was about  $(10^8 \text{ n/cm}^2 \cdot \text{s})$ . The equipment used for the outer end physics experiments were arranged around the horizontal channels as shown in fig. (1).

In this lecture a review on some research work carried out on the (ET-RR-1), in the fields of reactor and neutron physics, is given.

## RESEARCH ACTIVITIES OF RESEARCH REACTORS

Research reactors are designed and operated to carry out some basic and applied research works in the fields of reactor and neutron physics as mentioned above. This will be carried out in addition to, production of isotopes, industrial applications, education and training. The most important topics of these activities could be summarised as follows:-

- \* Neutron flux mapping.
- \* Burn - up data.
- \* Neutron and  $\gamma$  - dosimetry.
- \* Neutron optics including reflection and diffraction.
- \* Neutron cross - section measurements.
- \* Neutron capture gamma - ray spectroscopy.
- \* Neutron activation analysis (development and applications).
- \* Neutron scattering and neutron crystallography.
- \* Material testing (high flux is needed-over  $1 \times 10^{14} \text{ n / cm}^2 \cdot \text{s})$ .
- \* Radiation shielding experiments.
- \* Radio - isotopes production.
- \* Education and training.

## EXPERIMENTAL RESEARCH ACTIVITIES OF THE ET-RR-1

The experimental arrangements installed at the outer ends of the horizontal channels of the (ET-RR-1) as well as the thermal column and the Rabbit pneumatic Transfer System (RPTS) installed at the gamma - ray spectroscopy laboratories, could be described as follows:-

1- For radiation shielding materials testing, the first, second and third channels were prepared using different techniques. A computerized tomography system is recently used for neutrons and gamma - rays in this field. The determination of the change in material structure, elemental compositions, creation of gas bubbles and cavities, is considered as the main purpose of this system<sup>(1)</sup>.

The experimental and theoretical studies are carried out in the experimental physics division<sup>(2)</sup> to examine and evaluate the physical, mechanical and nuclear parameters of materials of prime importance in nuclear technology and general industries. These will be achieved through the following two main projects:

a- Non - destructive testing of materials by Computerized Tomography (CT) by fast neutrons, thermal neutrons and gamma-rays are applied for inspecting and testing the physical and mechanical properties. This will be performed by the methods of transmission and emission for non - radioactive and radioactive materials respectively.

b- Material testing by fast neutrons and gamma-ray spectra measurements.

The nuclear parameters and metal inclusions are studied by measuring the spectra of fast neutrons and gamma-rays transmitted through the materials under investigation. Measurements are performed by a neutron - gamma spectrometer with organic scintillator detector. Separation between neutron and gamma - events is achieved by a pulse shape discrimination technique based on the zero crossing method.

A block diagram of the electronic equipments of the neutron - gamma spectrometer with a dynode chain of the photomultiplier tube is shown in fig. (2).

In their paper, Pfister et al.<sup>(3)</sup> review a CT - measurements with fast, thermal and gamma-rays, just to demonstrate the capability of this nondestructive method in problems of research and technical applications. The following images figs. (3,4,5,6 and 7) for different samples have been selected from this work<sup>(3)</sup>, with some comments on each one.

Aluminum is nearly transparent for thermal neutrons, therefore other materials located inside an aluminum sample can be displayed with high contrast in a neutron-CT-image. Especially corrosion products, containing hydrogen can be detected very good. A fiber reinforced (AlSi) compound test sample was examined with thermal neutrons - CT. This test sample was prepared with defects (bore - holes filled with pure aluminum). The CT-image shows clearly a radial boring (1.6 mm diameter). Only the two largest of the 4 axial boreholes (0.35, 0.5 0.8 and 1.6 mm diameters) could

be localized inside this sample. A pure aluminum ring at the surface of the compound material and the notch (upper part) are seen in this image, Fig.(3).

Fig.(4) shows a cross section through a heat pipe (14 mm diameter) reconstructed from a thermal neutron-CT-measurement. This image clearly shows the steel tube (0.925 mm thick) and the capillary structure inside the heat pipe (4 layers of a net with total thickness of 0.9 mm). The 8 arteries inside the vapour zone have a net thickness of 0.14 mm and deformations can be seen. CT-measurements with heat pipes can be used to examine the geometry of the inner structures as well as the distribution of the heat carrier; especially if this medium contains hydrogen, thermal neutron-CT will be predestinated to show this. The heat pipe used in this tomography measurement was not in operation, therefore no heat carrier can be seen.

The high penetration capability of fast neutrons is especially useful in testing large metallic objects. Many of these objects in technical applications are made from austenitic steel or cast iron which, due to its granular structure, is less suited to ultrasonic test methods. A cast iron part of the hydraulics of a truck brake was examined with fast neutron CT. The aim was to show if there are porous parts inside the object. The reconstructed neutron CT image in Fig.(5) shows a porous part in the right lower region of the circular hole in the middle of the object. An aluminum screw with plastic screw inside can be seen in the upper part of the image. It can be clearly distinguished between the three different materials (iron, aluminum, plastics). The ring structure in the center of the object is a step in the hole which was exactly in the middle of the examined slice height.

Neutron- and gamma-CT-images were reconstructed from the transmission measurements in the fast neutron field. The detected beam had the dimensions of 1 mm in width and 5 mm in height. The neutrons and gamma-rays - both present in this radiation field - were discriminated and detected simultaneously. Fig.(6) shows the neutron-CT-image and Fig.(7) the  $\gamma$ -CT-image of a reflex camera. Both images show fine structures (rolls, levers, hinges etc.). It can be seen that two of the four achromatic lenses are manufactured out of two parts with different densities (refraction index). The neutron-CT-image shows all parts manufactured out of plastics (cover of the lenses, film, etc.) with higher contrast compared to the  $\gamma$ -CT-image. Even the film with a thickness of 0.15 mm can be seen in the neutron image.

In addition four CT-images have been taken for the ordinary concrete samples at 200 °C using the low and high threshold neutrons as well as the low and high threshold gamma-rays at the ET-RR-1 as shown in figs. (8,9,10 and 11) respectively.

2- The double crystal diffractometer placed at the hole number 5 of the ET-RR-1 running at a power of 2MW was used for neutron powder diffraction measurements. Fig. (12) shows a schematic diagram of the experimental arrangement of the neutron crystal spectrometer. An effective system of shielding is important to reduce the back ground of the scattered neutrons which would be picked up by the counter. Also, to insure that the general level of radiation in the neighborhood is sufficiently low from health and safety points of view.

The fast neutrons are slowed down by collision of hydrogen atoms in the borated paraffin shield and they are then subsequently absorbed by the boron which has a high absorption coefficient for slow neutrons. The  $\gamma$ -rays are absorbed by a lead screen<sup>(4)</sup>.

The powder sample  $\text{Co}_{0.6} \text{Fe}_{1.4} \text{O}_4$  contained in thin walled cylindrical (vanadium sample holder 16 mm in diameter) was used for obtaining neutron diffraction patterns.

Measurements were repeated twice<sup>(4)</sup> using  $1.08 \text{ \AA}$  neutrons reflected from a (zinc) monochromator cut along (002) plane. Measurements were made up to  $2\theta = 52^\circ$ , since only in this region well-resolved peaks were present. A collimator with angular resolution of  $20'$  was placed in the reactor hole and a second with the same resolution between the sample and the counter. Counts were taken for 7 minutes at  $10'$  intervals of the scattering angle. Neutron diffraction patterns at room temperature and at  $650^\circ\text{K}$  are shown in fig. (13). High temperature measurements were taken with the sample inserted in a special furnace. From this neutron diffraction pattern, the crystallographic parameters could be determined.

3- A simple slow neutron mechanical chopper is aligned at channel 6 of the ET-RR-1. A layout of the spectrometer<sup>(5)</sup> is shown in fig.(14).

The shielding materials used in building this spectrometer had provided a safe one. The spectrometer is well protected against the reactor hall radiation background and there is no significant radiation hazards comes out of it.  $^3\text{He}$  detector is used for measuring the slow neutron spectrum TOF american type detector used for Time of Flight experiments]. The spectrometer can be used for the neutron wavelength range (from  $0.5 \text{ \AA}$  up to  $6 \text{ \AA}$ ) [extended to  $10 \text{ \AA}$ ], by increasing the power of the reactor and using a higher vacuum flight path tube<sup>(5)</sup>. The

measured spectrum represents the thermal and cold neutron regions only as shown in fig. (15). The spectrometer was calibrated by using the accurate value of Be cut-off,  $[\lambda = 3.952 \text{ \AA}]$  which corresponds to time of flight value = 3744 s. (ref. 5)

4- Small angle neutron scattering (SANS) has now become an important technique in the study of metallurgical, polymeric, biological and nanocrystalline materials. The experimental aspects of neutron SANS has been given in details by several authors<sup>(6)</sup>. These instruments operated at high flux reactors equipped with cold neutron sources and use long neutron guide tubes.

However, under some conditions the measurements of the broadening of the incident narrow neutron beam after traversing the sample, due to SANS effect, can provide valuable information about its structural inhomogeneties of sizes up to several hundred times the size of individual atoms. The advantage of such measurements is that they can be carried out at low flux reactor which is equipped with neither cold neutron source nor guide tube.

A horizontal view of the general arrangement of SANS spectrometer<sup>(6)</sup> which was previously installed at channel no. 9 and it will be shifted to channel no. 7 is shown in fig.(16). Neutrons are emitted from the ET-RR-1 reactor channel (100 mm in diameter) passing through an in-pile collimator 60 cm long and a beam hole of 1 cm<sup>2</sup> (rectangular area) made from Lead, Paraffin and Boric acid.

The double-rotor consists of a rotating collimator (rotor 1) and curved slot rotor (rotor 2), each of them is mounted on its mobile platform inside an evacuated chamber. The rotors are suspended in magnetic fields and spinning synchronously up to a maximum speed of 16,000 rpm, producing bursts of polyenergetic neutrons. The curved slot rotor, 32 cm in diameter has two slots of 1 cm height and 0.7 cm width. The slot has a radius of curvature of 65.65 cm. The main parameters of the rotating collimator (diameter, slot shape, material) were selected to match the curved slot rotor.

The optimum operating condition of the double rotor facility was deduced using the computer program RCOL<sup>(6)</sup> for the case when the distance between the centers of the rotors was 66 cm.

A He-3 gas filled neutron detector was fixed inside a shield with a variable hole window, facing the neutron beam. The window was selected to be equal to the area of the of the neutron beam at the detector position. The neutron beam divergence was  $17.0' \pm 1.5'$ . As an application, the

neutron cross-sections in the wavelength range from 3.5 to 5.2 Å were measured for iron in both bulk and powder form. Fig. (17) displays the measured dependence of Fe metal total cross-section on neutron wavelength. Some values of  $\sigma_t$  for iron, reported in BNL-325 are also presented (open circles). One can notice the agreement of the measured values of  $\sigma_t$  and reported ones. Such agreement confirms that the SANS cross-section  $\sigma_{\text{SANS}}$  from metallic samples within the experimental accuracy is vanished.

5- Channel no. 8 was previously well prepared for external target measurements of the prompt gamma-rays emitted due to thermal neutron capture for many of samples. A single Bi plug was placed inside the hole of the channel, just to reduce the fission gamma - radiation, epithermal and fast neutrons to an acceptable level while thermal neutrons pass without any losses. In order to obtain an intense and narrow collimated neutron beam at the target position outside of the reactor, internal and external neutron collimators were placed inside and outside the reactor respectively. Lead and graphite materials were used as shown in fig (18). The thermal neutron flux was found to be in the order of  $10^6 \text{ n / cm}^2 \cdot \text{s}$ . at the target position, which was good enough to do the prompt gamma - ray experiment<sup>(7,8)</sup>. Blocks of lead and paraffin mixed with Boric acid were used to make a castle around the house of the gamma-ray detection system. Single, Pair and Anticompton gamma-ray spectrometers were used with success for investigation of different elements. The electronic block diagram for the Ge (Li) - Na (Tl) pair spectrometer as shown in fig. (19) was used<sup>(7,8)</sup>. Some rearrangements will be introduced for this experiments using more advanced computerized detection system. A portion of the neutron capture gamma-ray spectrum from  $^{39}\text{K} (n, \gamma) ^{40}\text{K}$  is shown in fig. (20), which was used for the level scheme investigation of  $^{40}\text{K}$ . [taken from ref. (7)]. A portion of the high energy part of the single and pair gamma-ray spectra of  $^{35}\text{Cl} (n, \gamma) ^{36}\text{Cl}$  taken by the Anticompton spectrometer is shown in fig. (21). The gamma-ray spectra emitted promptly due to neutron capture were very useful for nuclear structure studies and the applied nuclear science such as the elemental constituents investigations of different materials.

6- As mentioned above the neutron time of flight (TOF) method has proved to be one of the efficient tools for neutron diffraction studies. The TOF method is based on measuring the neutron time of flight through a



definite distance; using a neutron chopper which transmits short bursts of neutrons. Accordingly, neutrons of different energies, primarily present in the beam, will be sorted out; the fast neutrons will arrive at the end of the flight distance earlier than the slower ones. Most of the conventional TOF spectrometers apply the Fermi type disk chopper which makes use only of (0.1-0.5)% out of the available neutrons.

The Fourier TOF method has been of considerable interest prior to 1980 as a highly efficient alternative, of a Fermi chopper system, since it offers, regardless of resolution requirements, a high duty cycle combined with the possibility of exploiting a large beam area. The Fourier method has been improved by the reverse time of flight (RTOF) concept which is based on the triggering of the TOF analyzer by the detected neutrons instead of by the rotor's position. The use of the RTOF diffractometry at the ET-RR-1 reactor (2MW), was assessed in refs (9,10). Further developments of the suggested arrangement were represented in refs. (11-16); along with the main components required for the data acquisition. Moreover an RTOF diffractometer was recently installed at one of the ET-RR-1 reactor horizontal channels<sup>(9)</sup>, the Cairo Fourier Diffractometer Facility (CFDF). Such facility consists of a curved neutron guide tube (NGT) designed to deliver thermal neutrons; free from  $\gamma$ -ray and fast neutrons background, to a Fourier chopper which is followed by another straight NGT for collimation of the neutron beam before incidence on the sample. The optimized curved NGT has a radius of curvature  $\rho = 3388.5\text{m}$ , length  $L = 22\text{m}$ . and a rectangular cross sectional area  $S = 13.5 \times 90 \text{ mm}^2$  to give a characteristic wavelength of  $\lambda^* = 1.377 \text{ \AA}$ . The straight NGT is 3m long and with the same cross-sectional area of the curved one.  $^{58}\text{Ni}$  isotope is used as a coating layer for the mirror channel walls in both NGT. A schematic diagram for the NGT and the shielding around it is shown in fig. (22). (taken from references 9 and 10).

The neutron spectrum was measured after transmission through a Fermi disk type chopper. The chopper has been made of two aluminium disks attached to each other; with 0.5mm thick Cd foil pressed between them. The disk rotor has two radial slits,  $2.9 \times 80 \text{ mm}^2$  at the main radius of 200mm. The chopper was rotating at a constant speed 2840 rpm. At this speed the chopper produces approximately triangular pulses with the FWHM equals to  $48.8 \mu\text{s}$ . The pick up pulse is taken optically through two holes at the periphery. The width and timing of the pickup pulse with respect to the neutron pulse can be adjusted so that the logical "chopper open" pulse can be fully synchronized to the neutron pulse. Thus the neutron spectrum was measured with a  $^6\text{Li}$ -glass scintillator detector which

was set at a distance 3.45m from the Fermi chopper, being at the sample position, according to the arrangement schematically given in Fig. (23).

The neutron spectrum transmitted through 12cm thick beryllium filter was also measured for calibration of time of flight scale. The measured Be filtered spectrum is displayed in Fig. (24) where one can notice the well known Be cut-off at 3.952Å.

For the determination of the maximum resolution of the diffractometer, measurements of diffraction spectra in the RTOF-mode were performed. The samples of polycrystalline iron and diamond powder were used. The sample diameter and height were 5mm and 85mm, respectively. The measured diffraction patterns<sup>(9,10)</sup> are shown in figs. (25, 26 & 27). The width and position of the peaks for these spectra were defined with the help of the corresponding fit-software. The relative width of the peaks is shown in fig. (28). The minimum of the resolution curve determines the best experimental resolution of the diffractometer. This resolution is 0.55%. The true maximum resolution of a device is a little higher since the experiments measure the convolution of the instrumental resolution with the natural width of the sample diffraction line.

The iron sample was chosen from reasons of the possible scientific program of research of stress in materials with the composition close to various constructional steels. The difference between the diamond and iron data might be explained by the effects of strain in the iron sample. It shows that the iron sample should not be used for correct evaluation of the resolution<sup>(9,10)</sup>.

The iron diffraction pattern measured by the facility (see the layout at fig.(29) and treated with the proper software is displayed in fig. (30), along with that one which was measured for 120 minutes with the Fourier Stress Spectrometer (FSS) diffractometer installed at the FRG1 (5MW) Reactor (GKSS-Germany). The FSS facility is also a Fourier RTOF one, with a different arrangement and is also optimized for  $2\theta = 90^\circ$ . Despite the fact that the present iron diffraction pattern was obtained, with the CFDF, within 15 minutes measuring time, it is superior (concerning statistics) to that one measured by the FSS facility. This offers a chance for more accurate diffraction measurements with the CFDF and within less measuring time. It is concluded that the CFDF could be used efficiently for neutron diffraction measurements at D values between 0.7 Å - 2.9 Å.

7- In addition to the above experiments, the Rabbit Pneumatic Transfer System (RPTS) installed at the gamma-ray spectroscopy laboratories [of Inchass] was used for a series of irradiations of different

samples in a thermal neutron flux position of ( $\approx 2 \times 10^{11} \text{ n/cm}^2 \text{ .s.}$ ). Investigations of many important geological and biological samples using the (RPTS) facility as well as the core of the reactor are achieved on the basis of the non-destructive activation analysis project. Fig. (31) shows a sketch of the (RPTS) of ET-RR-1 and Fig. (32) shows - partial gamma-ray spectra of silver brazing alloy (CP2)\*. The gamma-ray spectra were collected by a HPGe detection system after irradiation time of 48h. at the core of the reactor and 30 s. irradiation time using the (RPTS)<sup>(7,8)</sup>.

8- Also, The thermal column of the ET-RR-1 is under preparation for neutron radiography measurements using thermal neutrons, through an IAEA technical project.

## REFERENCES

- 1- T.S. AKKi and R.M. Meghahid "Appl. of computer tomography for testing the Internal structure of concrete shield" Annual meeting of canadian radiation protection (1990).
- 2- R.M. Megahid, Reactor and Neutron physics Dept., AEA. (Private communication). (March 1997).
- 3- G. Pfister, A.K. Schatz, J. Gobel R. Kofler, "Computer ized Tomography with Fast and Thermal Neutrons, State of the Art and Future Prospectives. Int. Sym. on Computer ized Tomograhpy for industrial applications, Berlin (Germany) 8-11 June (1994).
- 4- S. Soliman, "study of the physical properties of some mixed cubic ferrites". M.Sc. Thesis, Facutly of science Cairo Univ. (1991).
- 5- M.A.Abu El-Ela, An Imporved Slow Neutron Spectrometer at the Research Reactor -. Proc. of 6<sup>th</sup> conf. of Nucl. Sci. and Applications (Cairo 15 - 20 March 1996) Vol. II PP (124 - 139).
- 6- M. Adib, A. Abdel-Kawy, K. Naguib, N. Habib, M. Kilany, M. Wahba and A. Ashry., "Small Angle Neutron Scattering From Iron" Proc. of 6<sup>th</sup> conf. of Nucl. Sci. and Appl. (Cairo-15-20 March 1996) Vol II PP. (88-101) and (M. Adib) (Priv. communications) (March 1997).
- 7- A.M. Hassan, "Neutrons as Research Tools and Elemental Analysis of Materials By Neutron Activation " Proc. of the symp on The Physics and Technology of Reactors Cairo 11-16/9/1993, Arab Atomic Energy Agency - Tunis - Nov. (1993).

- 8- E.A. Eissa, N.B. Rofail, A. El-Shershaky, N. Walley El-Dine, and A.M. Hassan "Elemental Analysis of Brazing Alloy Samples By Neutron Activation Technique", Third Radiation Physics Conf., Al-Minia, 13-17 Nov. (1996).
- 9- V.A. Trounov, A.P. Bulkin, D.Y. Cherenyshov, V.N.K. onechny, V.A. Kudryashev, V.G. Muratov, A.M. Pirogov, A.T. Titta and V.V. Chernyshov., "Report on the Test Experiments of the Multipurpose Diffractometer" Proj. EGY/1/022, IAEA, 1-April (1996).
- 10- R.M. Maayouf, L.A. Abdel-Latif and A.S. El-Kady, "Neutron Spectrum Measurements from a Neutron Guide Tube Facility at (ET-RR-1), Priv. Communications with R.M. Maayouf and L.A. Abdel-Latif., Reactor and Neutron physic Dept., AEA. (Cairo - Egypt) (March 1997).
- 11- R.M.A. Maayouf, et al., Report GKSS 91/E/65, Geesthacht, Germany, (1991).
- 12 - V.A. Kudruashev, V.A. Trounov, R.M.A, Maayouf, et al., Report LNPI 1732, Leningrad, (1991).
- 13 - R.M.A. Maayouf, A. Titta, P. Hiismaki, The RTOF Neutron Diffraction Facility at the ET-RR-1 Reactor, VTT Reactor Laboratory, Espoo, June (1991).
- 14 - R.M.A. Maayouf, et al., VTT Research Notes-1425, Espoo, (1992).
- 15 - R.M.A. Maayouf, A.T. Titta, VTT Research Notes-1502, Espoo (1993).
- 16- R.M.A. Maayoyf, P.E. Hiismaki, A.T. Titta. The Multipurpose TOF Fourier Diffractometer at the ET-RR-1 Reactor, VTT Reactor Laboratory, Espoo, Nov , (1993).

## ACKNOWLEDGEMENT

The great help given by the research Staff members of the RNPd , of the AEA, will not be forgotten.

## List of Figures

- Fig. (1) Experiments on the horizontal channels of (ET-RR-1).
- Fig. (2) A block diagram of the Electronic equipments of the neutron - gamma - spectrometer with a dynode chain at the photo-multiplier tubes [channels 1, 2 and 3].
- Fig. (3-11) Images using the computerized Tomography System for Neutrons and Gamma-Rays.
- Fig. (12) Schematic Diagram of the experimental arrangement of neutron crystal spectrometer [Chs. 4 and 5] (Double crystal Diffractometer).
- Fig. (13) Neutron Diffraction Pattern for the sample ( $\text{Co Mn}_{0.6}\text{Fe}_{1.4}\text{O}_4$ ) at Room Temperature and 650 °K.
- Fig. (14) Slow Neutron Mechanical Chopper Layout. Channel (6).
- Fig. (15) Reactor slow neutron spectrum, Angular velocity 1562 r.p.m.
- Fig. (16) The general arrangement of the (TOF) - (SANS) spectrometer (Channel. 7).
- Fig. (17) Total Neutron Cross-Section of Fe-Metal.
- Fig. (18) Neutron Capture Gamma-Ray Arrangements, (Channel 8).
- Fig. (19) Electronic Block Diagram for the Ge (Li) NaI (Tl) pair spectrometer.
- Fig. (20) A portion of the neutron capture Gamma-Ray spectrum of  $^{39}\text{K} (n, \gamma) ^{40}\text{K}$ .
- Fig. (21) A portion of the high energy part of the single and pair gamma-ray spectra of  $^{35}\text{Cl} (n, \gamma) ^{36}\text{Cl}$ .
- Fig. (22) A schematic Diagram of the NGT and shielding around it (Channel 9).
- Fig. (23) A schematic of the arrangement used for neutron spectrum measurements.
- Fig. (24) Neutron spectrum transmitted through the Be Filter.
- Fig. (25) Fe Sample Diffraction pattern - 1.
- Fig. (26) Fe Sample Diffraction pattern - 2.
- Fig. (27) Diamond sample Diffraction pattern .
- Fig. (28) Resolution of Diffractometer EGY1.
- Fig. (29) Layout of RTOF (CFDF) Spectrometer.
- Fig. (30) Iron Diffraction Patterns Measured by CFDF & FSS.
- Fig. (31) A Sketch of (RPTS of ET-RR-1).
- Fig. (32) Partial  $\gamma$ -ray spectra of Brazing alloy (CP2) using 48 hours and 30s. irradiation times.

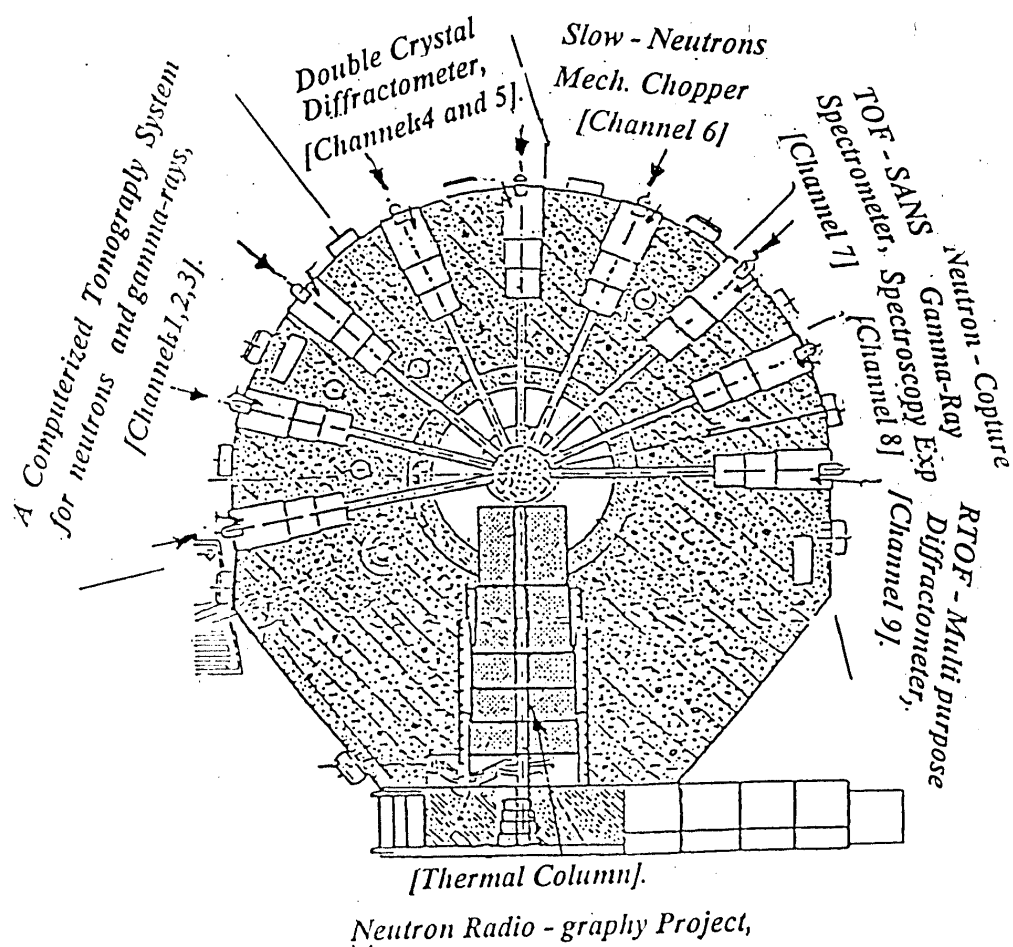


Fig. (1) Experiments on the horizontal channels of (ET-RR-1).

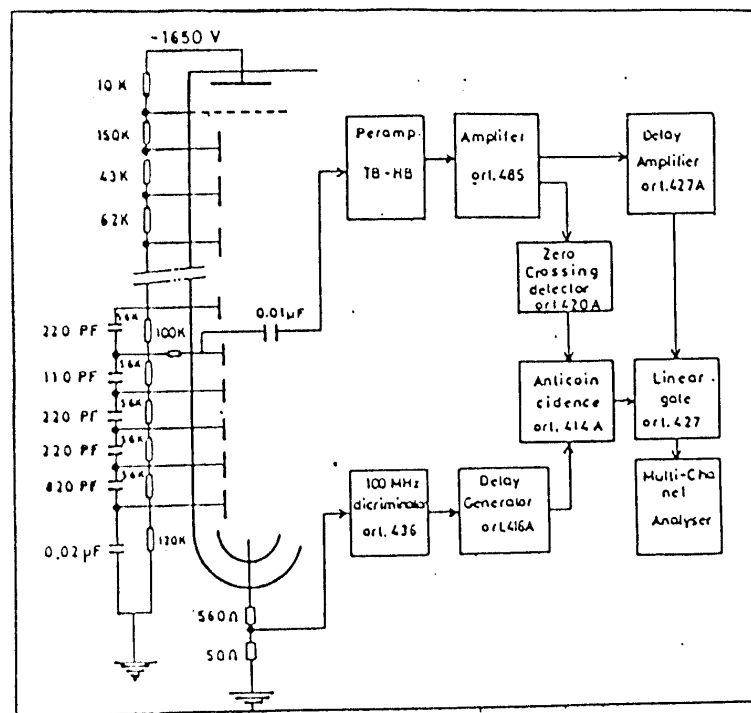


Fig. (2) A block diagram of the Electronic equipments of the neutron-gamma-spectrometer with a dynode chain at the photo-multiplier tubes [channels 1, 2 and 3].

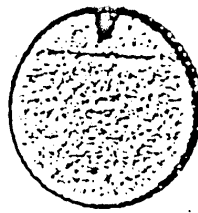


Fig. 3: Neutron-CT-image of a AISi compound sample

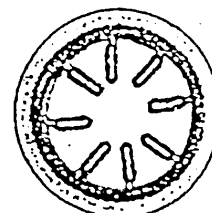


Fig. 4: CT-image with thermal neutrons of a heat pipe

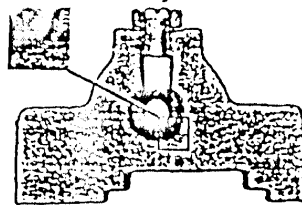


Fig. 5: CT-image with fast neutrons of a cast iron part of the hydraulics of a truck brake

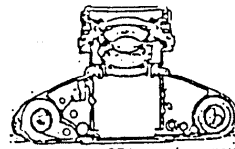


Fig. 6: Neutron CT-image of a camera

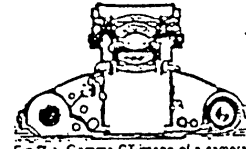


Fig. 7: Gamma-CT-image of a camera

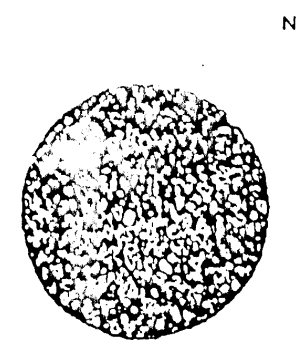


Fig. 8  
Low Neutron CT-image of Ordinary Concrete at 200 °C

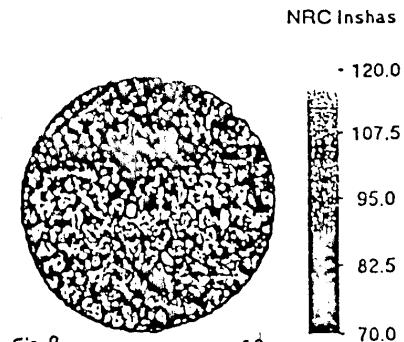


Fig. 9  
High Neutron CT-image of Ordinary Concrete at 200 °C

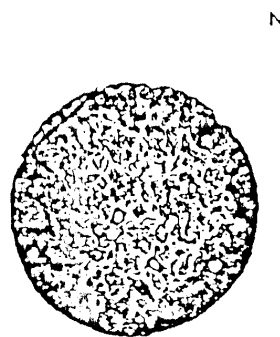


Fig. 10  
Low Gamma CT-image of Ordinary Concrete at 200 °C

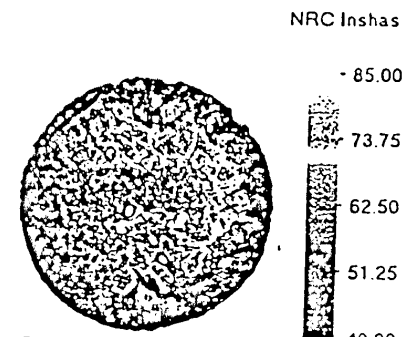


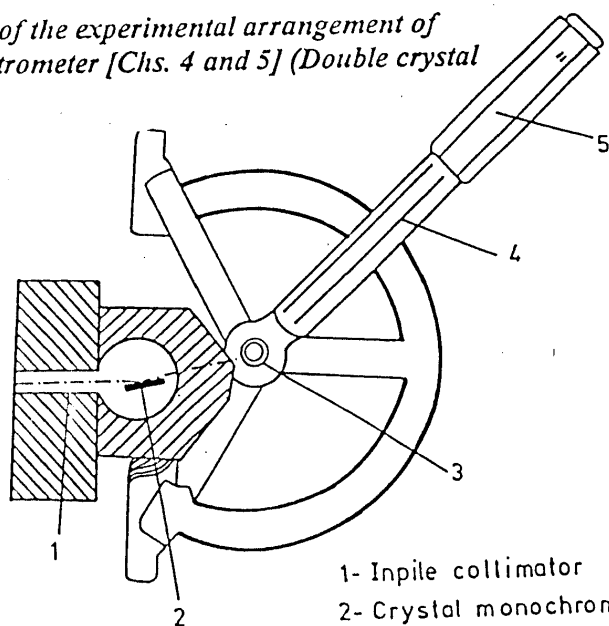
Fig. 11  
High Gamma CT-image of Ordinary Concrete at 200 °C

Figs. (3-11) Images using the computerized Tomography System for Neutrons and Gamma-Rays.



Fig. (12)

Schematic Diagram of the experimental arrangement of neutron crystal spectrometer [Chs. 4 and 5] (Double crystal Diffractometer).



- 1- Input collimator
- 2- Crystal monochromator
- 3- Sample
- 4- The outer collimator
- 5-  $\text{BF}_3$  detector

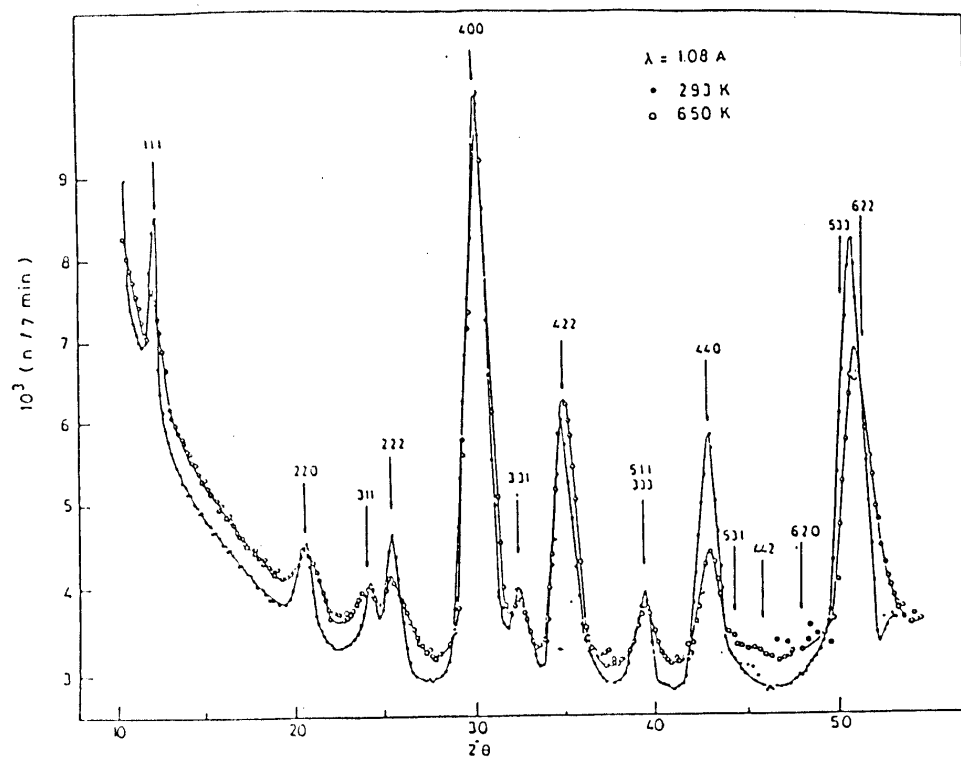


Fig.(13) Neutron Diffraction Pattern for the sample  $(\text{Co Mn}_{0.6}\text{Fe}_{1.4}\text{O}_4)$  at Room Temperature and 650 °K.

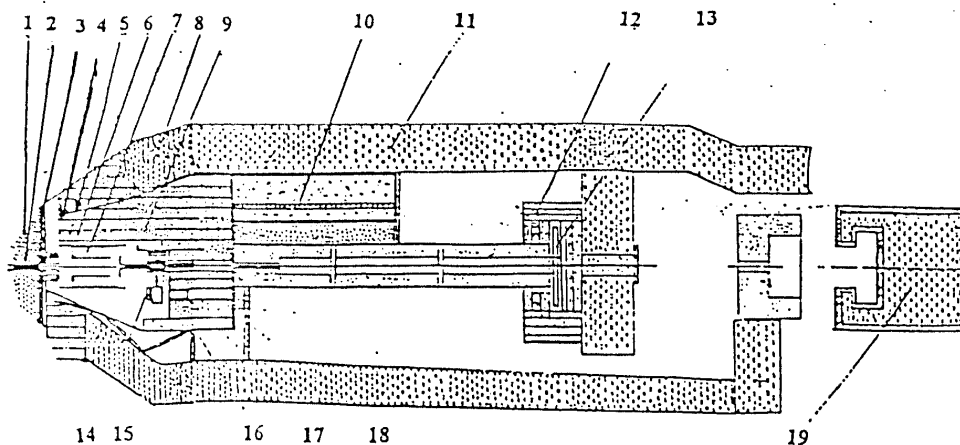


Fig.(14) Slow Neutron Mechanical Chopper Layout. Channel (6).

- 1- Inpile shield, 2- Inpile collimator, 3- Lead, 4- Outpile collimator, 5- Lead, 6- Iron, 7- Boric acid, 8- Cadmium, 9- Borated paraffin, 10- Lead, 11- Shielding wall, 12- Detector shield, 13- Detector, 14- fan, 15- Motor, 16- Rotor, 17- Magnetic phono preamplifier, 18- Borated polyethylene blocks, 19- Beam capture

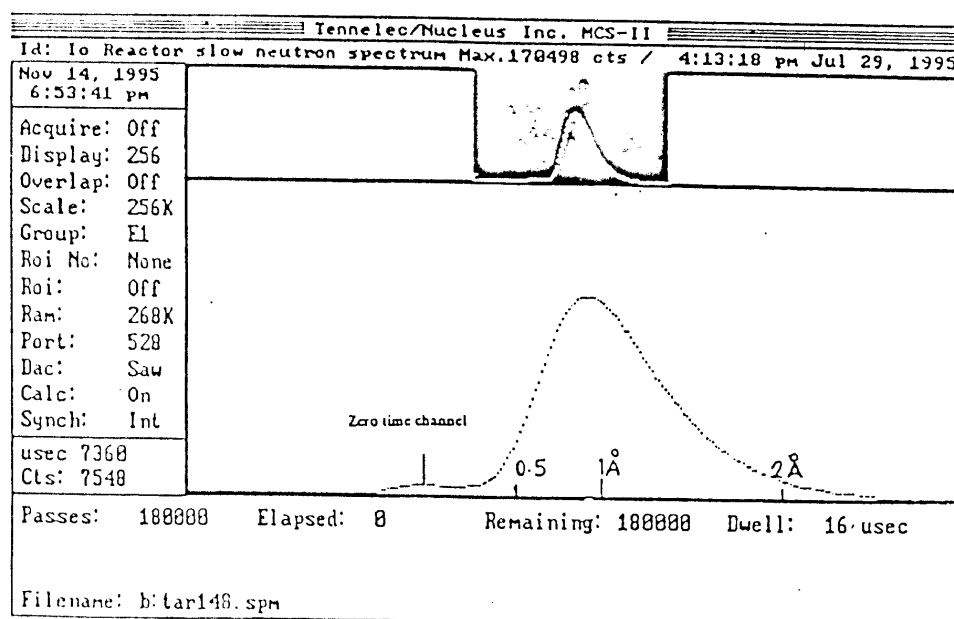


Fig. (15) Reactor slow neutron spectrum, Angular velocity 1562 r.p.m.

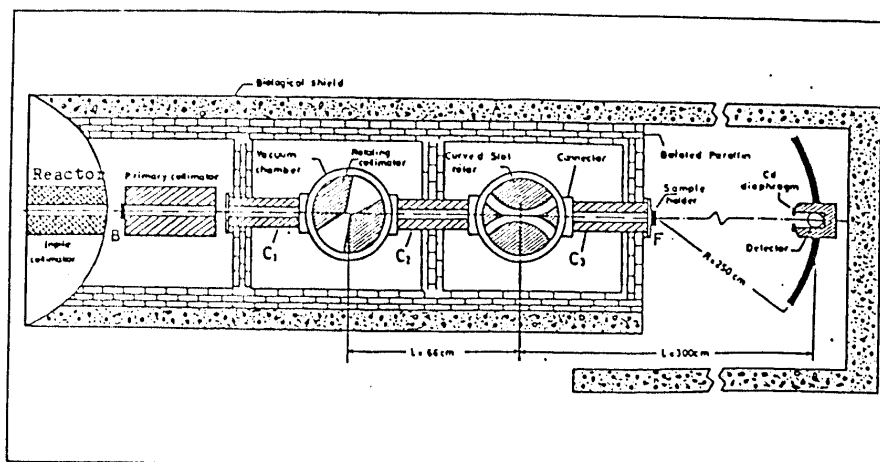


Fig. (16) The general arrangement of the (TOF) - (SANS) spectrometer (Channel. 7).

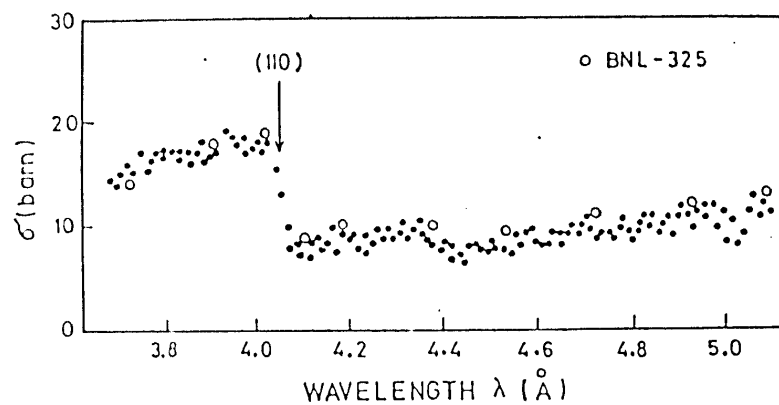
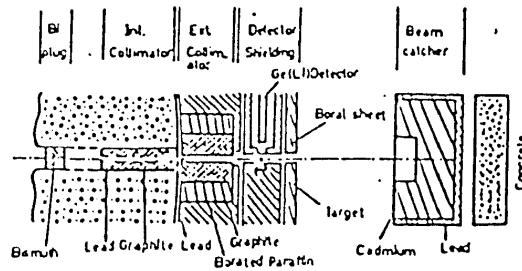


Fig. (17) Total Neutron Cross-Section of Fe-Metal.



Plan view of the experimental set up. A horizontal neutron beam extracted from the core of the ET-RR-1 Egyptian-Reactor passes through a 20 cm long of poly crystalline Bismuth plug reduce mainly the reactor gamma background, in front of the target is placed a 6mm graphite sheet in order to increase the thermal to fast neutron ratio. The Ge(Li) detector contained in a heavy lead shield is placed perpendicular to the beam at a distance of 25 cm.

Fig. (18) Neutron Capture Gamma-Ray Arrangements, (Channel 8).

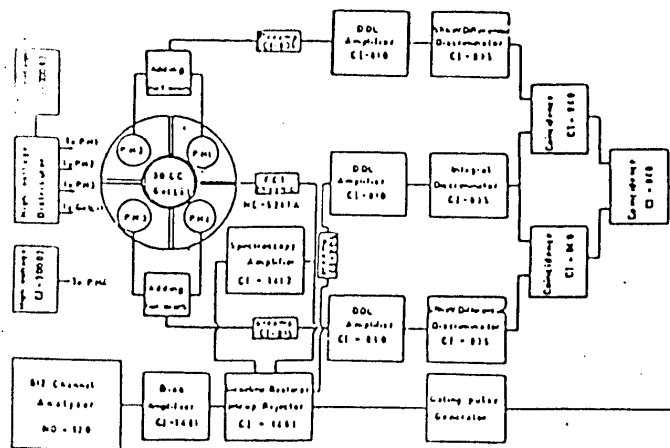
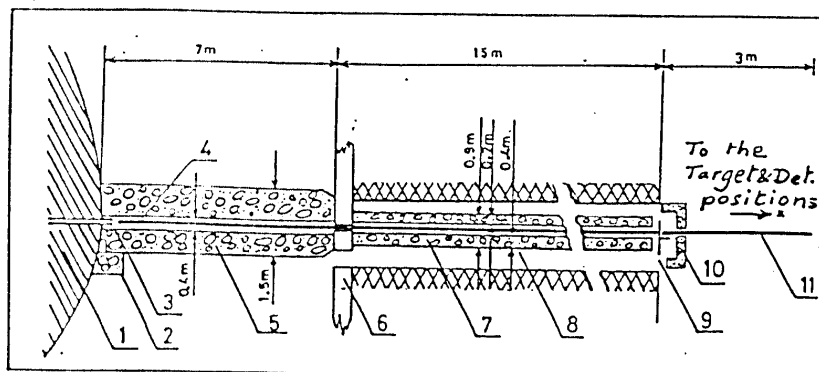


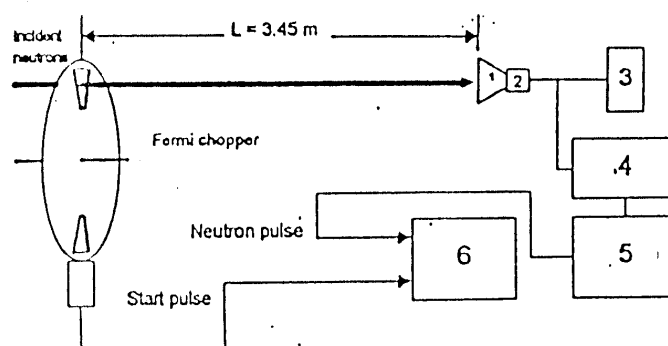
Fig. (19) Electronic Block Diagram for the Ge (Li) NaI (Tl) pair spectrometer.





- 1) Biological shielding of reactor, 2), 5), 7) & 10) Shielding (heavy concrete),  
 3) Inpile collimator, 4) Curved NGT,  
 6) Wall of reactor hall, 8) Corridor,  
 9) Fourier chopper, 11) Straight mirror collimator

Fig. (22) A schematic Diagram of the NGT and shielding around it (Channel 9).



- 1)  $^6\text{Li}$ -glass detector 2) Preamplifier 3) High voltage power supply  
 4) Main amplifier 5) Discriminator 6) Multichannel analyzer

Fig. (23) A schematic of the arrangement used for neutron spectrum measurements.

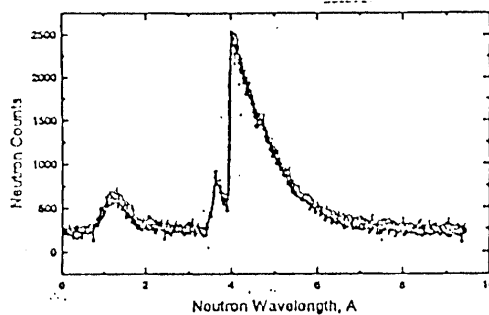


Fig. (24) Neutron spectrum transmitted through the Be Filter.

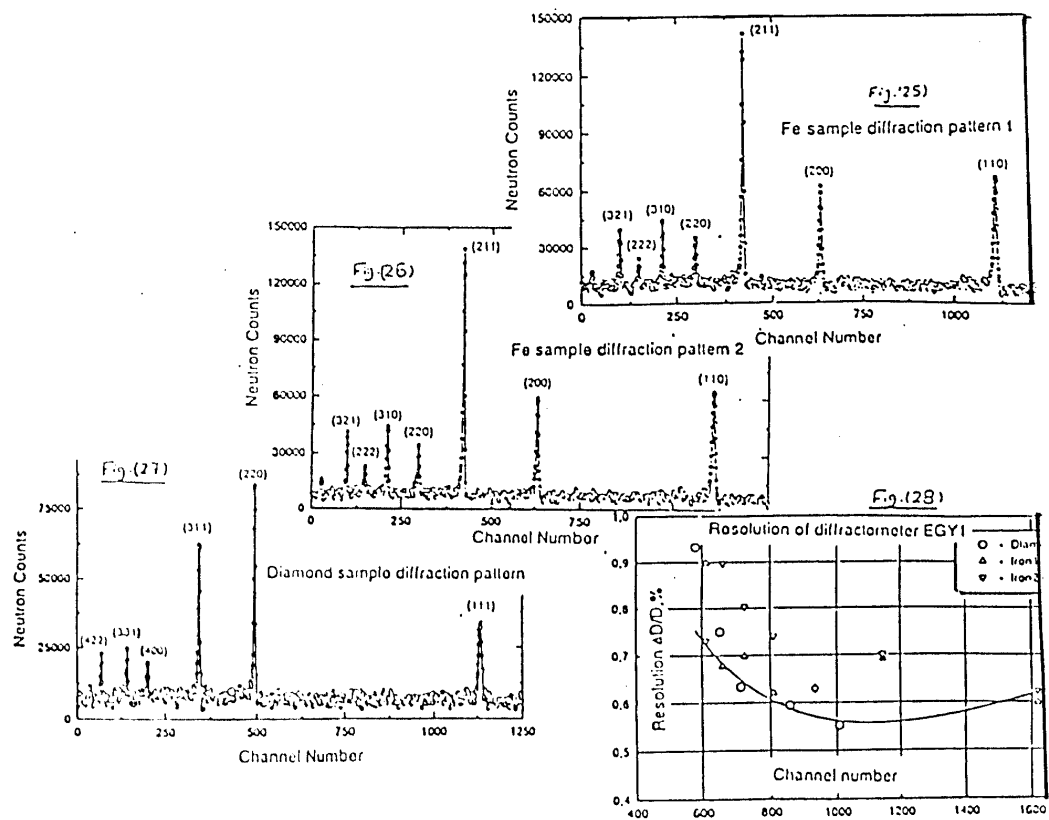


Fig. (25) Fe Sample Diffraction pattern - 1.  
 Fig. (26) Fe Sample Diffraction pattern - 2.  
 Fig. (27) Diamond sample Diffraction pattern.  
 Fig. (28) Resolution of Diffractometer EGY1.

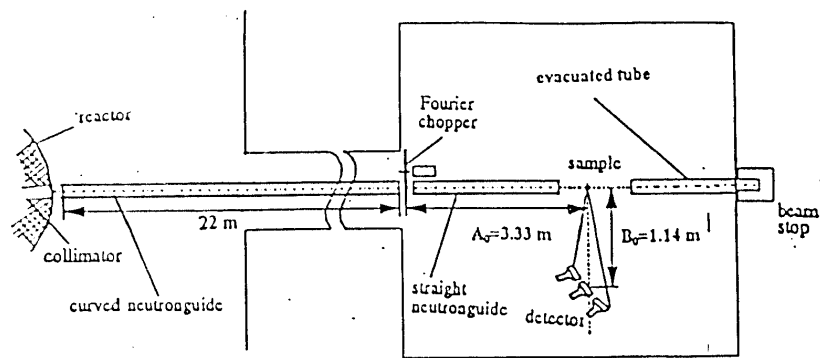
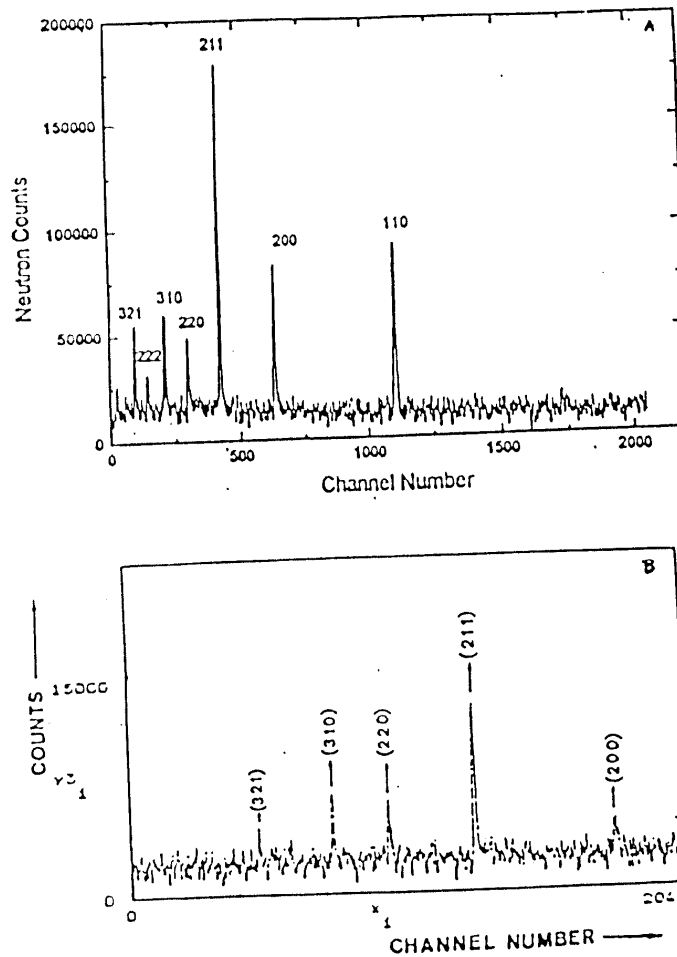


Fig. (29) Layout of RTOF (CFDF) Spectrometer.



Iron diffraction patterns:

A- Measured with the CFDF facility    B- Measured with the FSS facility

Fig. (30) Iron Diffraction Patterns Measured by CFDF & FSS.



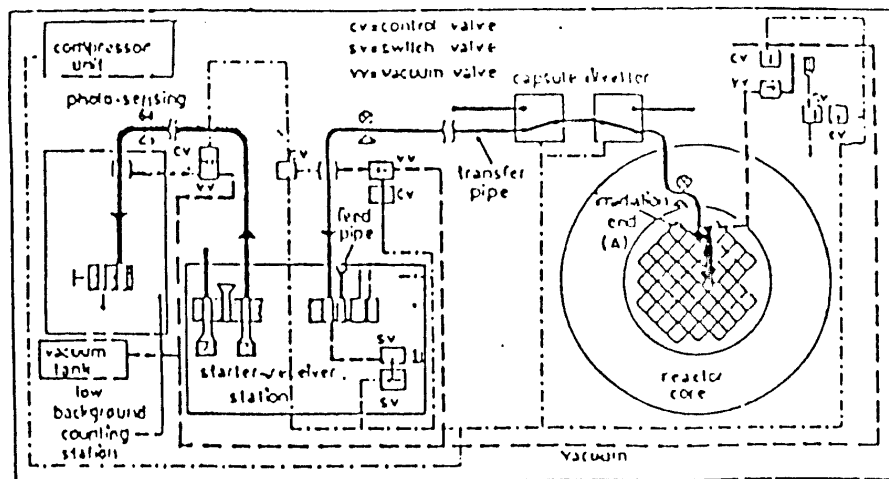


Fig. (31) A Sketch of (RPTS of ET-RR-1).

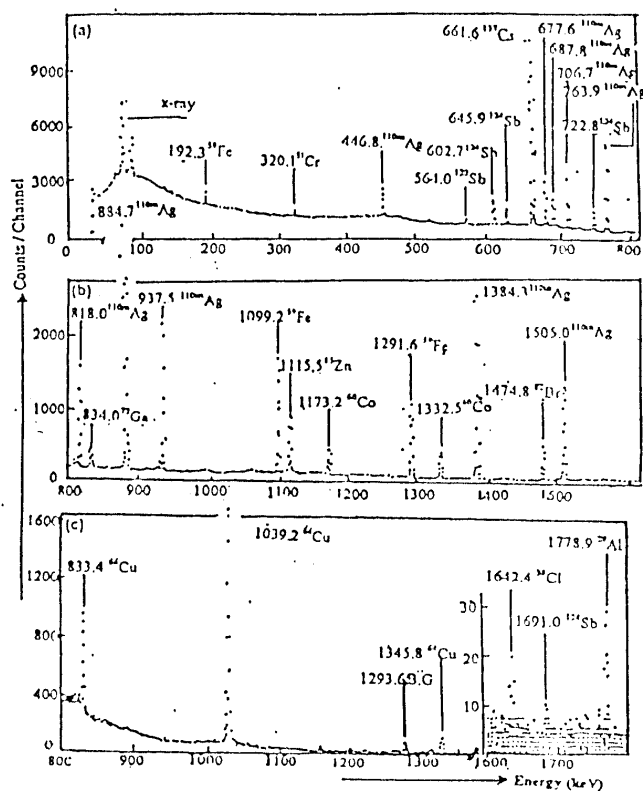


Fig. (32) Partial  $\gamma$ -ray spectra of Brazing alloy (CP2) using 48 hours and 30s. irradiation times.

# NEUTRON TRANSMUTATION DOPING OF SILICON IN RESEARCH REACTORS

M. A. Sultan

## *Utilization of Research Reactors :-*

Basic Applied research

Radio isotopes production :-

Silicon doping as an industrial application of  
research reactors :-

For many research reactors , the irradiation of silicon has become an important source of income , and in all likelihood this businesses going to develop further in coming years.

Technical progress , which took place in the last ten years , especially in the field of silicon doping , permitted to pass to production on a technical scale . As follows from the available information .

The world production of (NTD)-Si is estimated as sixty tones per year

Practical utilization of the nuclear of transmutation  $^{30}\text{Si}$  isotope to  $^{31}\text{P}$  and as a result , the homogeneous doping of semiconductor silicon by phosphorous started in mid 70's .

NTD of Silicon in Research Reactors has good properties:

Homogeneous Resistivity + Cheap to Produce

Therefore;

- The use of research reactors in NTD of silicon has been one of its important industrial applications
- The economic impact of this utilization of research reactors made some of them used only now for NTD of Si for the production of: Thyristors, Diodes, Integrated circuits.
- Work on NTD in reactors started in 1970.
- & A lot of developmental work was carried out since then to enhance the technological requirement in this important field.

The major advantage of the (NTD) of Silicon is the homogeneity which is the result of a homogeneous distribution of silicon isotopes in the target material and the long range of thermal neutron in Silicon. Research reactor facilities provide the best source of thermal neutrons for this purpose.

The absorption of a neutron and the emission of gamma in the case of Silicon is as follows :-

		<i>% In Natural Mixture</i>
$^{28}\text{Si} (n, \gamma) ^{29}\text{Si}$	$\sigma_c = 0.08 \text{ barns.}$	92.27 %
$^{29}\text{Si} (n, \gamma) ^{30}\text{Si}$	$\sigma_c = 0.28 \text{ barns.}$	4.68 %
$^{30}\text{Si} (n, \gamma) ^{31}\text{Si} \xrightarrow{2.62} ^{31}\text{P} + \beta^-$	$\sigma_c = 0.11 \text{ barns.}$	3.05 %

The first two reactions produce no dopants. The third reaction produces  $^{31}\text{P}$  the desired donor dopant.

The main object when a silicon sample is irradiated is to increase the number of phosphorous atoms in the target sample in order to obtain a required resistivity ( $\rho$ ) which is decreased by the transmutation of silicon, by neutron, to phosphorus.

Since the intention is to change the number of doped nuclei, the initial state of target material must be precisely known ( $\rho_{\text{final}} = \rho_{\text{initial}} + \Delta\rho_{\text{irradiation}}$ ). It is generally assumed that the accuracy will be acceptable if the ratio of the initial resistivity to the final resistivity is at least 10

$$\frac{\rho_{\text{initial}}}{\rho_{\text{final}}} \geq 10$$

An important factor is to use the ratio of the thermal to fast flux for a given location. In English speaking countries, the fast flux is considered to be the part of the spectrum above 0.18 MeV, whereas in French it is the spectrum above 1 MeV.

The French denomination includes :

$\phi_{\text{th}} / \phi_{\text{fast}} = 10 \rightarrow$  light water pool - type reactor : part of the spectrum corresponds to neutrons in the process of slowing down.

$\phi_{\text{th}} / \phi_{\text{fast}} = 1000 \rightarrow$  heavy water reactor highly thermalized spectrum.

Some recommendations are presented for NTD programs

1. It has been proven that even the reactor with the power of 250 kW and an average flux of about  $2 \cdot 10^{12}$  n/cm<sup>2</sup> s can be used for irradiation of Si ingots. In this limiting case the irradiation time is large (about 350 hours). With this fluence it is possible to achieve resistivities of about 50 OHM-CM. Therefore, irradiation of Si must be connected to other utilizations of the reactor: isotope production, neutron activation analysis, beam experiments, etc., otherwise the NTD method is too expensive a procedure for silicon doping.

2. For irradiation of silicon in the reactor, the following possibility are used:-

- radial beam ports
- channels in the reflector
- thermal to fast flux should be 7 : 1
- temperature of position should less than 180° C .

3. The ingot have to be treated very carefully to avoid mechanical damage and chemical impurities .

### procedure for irradiation of silicon

(5)

1. clean silicon ingot with Alcohol to reduce possible contamination
2. wrap up the ingot in Al foil to protect against contamination
3. Fix Al foil with Al wire
4. Measure the neutron flux at irradiation position
5. calculate the needed radiation time

$$t = \frac{1}{\phi} \left( \frac{1}{\rho_B} - \frac{1}{\rho_A} \right) \cdot$$

$$A = 7.3 \times 10^{15} \text{ } (\Omega \cdot \text{cm}^{-1} \cdot \text{n})$$

where:

A = irradiation constant (  $\Omega \text{ cm}^{-1} \text{ n}$  )

$\phi$  = neutron flux (  $\text{n} \cdot \text{cm}^{-2} \cdot \text{sec}^{-1}$  )

$\rho_B$  = demanded resistivity (  $\Omega \cdot \text{cm}$  )

$\rho_A$  = resistivity before irradiation (  $\Omega \cdot \text{cm}$  )

t = irradiation time (hr)

- The irradiation time needed to reach certain smaller resistivity is inreased with decresing desired resistivity . Fig( 2-6) illustrate this proportionality between irradiation time and required resistivity to be reach .

6. Irradiate the ingot

7. place irradiated ingot in a storage facility in the pool for about 7 : 14 days , depending on irradiation time and flux .

8. discharge the ingot from the pool and clean the sample with water and a solvent then measure activity and contamination .

9. clean the sample with acid solution if still contaminated .

10. the delivery paper .

6.

The irradiation of silicon can be made in very different ways, depending on the reactor facility and quantity of silicon processed, so the variety of irradiation rigs is broad.

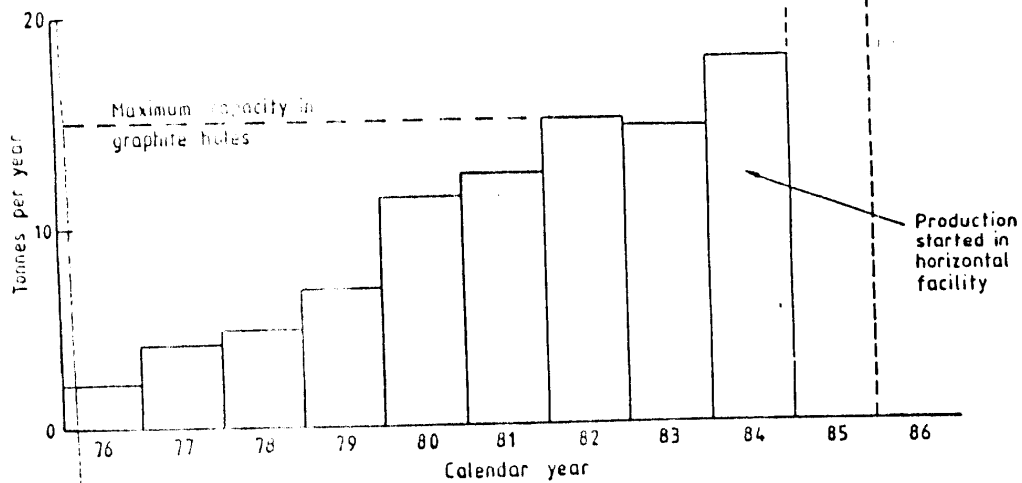
For the large production of NTD-Silicon, in the order of tens of tons per year, sophisticated irradiation rigs seem to be needed, whereas for small quantities, simple devices or even no special facilities are needed.

Large producers of NTD-Silicon

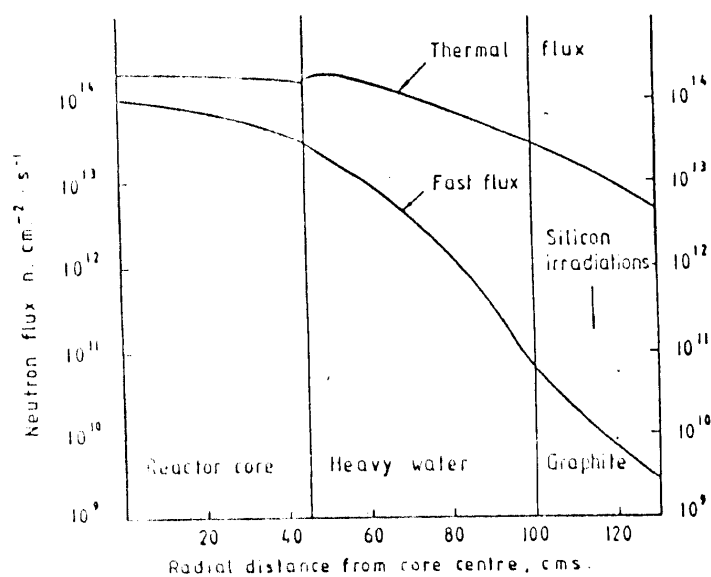
Harwell describes two irradiation facilities in the heavy water reactors DIDO and PLUTO. Irradiation is performed in vertical tubes in the graphite reflector. Boron doped aluminum is used in order to flatten the vertical flux profile to  $\pm 5\%$ , and by rotating the device, the radial flux gradient will be smoothed out.

The second irradiation facility consists of a water tank connected to a tangential beam tube which contains a storage rack for the silicon crystals encapsuled in a graphite container. A computer controlled travelling system automatically moves the samples in and out to the irradiation position and changes the samples. Crystals with a length of 600mm and diameter of up to 127mm can be irradiated and the capacity of this facility is about 20 tonnes/year.

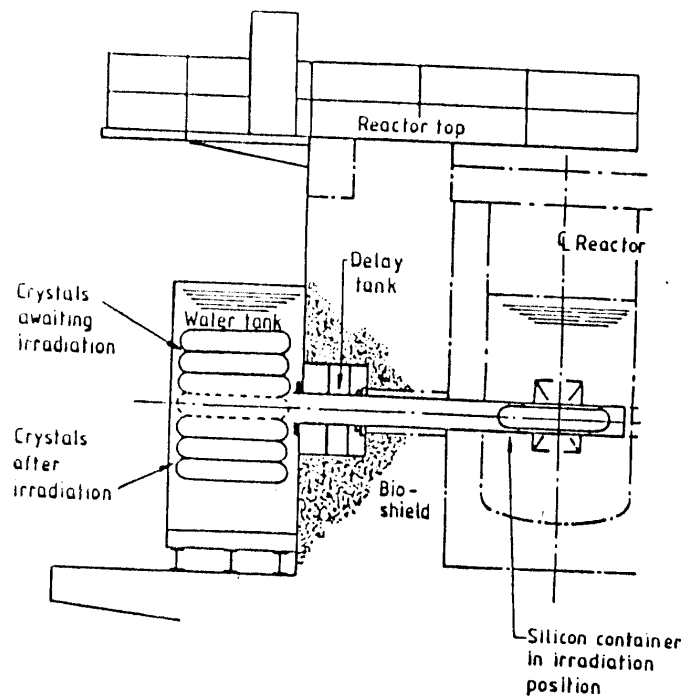




SILICON IRRADIATIONS AT HARWELL TONNES PER YEAR



COMPARISON OF THERMAL AND FAST FLUXES IN PLUTO REACTOR



HORIZONTAL SILICON IRRADIATION FACILITY

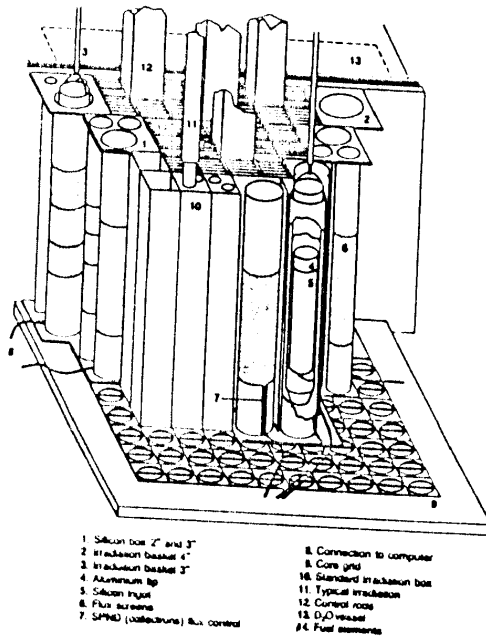
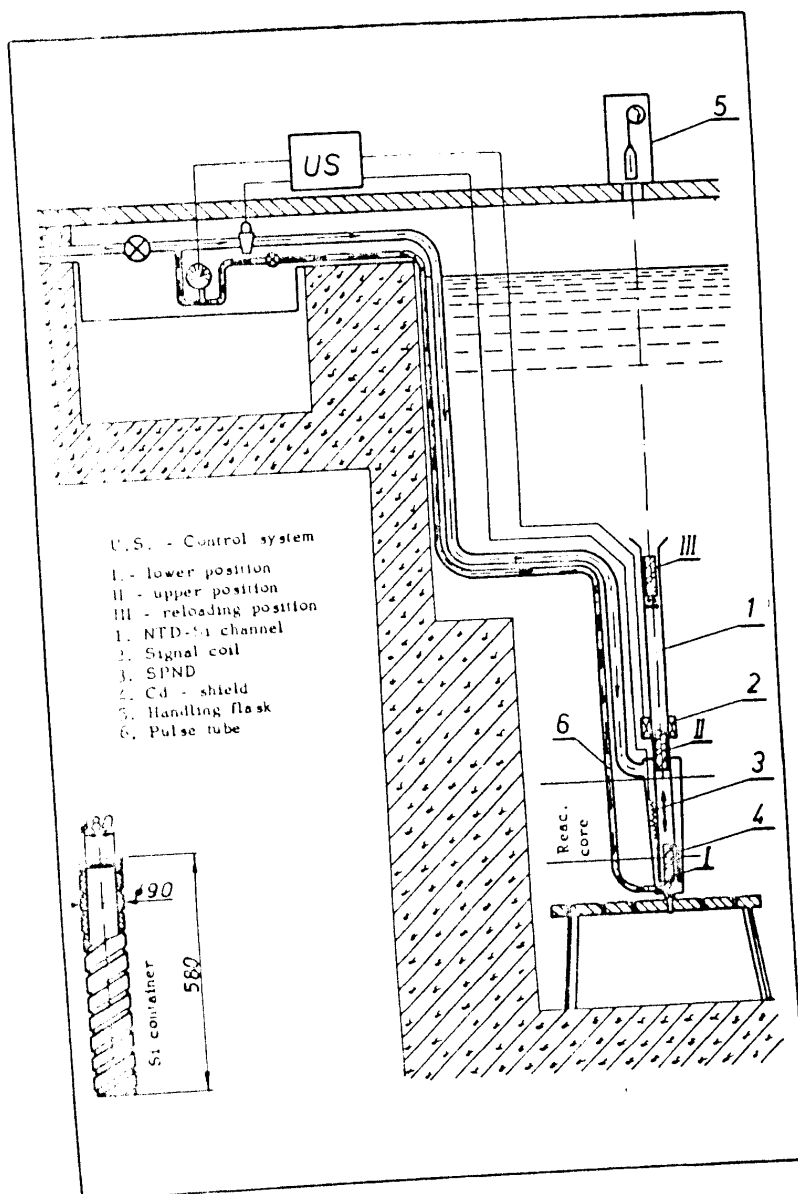


FIG.1. Swimming pool silicon irradiation locations (Melusine).

fluence is controlled by self-powered neutron detectors (SPND) of the vanadium type placed in the guide tube in the irradiation zone of the rig.

For relatively small NTD silicon production, e.g. around 1T/y or smaller quantities, there exists several simple irradiation facilities which can be built at very low cost.



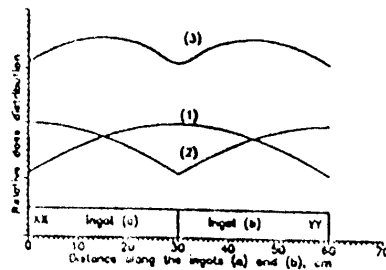
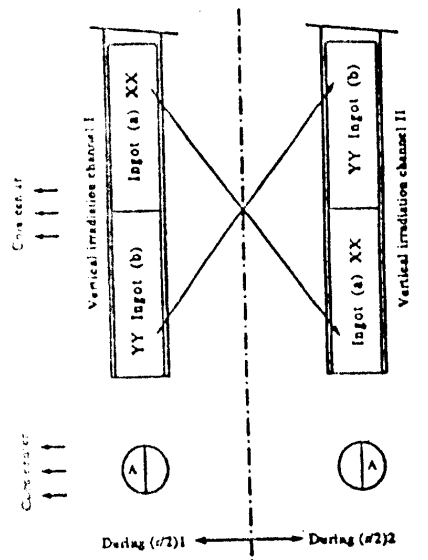
Schematic diagram of NTD-Si irradiation facility on MARIA reactor.

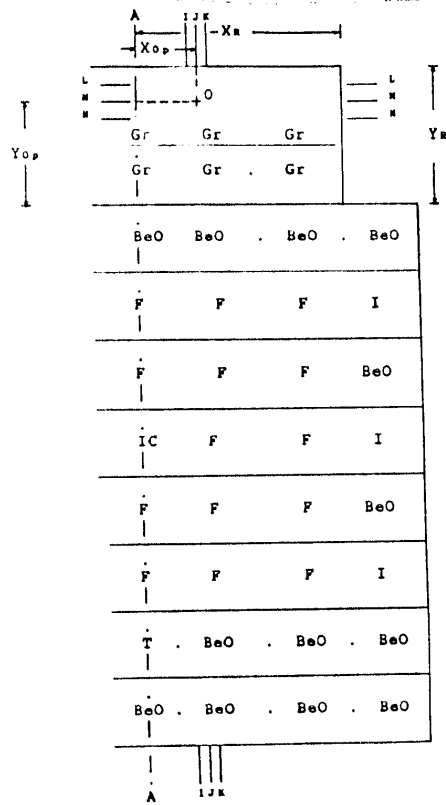
(3-4) A Method For Neutron Transmutation doping Of

Silicon In Research Reactor :-

(Inshast Nuclear Research Centre)

Ann. of Nuclear Energy - Vol. 22 No. 5 (pp. 303-310)  
(1995)





Neutron transmutation doping of Si

M. Sultan *et al.*

Calculated Optimum Parameters:

(Radius of irradiation channel = 3.45 cm.)

$X_{0p} = 7.5$  cm       $Y_{0p} = 12.75$  cm  
 $X_a = 20.25$  cm       $Y_a = 16.2$  cm

Fig. 4. Modified half core symmetry configuration showing center of Si irradiation channel (O); fuel elements (F); beryllium reflector (BeO); other irradiation channels (I); and graphite partial reflector (Gr).

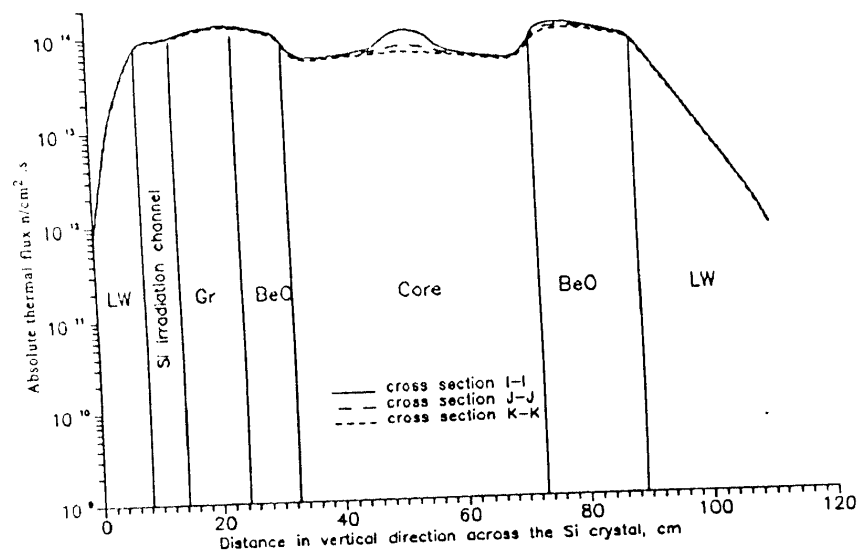


Fig. 5. Absolute thermal flux distributions in vertical direction across the Si crystal.

## Decontamination of Irradiated Si

The Si (doped) is washed with pure water and stored in the pool of the reactor for few days.

The listed regulations:

- The  $P^{32}$   $\beta$ -activity  $< 2 \times 10^4$   $\mu\text{Ci/g}$ .
- The total specific activity  $10^5$   $\mu\text{Ci/g}$ .
- The removal surface contamination  $< 10^4$   $\mu\text{Ci/g}$ .

N.B.

4 days after irradiation the activity of  $^{31}\text{Si}$  decays significantly. The total activity after that is from the  $\beta$  particles from  $P^{32}$  which has a Half-Life  $\rightarrow 14.5$  days.

CONTROL ROD CALIBRATION AND TEMPERATURE  
COEFFICIENT OF REACTIVITY

By

Dr. ENG. SAMIR SHEHL ABDOU EL-SEoud

Reactors Department, Nuclear Research Centre  
Atomic Energy Authority

SUMMARY

The calibration of control rods is important for both operation and safety of nuclear reactors, so this lecture demonstrated theoretical and experimental aspects of this subject. This calibration also concluded the temperature variation which has a noticeable effect on reactivity, control, and safety. Applications to these two subjects on the ETRR-1 reactor are illustrated.

معايرة قضبان التحكم والمعامل الحراري للفاعلية

معايرة قضبان التحكم ذات أهمية لمن من شغلها وأمان المفاعلات النووية لذلك فإن هذه المناقشة توضح الجوانب النظرية والتجريبية لهذا الموضوع. لهذا الموضوع. يشمل هذا الأيضاح أيضا على التعديل الحراري للفاعلية. على الفاعلية والتحكم والأمان. ثم الأيضاح التجريبي. وتطبيقات هذين الموضوعين على المفاعل البحثي المسمى الأول.

(2)

## I. CONTROL ROD CALIBRATION

### INTRODUCTION

Keeping a reactor operating at a constant power level requires the maintenance of a delicate balance between neutron production and absorption. Neutrons are the currency of the reactor economy, and as few of them should be wasted as possible. Some are lost through other processes, the most useful of which is absorption by control elements in the form of control rods or other mechanisms.

Control is necessary, because it is not possible to design a reactor so that the number of neutrons in successive generations is exactly constant. Therefore, extra fissile material is included in the fuel, and control elements rob the system of enough neutrons to maintain a balance. This extra fissile material is needed, because over a long period of time, enough fissile material would be destroyed to turn the reactor off. This control is necessary for other reasons, the most prominent of which is the buildup of neutron poisons as a result of reactor operation.

In a thermal reactor, the time needed for a neutron to slow down and induce a subsequent fission (releasing neutrons) may be about  $10^{-4}$  sec. Not all neutrons generated in the reactor appear "Promptly". Most neutrons appear within times like  $10^{-17}$  sec of



the time of fission, which is what we mean by prompt. However a small portion of them, about 0.5% for uranium-fueled thermal reactors, result from the decay of fission products which have half-lives on the order of seconds which are so much greater than the  $10^{-4}$  sec. mentioned above that this small number of "delayed" neutrons substantially reduces the rate of which the neutron population changes, and as a result control can be achieved.

One universal form of control is to provide a number of rods, loaded with neutron-absorbing elements such as boron or cadmium, which can be moved in and out of the core to select the portion of neutrons absorbed.

The time dependence of the appearance of delayed neutrons makes it clear that they have a number of different precursors (fission products leading to these neutrons) with a range of half-lives. Historically, these delayed neutrons have been fit into six relatively well-defined groups, corresponding to half-lives from 0.2 to 56 sec. Table 1 gives the measured half-lives of the six groups for thermal-neutron fission of  $^{233}\text{U}$ ,  $^{235}\text{U}$  and  $^{239}\text{Pu}$ . The table also give the neutron yield of each group, and the total delayed fraction " $\beta$ ", the ratio of delayed neutron yield to total neutron yield from fission.

(4)

The characteristic curve of reactivity " $\rho$ " versus " $T$ " the doubling time, can be plot from the inverse or inhour equation:

$$\rho = \frac{1}{TK_{\text{eff}}} + \sum_{i=1}^m \frac{\beta_i}{1 + \lambda_i T}$$

Where  $\beta_i$  is the fraction of the  $i^{\text{th}}$  group delayed neutrons,  $\lambda_i$  is the radioactive decay constant, and  $K_{\text{eff}}$  is the effective multiplication factor.

If  $T$  is large as is usually the case in calibration measurements, the  $\frac{1}{TK_{\text{eff}}}$  term of the above equation may be neglected, then:

$$\rho = \sum_{i=1}^m \frac{\beta_i}{1 + \lambda_i T}$$

Fig. (1) shows a plot of the reactivity versus the doubling time, which is the twice folding time, and defined as the time required for the flux to change by a factor 2. Three curves are drawn based on three sets of delayed neutron constants.

Reactivity  $\rho$  sometimes is replaced by different notations such as  $\Delta k/k$  or  $\delta k/k$  but it has the same meaning. The inverse hour or "inhour" unit of reactivity is defined as the reactivity which makes the stable period of the reactor equal to one hour. The "dollar" unit is the reactivity when equal to  $\beta$  the total fraction of delayd neurons, so, the reactivity in dollars equals  $(\rho/\beta)$ , and a "cent" represents a 1/100 of a dollar.

TABLE (1): Delayed Neutron Data for Thermal Fission in  
 $^{233}\text{U}$ ,  $^{235}\text{U}$  and  $^{239}\text{Pu}$  :

Group	$^{233}\text{U}$		$^{235}\text{U}$		$^{239}\text{Pu}$	
	Half-life (second)	Yield (Neutrons/ fission)	Half-life (second)	Yield (Neutrons/ fission)	Half-life (second)	Yield (Neutrons/ fission)
1	55.00	0.00057	55.72	0.00052	54.28	0.00021
2	20.57	0.00197	22.72	0.00346	23.04	0.00182
3	5.00	0.00166	6.22	0.00310	5.60	0.00129
4	2.13	0.00184	2.30	0.00624	2.13	0.00199
5	0.615	0.00034	0.61	0.00182	0.618	0.00052
6	0.277	0.00022	0.23	0.00066	0.257	0.00027
Total yield	-	0.0066	-	0.0158	-	0.0061
Total delayed fraction: $\beta$		0.0026	-	0.0065	-	0.0021

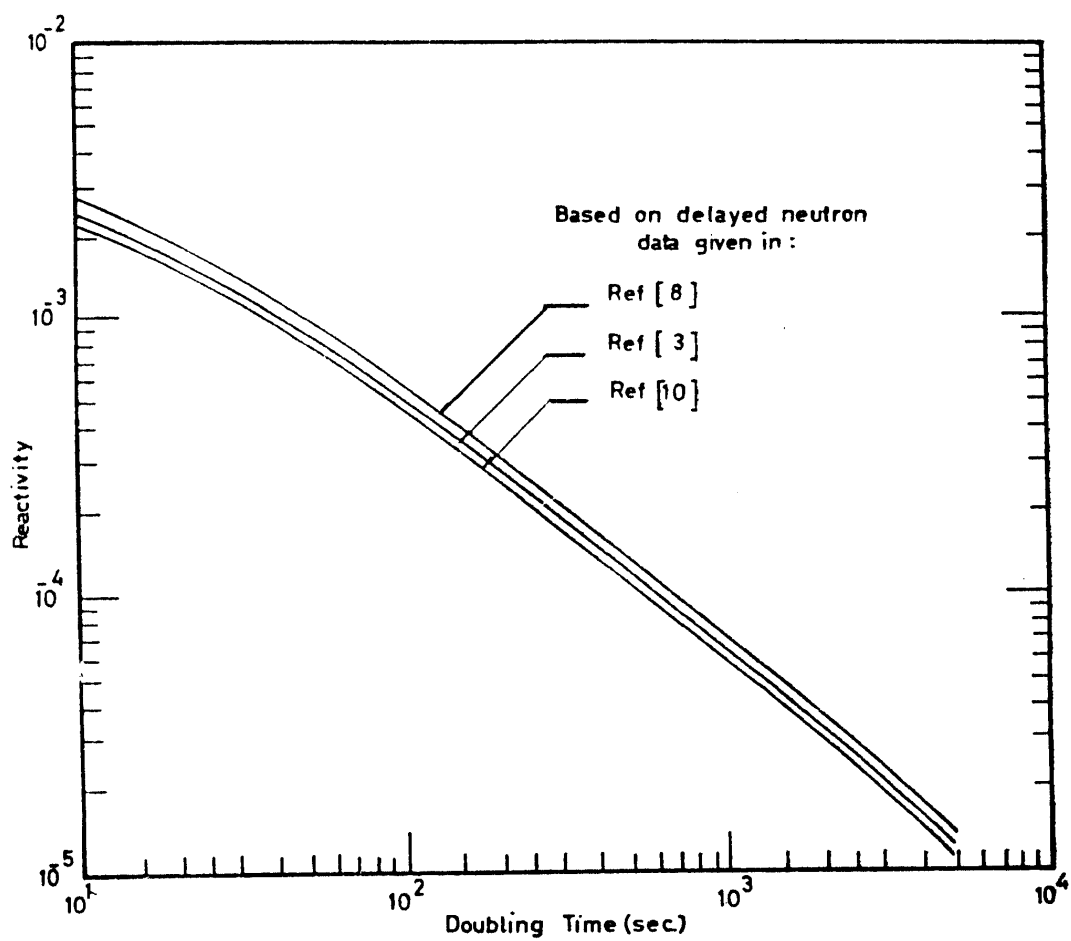


FIGURE (1): REACTIVITY VERSUS DOUBLING TIME CHARACTERISTICS

METHODS OF CONTROL ROD CALIBRATION

For large reactors the problems of calibration are numerous due to the complexity of the control system involved. Most research reactors have the flexibility in using the control rods in different ways. For great number of control rods perhaps 100 rods, the problem needs some regulating arrangements, some of these control rods are fully withdrawn through operation, some, groups of control rods for control and some for getting neutron flux flattening. The calibration of the control rods plays an important role in reactor operation, since through it we can predict the number and distribution of the control rods to be used under any circumstances throughout the life of the reactors. So many methods are in use for control rod calibration, but the method to be adopted is largely dependent on the total reactivity worth of the control rod to be calibrated and on the reactor type too.

1. DOUBLING TIME METHOD

This method is based on bringing the reactor to criticality while the rod to be calibrated is fully inserted. The reactor is then shut down and the control rod is withdrawn a small distance. The height of the rod is fixed while the other rods are withdrawn to the previously recorded situation. The doubling time is

measured and then the reactor is shut down. From the characteristic equation, the reactivity worth of the distance withdrawn by the rod can be calculated. The procedure is repeated in stages until the control rod is completely withdrawn. In this way we can plot the calibration curve of the control rod under consideration.

## 2. ANALOG COMPUTER TECHNIQUE:

This method has been widely used recently. The idea is the analog computer is used as a simulator. The computer is innersly simulate the kinetic equation. The input signal to the computer is the output current from the ionization chamber, this current is proportional to the reactivity.

## 3. ROD DROP METHOD

This method is carried out by the observation of the decay of the reactor power following the sudden insertion of the control rod to be calibrated. The resulting negative reactivity change causes the neutron flux to decay. From the neutron density calculated from the kinetic equation at different times the reactivity change and consequently the worth of the control rod can be determined.

### 3. INTERCALIBRATION METHOD

This method depends on calibrating the control rod under consideration with respect to a previously calibrated one.

The procedure is to bring the reactor critical at low power level using the calibrated rod with the uncalibrated one fully inserted. Insert the calibrated rod a certain distance  $\Delta x$ , and return to the criticality by withdrawing the uncalibrated rod a corresponding distance  $\Delta y$ . This means that the reactivity worth of the first  $\Delta y$  of the uncalibrated rod is equivalent to the  $\Delta x$  of the calibrated one. The procedure is repeated until the whole control rod is calibrated.

### 5. SOURCE JERK METHOD

The basic idea of this method is to introduce a neutron source into the reactor core in a subcritical state, the source is suddenly withdrawn and the variation in the neutron density following this Jerk can be measured. The basic equations are the kinetic equation for the neutron density, and precursors concentrations with the delayed neutron properties as parameters. By determining the neutron density in or near the core before and after the source Jerk, the corresponding negative reactivity of the core can be calculated.

### CALIBRATION OF THE ETRR-1 CONTROL RODS

#### Control Rods of The ETRR-1 Reactor

The reactor uses nine control rods for normal operation, start up, power level control, and shut down. Three (AZ) of reactivity worth 6% are safety rods which are used in all cases of shut down. Two pairs ( $PP_1$  and  $PP_2$ ) of reactivity worth 2.8% and 3.2% respectively are shim rods for coarse control to provide adjustment for long time cycles, and each pair of these manual rods is designed to move simultaneously. One (MP) of reactivity worth 1.5% is a fine manual rod for the precision regulation and adjustment, and one (AP) of reactivity worth 0.8% is an automatic control rod to adjust power at steady level. Fig. (2) shows a schematic illustration of the control rod configuration inside the reactor core. All the control rods except the automatic rod contains boron carbide  $B_4C$  as neutron absorber, the automatic rod is made of steel. The maximum built in (cold clean) reactivity in the reactor core is 5%. This is to compensate, the reactivity change due to the increase in the cooling water temperature within 20-30°C (~ 0.1%), the poisoning by xenon-135 (~ 1.6%), and the reactivity change during experiments (~ 1.8%). Burnup and poisons are compensated by adding more fuel baskets.



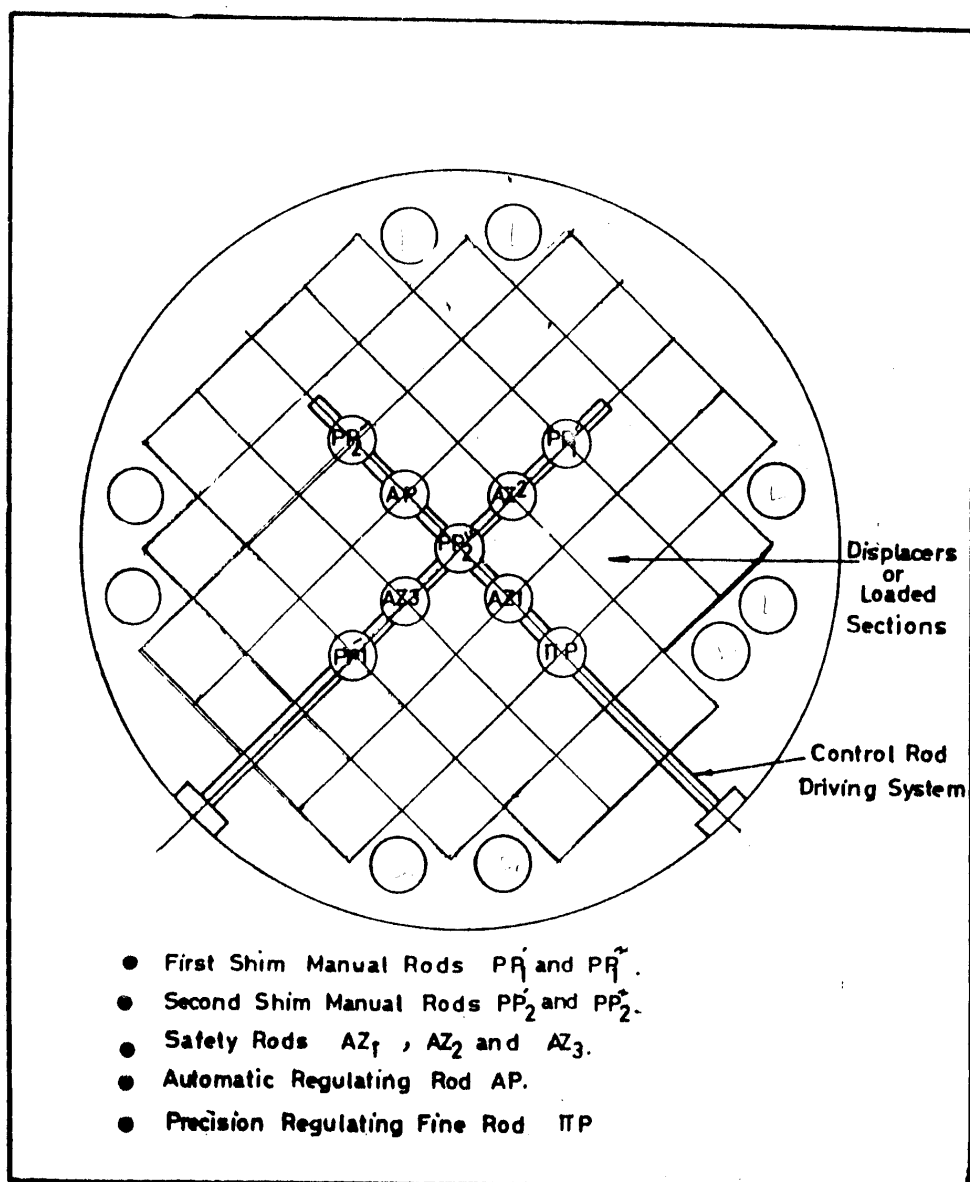


FIGURE (2) DISTRIBUTION OF THE CONTROL RODS IN THE ETPR-1 REACTOR

### Introduction On The Experimental Procedure:

Starting by calibrating the automatic control rod AP or the rod BP. The idea of the method is based on introducing a reactivity disturbance inside the reactor core, which causes a deviation from the critical condition on a pre-established power level. By raising the control rod manually, from the extreme lower position in steps, the power increases at a certain rate by which the doubling time  $T$  can be recorded. By the aid of the reactivity-doubling time curve, the value of  $\delta k$  corresponding to each step can be determined. When the rod to be calibrated is at the upper position, the values of  $\delta k_i$  corresponding to each step  $i$ , are added to obtain the total reactivity effect of the rod  $\Delta k_N$ .

The calibration curve represents the relation between the distance travelled by the rod,  $x_i$ , and the corresponding reactivity  $\Delta k_i$ . The reactivity is small, when the rod is near the upper or lower positions. On the otherhand, the maximum rate when the rod is in its halfway.

After calibrating the automatic rod, other rods can be calibrated by utilizing the results obtained for the automatic rod. The method is based on raising the control rod and compensating the resulting effect automatically by the automatic rod. A precaution should be made that is to restrict the compensation by automatic control rod along the linear part of the relation between

its degree of insertion in the core and the corresponding reactivity.

Calibration of The Automatic Control Rod AP:

In the following steps, we consider the lower position of the control rod (Full insertion) at 0.0 cm, and the upper position (complete withdrawal) at 60.0 cms.

- (1) Start up the reactor and bring it to criticality at low power (500 watts) on automatic operation.
- (2) Record the position of the control rods e.g. AP (30 cms), PP<sub>1</sub> (0.0), PP<sub>2</sub> (43.3 cms), and NP (0.0).
- (3) On automatic operation, lower the automatic rod and raise the PP<sub>1</sub> until the AP rod approaches the lower position. It is recommended not to reach the extreme lower position on automatic operation to avoid tripping (scram) of the reactor.
- (4) Switch off the automatic operation and lower the automatic rod AP manually to the extreme lower position and compensate by the manual PP rods. Record the new positions of the control rods for the same criticality and power conditions, e.g. AP (0.0), PP<sub>1</sub> (30.0 cms), PP<sub>2</sub> (34.0 cms), and NP (0.0) cm.
- (5) Raise the automatic rod AP a certain distance e.g. 10% of its total length, and record the resulting doubling time  $T_1$  and the corresponding reactivity  $\delta k_1$ .

- (6) Compensate with  $PP_1$  only to return to criticality again. The reason for lowering the  $PP_2$  rods from 43.3 cms in step (2) to 34 cms. in step (4) then fixing its motion throughout the calibration procedure is to avoid the uneven influence they may cause during the experiment on the automatic rod AP since the  $PP_2$  rods are adjacent to AP.
- (7) Steps (5), (6) are repeated successively until the extreme upper position of the automatic control rod is reached.
- (8) Construct a table, connecting the rod position, the other control rod positions, the doubling time, the corresponding reactivity and the total reactivity equivalence.

Plot the variation of  $x_n$  with  $\Delta k_n$ , which shows the required calibration curve for the control rod under consideration. From this curve one can determine the linear range of the rod characteristics. The maximum reactivity effect is  $\Delta k_N$ , which gives the reactivity effectiveness of the whole control rod.

#### Calibration of the First Manual Control Rods $PP_1$ :

- (1) Start up the reactor and bring it to criticality at low power on automatic operation where the  $PP_1$  rods are in the lowest position.
- (2) Lower the  $PP_2$  manual rods until the automatic control rod AP comes to a position corresponding to the maximum point of

linearity on its characteristic curve e.g (37.4 cms) Record the positions of the control rods as e.g:

AP(37.4 cms),  $PP_1(0.0)$ ,  $PP_2(-11.6)$ , and  $\Pi P(0.0)$

- (3) Start to raise the  $PP_1$  rods in steps and record the position of different control rods. Keep the movement of the automatic rod AP in its linear range by lowering the  $PP_2$  manual rods.
- (4) Construct a similar table as in AP calibration experiment and plot the corresponding characteristic curve.

Since the positions of the two manual control rods are symmetrical in the core, one can assume their effect to be equal, and the effect of each rod equals  $(\Delta k_N/2)$ .

(16)

## II. TEMPERATURE COEFFICIENT

The temperature of the core, including the moderator, the fuel, the coolant, the reflector and the structural material has a noticeable effect on the reactivity.

This has very important reflections on problems of control and safety. Beside being an important operational parameter, it actually adds a stabilising effect to the characteristics of the control since for each power level, there exists a different average temperature and hence a different equilibrium position of control rods. Without the variation of reactivity with temperature, the power level will be an arbitrary parameter in the criticality equation, and the position of the control rods will be defined for criticality independent on the power level.

On the other hand, if the coefficient of dependence of reactivity on temperature is zero or positive the equilibrium of the system will be critical or unstable respectively. For zero coefficient there will be no restoring effect to damp the effects of an assumed accidental change in reactivity, while the presence of a positive coefficient creates a condition of unstable equilibrium in which an assumed accidental change tends always to proceed increasingly fast in the initial direction. This is a very important feature affecting the safety consideration of a reactor.

This experiment is carried out to determine the dependence of reactivity on the average temperature of the moderator coolant medium.

#### Description and Procedure

In nuclear reactors, and especially those primarily concerned with energy production in the form of heat, temperature transients are inevitable. For this reason, the operation of a reactor in the practical sense required that the temperature coefficient of reactivity be small, so that a steady state can be maintained by means of the control system. The reactor will then remain essentially stable in spite of moderate fluctuations in temperature.

The qualitative relationship between temperature and reactivity will be developed from a consideration of the effect of temperature on the individual factors of the two group criticality equation.

$$K_{eff} = \eta \epsilon P f \left[ \frac{1}{1 + L^2 B^2} \right] e^{-\tau B^2} \quad (1)$$

where  $\eta$  = number of fast neutrons born per thermal neutron captured in the fuel,

$\epsilon$  = fast fission factor,

$P$  = resonance escape probability,

$f$  = thermal utilization,  
 $e^{-\tau B^2}$  = fast nonleakage probability ( $L_1$ ), where  $\tau$  is the  
 neutron age and  $B^2$  the geometric buckling,  
 $\frac{1}{1+L^2 B^2}$  = thermal nonleakage probability ( $L_2$ ), where  $L$  is the  
 thermal diffusion length.

The reactor is critical where  $K_{eff} = 1$ , that is on the average one of the neutrons born in a thermal fission cause another fission. Then, the neutron population is independent of time and is said to be self sustaining. If  $K_{eff} \neq 1$  the population will continuously change, increasing if  $K_{eff} > 1$  and otherwise decreasing. The rate of change of population is a function of the reactivity  $\rho$ , defined as:

$$\rho = \frac{K_{eff} - 1}{K_{eff}}$$

The temperature coefficient of reactivity is given by:

$$\frac{d\rho}{dT}$$

Where  $T$  is usually in  $^{\circ}\text{C}$ .

Usually as a safety feature, and for stability reasons, the overall reactivity temperature coefficient is designed to be negative. If the temperature of a critical reactor increases,  $K_{eff}$  becomes less than one, and the reactor is then subcritical at the new temperature. On the other hand, if  $d\rho/dT$  were positive and as the fission process releases heat, the reactor would be unstable



and become increasingly more supercritical as the temperature increased.

The effect of temperature on the factors of Eq. (1) arise mainly from the neutron energy dependence of the microscopic absorption and to a lesser extent scattering cross-sections and from the variation of the macroscopic cross-sections due to variations in core density. Also the effect of volume changes on the geometrical buckling is an important effect. With increasing temperature some factors increase, some decrease, and some hardly change, so that overall coefficient depends on which factors dominate.

The temperature coefficient is not easily calculated, it is usually confirmed or determined experimentally. In the following discussion the coefficient is considered separable into a density and nuclear coefficient as is usually done for large fueled thermal reactors.

For the density coefficient, as the temperature increases, the core material densities decrease while the core volume increases, and the reactivity associated with these physical changes is of opposite sign.

A decrease in density decreases the macroscopic cross-sections and increases the mean free pathes for absorption and scattering and the thermal diffusion length increases. But partially if not completely compensating for the increase in  $L^2$  is the decrease in  $B^2$  due to increased core volume. Generally, the net result of the density decrease is a decrease in thermal non-leakage probability.

Another effect of a density decrease which can be very important in over-moderated liquid or gas cooled heterogeneous reactors, is the decrease of poison in the core due to the expansion of the coolant-moderator.

For the nuclear coefficient, as the core temperature increases the neutron energy increases as does the vibratory energy of the core atoms. With increasing neutron energy, the microscopic absorption cross-section (excluding resonances) and the scattering cross-section decrease. Generally, for neutron energies less than of the first resonance, absorption cross-section vary as  $1/v$  for most materials.

The temperature dependence of  $\tau$  and  $\epsilon$  will be considered negligible, because they are functions of high energy cross-sections which are hardly temperature dependent.

With increasing neutron energy beyond 0.025 eV,  $\eta$  decrease for natural or slightly enriched uranium reactors because whereas  $^{238}\text{U}$  is a  $1/v$  absorber,  $^{235}\text{U}$  is less than  $1/v$ . Hence, as the temperature increases,  $^{238}\text{U}$  will non-fission capture, an increasingly larger fraction of thermal neutrons. However, the change in  $\eta$  is small, and it usually is considered to be temperature independent.

Because of Doppler broadening of the  $^{238}\text{U}$  resonance peaks with increasing temperature,  $\rho$  decreases. The Doppler broadening arises from the thermal vibration of the  $^{238}\text{U}$  atoms.

The thermal utilisation is often considered to be temperature independent because all cross-sections would vary as  $1/v$ , but  $^{235}\text{U}$  is not  $1/v$ , so a slight decrease of  $f$  with increasing temperature is expected. In the case of heterogeneous reactors, the decrease in uranium absorption with increasing temperature will decrease the disadvantage factors. This effect can be quite large and can even result in a positive fuel temperature coefficient.

The decrease in microscopic cross-section will increase  $L^2$  and decrease the thermal non leakage probability.

In carrying out the experiment, the reactor was made critical at a very low power level (few milliwatts), with no circulation and the positions of control rods were recorded. The reactor was then shutdown and the temperature of the moderator was measured ( $t_1$ ). The circulation of the pumps of the primary cooling circuit was started in order to heat the coolant. This dissipates a heat energy to the coolant, and after considerable temperature rise the reactor was brought back to critical, and positions of control rods were recorded and the temperature measured ( $t_2$ ). The decrease of reactivity due to temperature rise was then calculated from the control rods positions.

#### RESULTS:

- (1) Reactor critical at  $t_1 = \text{ }^\circ\text{C}$ , control rods positions are:

$$l_1(\text{cm}), l_2(\text{cm}), l_3(\text{cm}), l_4(\text{cm})$$

- (2) Reactor critical at  $t_2 = \text{ }^\circ\text{C}$ , control rods positions are:

$$l_1(\text{cm}), l_2(\text{cm}), l_3(\text{cm}), l_4(\text{cm})$$

- (3)  $dt = t_2 - t_1 \text{ }^\circ\text{C}$ ,

and  $d\rho$  equivalent to the difference in rod positions may be calculated from their calibration curves.

- (4) Temperature coefficient =  $(d\rho/dt) \text{ } \delta k/\text{ }^\circ\text{C}$ .

REFERENCES

- [1] Anthony. V. Neor. JR., " A Guidebook to Nuclear Reactor", University of California Press. (1979).
- [2] J.Shaw. "Reactor Operation", Pergamon Press Ltd. Oxford, (1969).
- [3] S.Glasstone, "Principles of Nuclear Reactor Engineering" D. Van Nostrand Co., Inc., New York, (1955).
- [4] M.G. Zaidouk et al. UAR. AEE, Int. Rep. 25 (1968)
- [5] O.H. Marty et al. UAR AEE, Int. Rep. 6 (1963).
- [6] O.H. Marty et al. UAR AEE, Int. Rep. 11(1965).
- [7] M.A. Sultan et al. UAR AEE, Int. Rep. 100 (1983).
- [8] ANL-6990, A Manual of Reactor Laboratory Experiments, Jan., (1965).
- [9] "Delayed Fission Neutrons, "Proceeding of a Panel Held in Vienna 24-27 April 1967, IAEA Vienna (1967).
- [10] REGAR "Reference Safety Analysis Report", Vol. 8, Technical Description for Proposed Egypt's First Nuclear power Plant (600 MW Westinghouse Electric Corp.) (1976).

# SHIELDING CALCULATIONS

Prof. Dr. M. E. Nagy  
Nuclear Engineering Department  
Faculty of Engineering, Alex. Univ.

## ABSTRACT

Radiation shielding serves a number of functions. Foremost among these is reducing the radiation exposure to persons in the vicinity of radiation sources. Shielding used for this purpose is called biological shielding. The present work is devoted to biological shielding of  $\gamma$ -rays. Shields are also used in some reactors to reduce the intensity of  $\gamma$ -rays incident on the reactor vessel. This protects the vessel from excessive heating due to  $\gamma$ -ray absorption, and these shields are called thermal shields. Sometimes shields are used to protect delicate electronic apparatus that otherwise would not function properly in a radiation field. Such apparatus shields are used, for example, in some types of military equipment. Ordinarily it is necessary to shield only against  $\gamma$ -rays and neutrons, not against  $\alpha$ -particles or  $\beta$ -rays. This is because the ranges of charged particles in matter are so short. In all cases, the central problem is to determine the thickness and / or composition of shielding material required to reduce biological dose rates to predetermined levels, frequently the maximum permissible dose rates at certain points for either occupational or general population exposure.

## 1. Buildup Factors :

Consider a monodirectional beam of  $\gamma$ -rays of intensity (or flux)  $\phi_0$  and energy  $E_0$  which is incident upon a slab shield of thickness  $a$  as shown in Fig. 1. If there were no shield, the exposure rate at P would be :

$$\dot{X}_0 = 0.0659 \phi_0 E_0 (\mu a / l)^{\text{air}} \quad \text{mR / hr} \quad (1)$$

where  $\phi_0$  is in units of  $\gamma$ -rays /  $\text{cm}^2 \cdot \text{sec}$ ,  $E_0$  is in Mev, and  $(\mu a / l)^{\text{air}}$  is in  $\text{cm}^2 / \text{g}$  and is evaluated at the energy  $E_0$ . It is convenient to write Eq.(1) in the form :

$$\dot{X}_0 = c \phi_0 \quad (2)$$

where

$$c = 0.0659 E_0 (\mu a / l)^{\text{air}} \quad (3)$$

is a function of  $E_0$ . With the shield in place, the  $\gamma$ -ray flux  $\phi$  emerging from

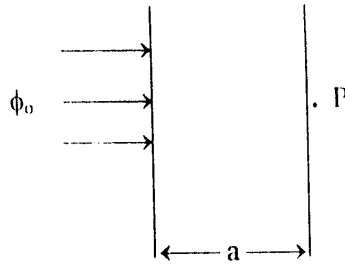


Fig. 1: Monodirectional beam of  $\gamma$ -rays incident on slab shield

the shield is different from  $\phi_0$  and the problem of determining the actual value of  $\dot{X}$  at P reduces to the problem of computing  $\phi$ .

It would be easy to compute  $\phi$  if over time a photon interacted with matter it disappeared, then  $\phi$  would be equal to the flux of uncollided  $\gamma$ -rays

$$\phi_u = \phi_0 e^{-\mu x} \quad (4)$$

where  $\mu$  is the total attenuation coefficient at the energy  $E_0$ . Unfortunately,  $\gamma$ -rays do not disappear at each interaction. In the Compton effect, for instance, they are merely scattered with a loss of energy, and even in the photoelectric effect and in pair production, although the incident photon is absorbed, X-rays are usually produced subsequent to the photo effect, and annihilation radiation inevitably follows after pair production. As a result a monoenergetic beam incident on a shield with energy  $E_0$  emerges from the shield with a continuous spectrum with sharp peak at  $E_0$  corresponds to the unscattered photons and is reduced in size over the peak by the exponential factor in Eq.(4). The continuous part of the spectrum is due for the most part to Compton scattered photons, with some contribution from photoelectric X-rays and annihilation radiation.

The exact calculation of a spectrum like that shown in Fig. 3 is very difficult and it has been carried out for a variety of shielding materials as a function of the incident  $\gamma$ -ray energy and shield thickness. The computed value of  $\phi_{(E)}$  were then used to compute the exposure rate from the formula :

$$\dot{X} = 0.0659 \int_0^{E_0} \phi_{(E)} E (\mu_a / l)^{air} dE \quad (5)$$



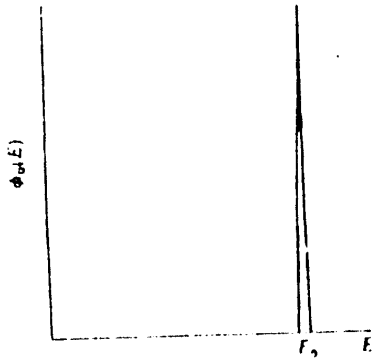


Fig. 2 Energy spectrum of incident  $\gamma$ -ray beam.

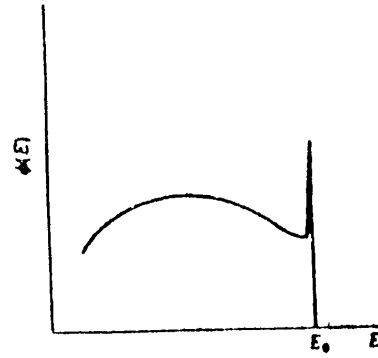


Fig. 3 Energy spectrum of  $\gamma$ -rays emerging from shield.

The results of these computations are written as :

$$\dot{X} = \dot{X}_0 B_m(\mu a) e^{-\mu a} \quad (6)$$

where  $\dot{X}_0$  is the exposure rate in the absence of the shield as given by Eq.(1),  $B_m(\mu a)$  is called the exposure buildup factor for a monodirectional beam and  $\mu$  is again the total attenuation coefficient at the energy  $E_0$ . Values of  $B_m$  are usually given in tables as a function of the incident energy for several materials.

Numerical values of  $B_m$  can be very large, which shows the importance of the buildup of scattered radiation in shielding calculations. With a water shield, for example, which is  $\mu a=10$  mean free paths thick at 2 Mev,  $B_m$  is approximately equal to 10. This means that if buildup were omitted from a calculation of the effectiveness of such a shield, the resulting exposure rate would be in error by a factor of 10. The buildup factor,

therefore, cannot be ignored. Since  $B_m$  is a continuous function of atomic number, values of  $B_m$  for materials not given in the table can be obtained by plotting  $B_m$  versus  $Z$  for the energy in question and interpolating from the curve.

According to Eq.(1)  $\dot{X}_0$  is proportional to  $\phi_0$ , and it is reasonable, by analogy, to write  $\dot{X}$  in the same form, namely

$$\dot{X} = c \phi_b \quad (7)$$

where  $c$  is again given by Eq.(3). The quantity  $\phi_b$  will be called the buildup flux and is clearly equal to that flux of monoenergetic  $\gamma$ -rays of energy  $E_0$  which gives the same exposure rate at P in Fig. 1 as the actual  $\gamma$ -ray flux at that point.

Introducing Eqs. (2) and (7) into Eq.(6) shows that

$$\phi_b = \phi_0 B_m(\mu a) e^{-\mu a} \quad (8)$$

or equivalently

$$\phi_b = \phi_u B_m(\mu a)$$

where  $\phi_u$  is the uncollided flux of Eq.(4).

The above discussion pertains exclusively to a monodirectional beam normally incident upon a slab shield, and the buildup factor  $B_m(\mu a)$  can be used only in problems of this type. Buildup factors have also been computed for other types of shielding problems. Consider, for instance, a point isotropic source emitting  $S$   $\gamma$ -rays surrounded by a spherical shield of radius

R. In this case, the exposure rate at a point on the surface of the shield is written as

$$\dot{X} = \dot{X}_0 B_p(\mu R) e^{-\mu R} \quad (10)$$

Here  $B_p(\mu R)$  is the point isotropic exposure buildup factor and  $\dot{X}_0$  is the exposure rate in the absence of the shield, specifically :

$$\dot{X}_0 = c \phi_0 \quad (11)$$

where

$$\phi_0 = \frac{S}{4\pi R^2} \quad (12)$$

is the flux from a bare point source. The uncollided flux in this problem is :

$$\phi_u = \frac{S}{4\pi R^2} e^{-\mu R} \quad (13)$$

and the buildup flux is :

$$\phi_b = \frac{S}{4\pi R^2} e^{-\mu R} B_p(\mu R) \quad (14)$$

Computed values of  $B_p$  are given in table for several materials used for shielding. It should be noted especially that  $B_p$  and  $B_m$  are entirely different functions, which must be used only in appropriate problems.

For computational purposes it is convenient to express the tabulated point buildup factor as a mathematical function, and several functions have

been developed. One of the most useful of these is the sum of exponentials, namely,

$$B_p = A_1 e^{-\alpha_1 r} + A_2 e^{-\alpha_2 r} = \sum A_n e^{-\alpha_n r} \quad (15)$$

where  $A_1$ ,  $A_2$ ,  $\alpha_1$  and  $\alpha_2$  are functions of energy. Eq.(16) is known as the Taylor form of the buildup factor, and it is sufficiently accurate to be used in many practical shielding problems. As  $r$  goes to zero,  $B_p$  must approach unity, since can be no buildup of scattered radiation in a shield of zero thickness. It follows that :

$$A_1 + A_2 = 1 \quad (16)$$

Thus it is sufficient to specify  $A_1$ , which here in after will be denoted as  $A$ ; then  $A_2$  is equal to  $1-A$ . Values of  $A$ ,  $\alpha_1$  and  $\alpha_2$  are given in tables.

## 2. Infinite Planar and Disk Sources :

Consider an infinite planar source emitting  $S$   $\gamma$ -rays/cm<sup>2</sup>.sec isotropically from its surface, which is located at the back of a shield of thickness  $a$  as shown in Fig. 4. The sources located on the differential ring of width  $dz$  at  $z$  emit  $2\pi S z dz$   $\gamma$ -rays/sec and make a contribution to the uncollided flux at  $P$  which is equal to :

$$d\phi_u = \frac{2\pi S z dz e^{-\mu r}}{4\pi r^2} = \frac{S z e^{-\mu r} dz}{2r^2} \quad (17)$$

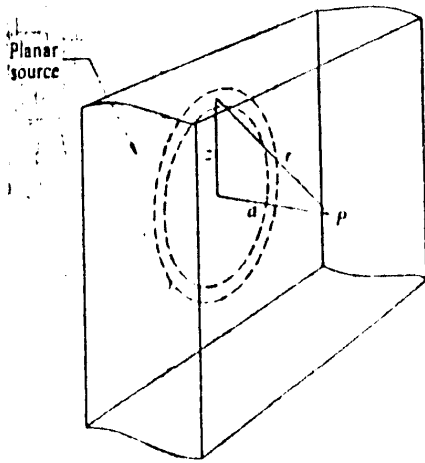


Fig. 4 Isotropic planar source behind slab shield.

The total flux at P is then :

$$\phi_u = \frac{S}{2} \int_0^{\infty} \frac{ze^{-\mu r}}{r^2} dz \quad (18)$$

It is convenient at this point to change the integration variable from  $z$  to  $r$ .

Then, since  $r^2 = a^2 + z^2$  and  $rdr = zdz$ , it follows that :

$$\phi_u = \frac{S}{2} \int_a^{\infty} \frac{e^{-\mu r}}{r} dr \quad (19)$$

Finally, letting  $\mu r = t$ , the integral may be put in the form :

$$\phi_u = \frac{S}{2} \int_{\mu a}^{\infty} \frac{e^{-t}}{t} dt \quad (20)$$

The integral in Eq.(20) cannot be evaluated analytically, but can be expressed in terms of one of the  $E_n$  functions defined by the integral :

$$E_n(x) = x^{n-1} \int_x^{\infty} \frac{e^{-t}}{t} dt \quad (21)$$

where  $n$  is an integer. Comparing Eqs.(20) and (21) one gets :

$$\phi_u = \frac{S}{2} E_1(\mu a) \quad (22)$$

The function  $E_1(x)$  occurs in many shielding problems. Fig.5 shows this function, together with  $E_2(x)$  for values of  $x$  up to  $x=14$ . For larger values of  $x$ ,  $E_n(x)$  can be computed with sufficient accuracy for most purposes from the following approximate formula :

$$E_n(x) \cong e^{-x} \left[ \frac{1}{x+n} + \frac{n}{(x+n)^3} \right] \quad (23)$$

To return to the shielded planar source, it is possible to calculate the buildup flux by noting that the contribution to  $\phi_b$  due to the differential ring at  $z$  is :

$$d\phi_b = B_p(\mu r) d\phi_u \quad (24)$$

so that :

$$d\phi_b = \frac{SB_p(\mu r)ze^{-\mu r}dz}{2r^2}$$

The total buildup flux is therefore :

$$\phi_b = \frac{S}{2} \int_0^{\infty} \frac{B_p(\mu r)ze^{-\mu r}dz}{r^2}$$

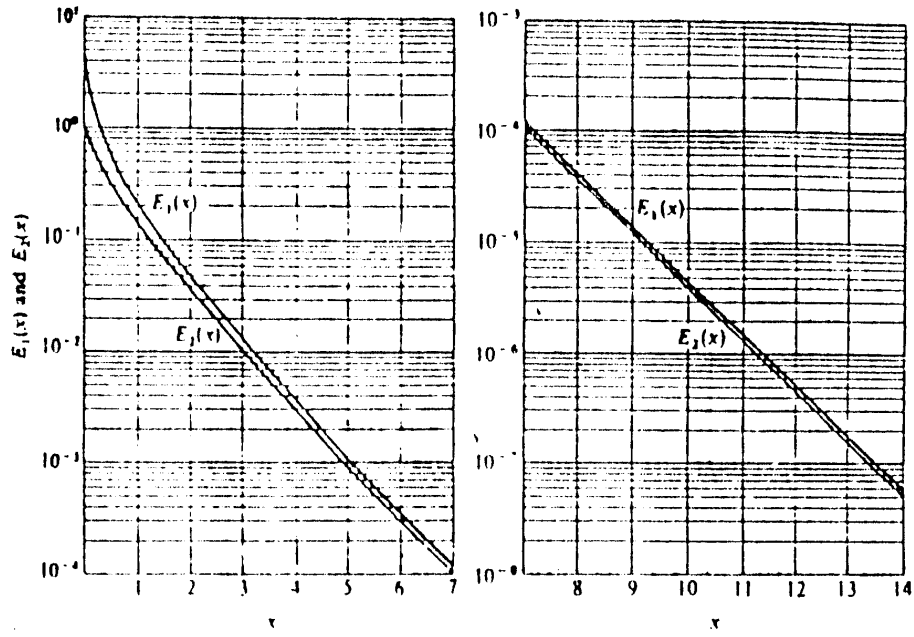


Fig. 5 The functions  $E_1(x)$  and  $E_2(x)$ .

Introducing  $B_p(\mu r)$  from Eq.(15) gives :

$$\phi_b = \frac{S}{2} \sum A_n \int_0^{\infty} \frac{z e^{-(1+\alpha_n)\mu r}}{r^2} dz \quad (25)$$

The integral can be transformed as in the uncollided case and written in terms of the  $E_1$  function. The final result is :

$$\phi_b = \frac{S}{2} \sum A_n E_1[(1+\alpha_n)\mu a] \quad (26)$$

In case of disk source of radius  $R$  emitting  $S$  photons/cm<sup>2</sup>.sec shielded by a slab of thickness  $a$ , the uncollided and buildup fluxes at the point  $P$  on the

axis of the disk can be computed as in the infinite planar case by integrating the contributions from differential rings. Thus  $\phi_u$  is given by Eq.(18) but with an upper integration limit of  $z = R$ . In a similar way one can calculate the buildup flux.

### 3. The Line Source :

Figure 6 shows a line source of length  $l$  surrounded by a cylindrical shield of radius  $R$ . If there are  $S$   $\gamma$ -rays emitted isotropically per unit length of the source, then the uncollided flux at  $P$  from sources in  $dz$  is :

$$d\phi_u = \frac{S e^{-\mu r} dz}{4\pi r^2} \quad (27)$$

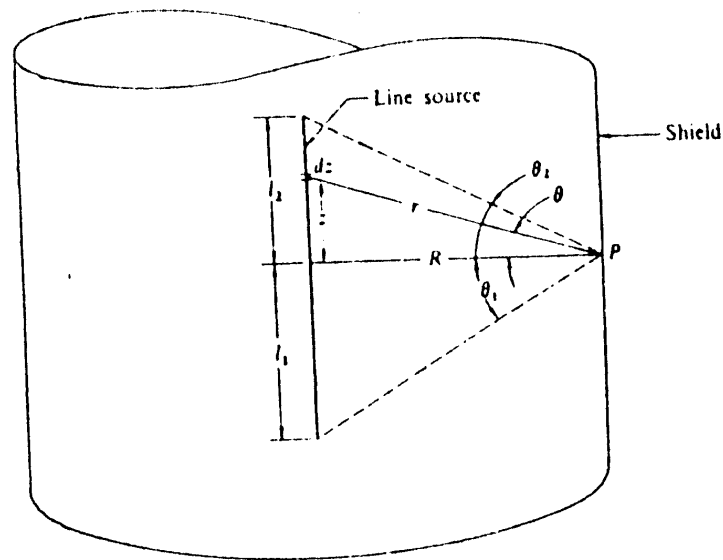


Fig. 6 Isotropic line source imbedded in a cylindrical shield.



and  $\phi_u$  is :

$$\phi_u = \frac{S}{4\pi} \int_{-l_1}^{l_2} \frac{e^{-\mu r}}{r^2} dz \quad (28)$$

where  $l_1$  and  $l_2$  are the lower and upper portions of  $l$ , respectively.

It is convenient to change the integration variable in Eq.(28) from  $z$  to the angle  $\theta$ . Then since

$$r = R \sec\theta$$

$$z = R \tan\theta$$

$$dz = R \sec^2\theta d\theta,$$

The uncollided flux becomes :

$$\phi_u = \frac{S}{4\pi R} \int_{-\theta_1}^{\theta_2} e^{-\mu R \sec\theta} d\theta \quad (29)$$

The integral in Eq.(29) cannot be evaluated analytically but it can be expressed in terms of the Sievert integral function. This is a function of two variables which is defined as :

$$F(0, x) = \int_0^{\theta} e^{-x \sec\theta} d\theta \quad (30)$$

where  $\theta$  is restricted to values less than  $\pi/2$ .  $F(0, x)$  is found to decrease more or less exponentially with  $x$  and increase with  $\theta$ . For large value of  $\theta$  (near  $\pi/2$ ) and  $x$ ,  $F(0, x)$  can be computed from the formula :

$$F(0, x) \cong \sqrt{\frac{\pi}{2x}} e^{-x} \left(1 - \frac{5}{8x}\right) \quad (31)$$

Since  $\sec(-0) = \sec 0$  the integrand in Eq.(30) is an even function of  $0$ , and since the integral of an even function is always an odd function it follows that :

$$F(-0, x) = -F(0, x) \quad (32)$$

In view of these properties of  $F(0, x)$ , Eq.(29) for the uncollided flux at P can be written as :

$$\phi_u = \frac{S}{4\pi R} [F(0_1, \mu R) + F(0_2, \mu R)] \quad (32)$$

The calculation of the buildup flux is essentially the same in this problem as in the slab and disc problems, thus  $\phi_b$  is given by :

$$\begin{aligned} \phi_b &= \frac{S}{4\pi R} \sum A_n \int_{-0_1}^{0_2} e^{-(1+\alpha_n)\mu R \sec 0} d0 \\ &= \frac{S}{4\pi R} \sum A_n \{F[0_1, (1+\alpha_n)\mu R] + F[0_2, (1+\alpha_n)\mu R]\} \end{aligned} \quad (33)$$

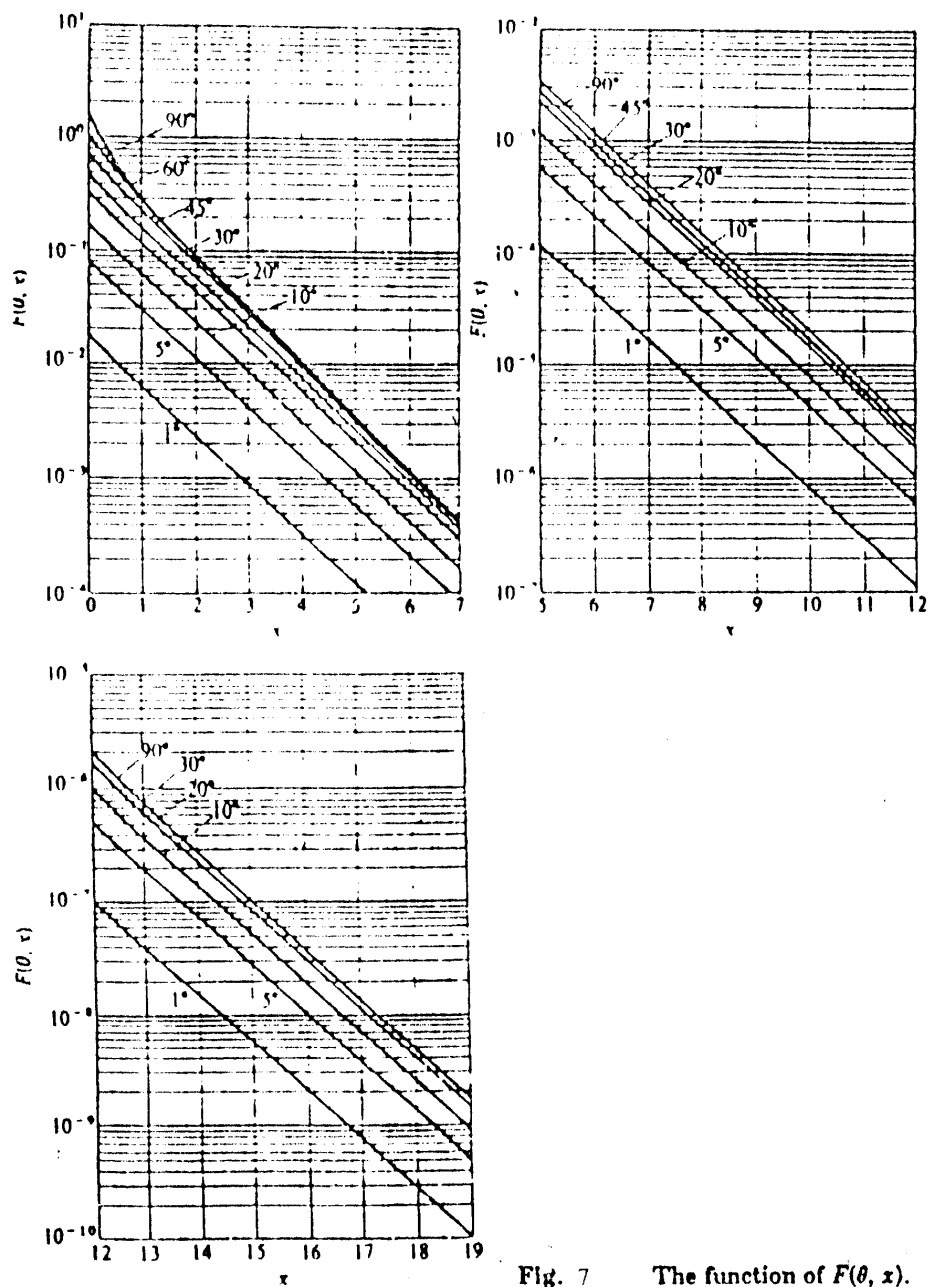


Fig. 7 The function of  $F(\theta, x)$ .

#### 4. Internal Sources :

Circumstances often arise in which  $\gamma$ -ray sources are distributed in the interior of attenuating media. This occurs, for example, in shields for reactors. Energetic fission neutrons inelastically scattered within the shield give rise to sources of inelastic  $\gamma$ -rays, while thermalized neutrons undergo radiative capture and produce capture  $\gamma$ -rays. Reactor shields must include provisions for the shielding against such secondary  $\gamma$ -rays. Consider a slab of thickness  $a$  containing sources of  $\gamma$ -rays emitting  $S(x)$  photons/cm<sup>3</sup>.sec at the distance  $x$  as shown in Fig. 8. It is required to find the exposure rate at P. The uncollided flux at P from the planar source of thickness  $dx$  at  $x$  is given by :

$$d\phi_u = \frac{S(x)}{2} E[\mu(a-x)] dx \quad (34)$$

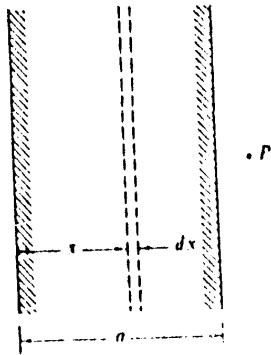


Fig. 8 Slab containing  $\gamma$ -ray sources.

and the total flux is then :

$$\phi_u = \frac{1}{2} \int_0^a S(x) E_1[\mu(a-x)] dx \quad (35)$$

As a special case, suppose that  $S(x) = S$  is a constant then Eq.(35) becomes

$$\phi_u = \frac{S}{2} \int_0^a E_1[\mu(a-x)] dx \quad (36)$$

To evaluate this integral, let  $t = \mu(a-x)$ , so that  $dx = -dt/\mu$ . Eq.(36) then becomes :

$$\phi_u = \frac{S}{2\mu} \int_0^{\mu a} E_1(t) dt \quad (37)$$

In view of this identity

$$\int_0^x E_1(t) dt = 1 - E_2(x) ,$$

Eq.(37) reduces to :

$$\phi_u = \frac{S}{2\mu} [1 - E_2(\mu a)] \quad (38)$$

The buildup flux, computed in the usual way, is

$$\phi_b = \frac{S}{2\mu} \sum \Lambda_n \{1 - E_2[(1 + \alpha_n)\mu a] / (1 + \alpha_n)\} \quad (39)$$

A source distribution that more realistically reproduces the  $\gamma$ -ray sources in a shield where the neutron flux decreases approximately exponentially, is the function :

$$S(x) = Se^{-kx}$$

where  $k$  is a constant.

For an arbitrary source distribution  $S(\mathbf{r}')$  in a volume of an arbitrary shape, the  $\gamma$ -ray flux at the point  $\mathbf{r}$  on the surface can be found by evaluating the integral

$$\phi_u(\mathbf{r}) = \frac{1}{4\pi} \int \frac{S(\mathbf{r}') e^{-\mu|\mathbf{r}-\mathbf{r}'|}}{|\mathbf{r}-\mathbf{r}'|^2} d\mathbf{v}'$$

over the source volume. This can be done either on a computer or by a hand calculation by dividing the source volume into convenient subvolumes  $V_i$ , which need not be the same size. The number of  $\gamma$ -rays  $S_i$  emitted from  $V_i$  is then computed from the source function. The contributions to the flux from each volume are then added, taking  $S_i$  to be a point source. The result for the buildup flux is :

$$\phi_b = \frac{1}{4\pi} \sum \frac{S_i B_p(\mu r_i)}{r_i^2} e^{-\mu r_i}$$

where  $r_i$  is the distance from some point in  $V_i$  to the observation point.

### References :

- [1] Glasstone S. and A. Sesoske, Nuclear Reactor Engineering, D. Van Nostrand Co., Inc., Princeton, N.J., 1963.
- [2] Lamarsh, J. R., Introduction to Nuclear Engineering, Reading Mass, Addison Wesley, 1983.

## WATER TREATMENT IN NUCLEAR PLANTS

Prof. M. A. Marawan.

### INTRODUCTION

Reactor Dept.

Water in a steam-water cycle of a conventional power plant utility and a nuclear plant is treated, before its introduction into the utility. Moreover this Working fluid is continuously monitored during operation.

Water quality requirement differ with each power cycle. For example, in conventional steam - water cycles, water quality requirement is less stringent in boilers with steam drum, than the once through super critical boilers.

The reason for this, is that, water drums act as mechanical barriers to the contaminants formed in the water during its cycle through the plant. On the other hand super critical boilers don't have such mechanical barriers.

These contaminants are mainly corrosion products which could accumulate on tubes of the boiler, causing the concentration of corrosive materials e.g. Sodium hydroxide, which may cause tube failure, by means of a mechanism called "ductile gouging".

In nuclear plants, the contamination of water used as a coolant and moderator, with corrosion products and water soluble material are subjected to high neutron flux. These contaminants are transformed to longlived isotopes which emit radiations. These radiations have dangerous effects on the operation and maintenance processes.

Therefore special measures are taken to sustain the water quality required for prolonged operation of the nuclear plant. These measures are implemented through some major steps

- A- Selection of high corrosion resistance materials
- B- Ion exchange polishers for the removal of corrosion and water soluble products, from the circulating water.

- C- PH is an important factor in minimizing corrosion of metals
- D- Water oxygen content has a great bearing on metal corrosion

The permissible residue limit depend on the pressure and temperature of operation.

In the next paragraph we will discuss the nature and design of the equipment encountered in feed and working water treatment in nuclear facilities .

### WATER DEMINILIZERS

Ion exchanger removes unwanted ions, from raw water , by transforming them to a solid material , while giving back an equivalent number of a desirable species stored on the ion exchange skeleton.

The ion exchanger has a limited capacity for storage of ions on its skeleton , called its exchange capacity .

Because of this , the ion exchanger eventually becomes depleted of its desirable ions, and becomes saturated with unwanted ions. Consequently , it is washed with a strong regenerating solution , containing the desirable species of ions. These replace the accumulated undesirable ions , returning the exchange material to a usable condition . This operation is a cyclic chemical process. the complete cycle usually includes backwashing, regeneration , rinsing and then service.

Ion exchangers are related to polyelectrolytes used for coagulation and flocculation , but deliberately made so high in molecular weight as to be essentially insoluble.

Exchangers with negatively charged sites are cation exchangers because they take up positively charged ions . Anion exchanger have positively charged sites and , consequently , take up negative ions .

The plastic structure is porous and permeable so the entire ion exchange particle participate in the exchange process.



## FEED WATER TREATMENT

Feed water for a high pressure conventional utility is of the same quality as a nuclear plant .

There are numerous possibilities for the design engineer in putting together individual units , utilized in water treatment , to suit the type of raw water being processed , to give the quality demanded by the process. Some options are illustrated in Fig (1).

Some general rules for the selection of individual components of a demineralizing system, based chiefly on economics of operation are given in Table' (1).

The ratio of feed water to that of the working fluid , in a conventional or nuclear utility is relatively small . Therefore , special measures are taken to continually keep the working fluid free from contaminations , which could have a detrimental effect on the safety of the process and personnel.

## WORKING FLUID TREATMENT

For conventional power cycle condensate polishers, are generally located between the condenser and the first feed water heater as shown in Fig (2) .

A polisher is generally a mixed bed ionizer, and in some cases a cation ion exchanger unit is utilized instead .

Nuclear pressurized water reactors ( PWR ) has two major water systems Fig (3).

- 1- The primary loop , or reactor coolant system
- 2- The secondary loop , or steam generator - turbine cycle.

High purity must be maintained in the primary loop to minimize fouling of the reactor , and to avoid contaminants that could create undesirable radioactive isotopes under neutron flux.

PH control in the PWR is done by the addition of a chemical such as lithium hydroxide , which does not leave any solid residue

To suppress oxygen generation and to scavenge oxygen entering the system, which may initiate corrosion, by the addition of hydrogen gas.

Primary loop water purity is usually maintained by continuously circulating a portion of the cooling water through a polisher as shown in Fig (3).

In the boiling water reactor ( BWR ) Fig (4), boiling of water occurs in the reactor itself in contrast with the ( PWR ). This is because, the cycling water serves as the working fluid, the reactor coolant, and reactor moderator.

An important aspect of BWR operation is the effect on the working fluid by the direct exposure to nuclear radiation. Some of the water is decomposed into hydrogen and oxygen. In contrast to PWR hydrogen cannot be injected because of the need for continuous removal of all non condensable gases at the condenser to maintain the vacuum required for turbine efficiency.

Thus, steam produced by a BWR contains high concentrations of oxygen, an important factor in the corrosion process.

Additives, for pH control and oxygen scavenging such as hydrazine are not permissible in BWR cycles because they are subject to nuclear decomposition.

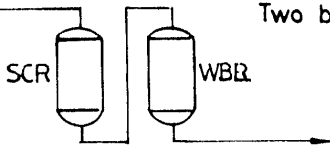
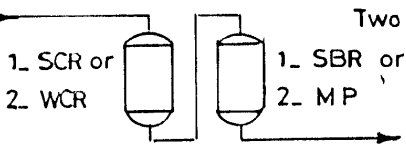
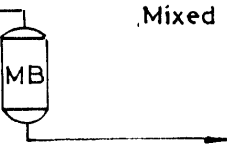
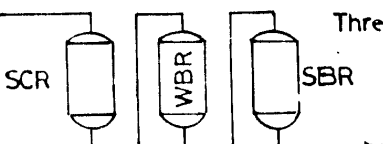
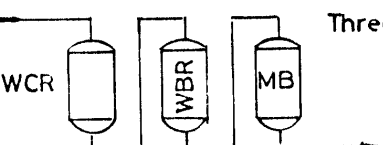
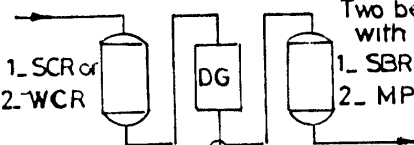
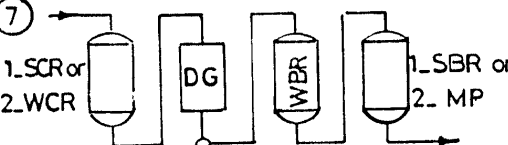
Thus, corrosion control relies primarily on the corrosion resistant materials. Full flow condensate in deminilization is then employed, to maintain cycle water purity at standards established by the manufacturer.

The cycle water treatment in the Egyptian research reactor is kept clean by passing a portion of the cyclic water through a mixed bed polisher. This portion is 1 % of the recycling water which has a flow rate of 900 m<sup>3</sup> / hr.

	Amount of impurity to be removed mg/L			Resins required			Units to be used				
	FMA	CO <sub>2</sub>	SiO <sub>2</sub>	C	WB	SB		C	DG	A	MB
1	Any	None	None	x	x	—	1 2	x —	— —	x —	— x
2	Any	Any	None	x	x	—	1 2	x —	x x	x —	— x
3	Any	Any	Any	x	—	x	1 2	x —	— —	x —	— x
4	A	0-50	Any	x	x	x	1 2	x —	— —	x —	— x
5	0-100	Over 100	Any	x	—	x	1 2	x x	x x	x —	— x
6	Over 200	Over 100	Any	x	x	x	1 2	x x	x x	x x	— x

C: cation   A: anion   DG: degasifier   MB: mixed bed   WB: weak base  
SB: strong base   FMA: free mineral acidity (SO<sub>4</sub> + Cl + NO<sub>3</sub>)

Fig (1)

Scheme	
①	Two bed 
②	Two bed 
③	Mixed bed 
④	Three bed 
⑤	Three bed 
⑥	Two bed with DG 
⑦	Two bed with DG 

SCR: Strong cation resin  
SBR: Strong base resin  
DG: Degasifier MB: mixed bed  
WCR: Weak cation resin  
WBR: Weak base resin

Table (1)

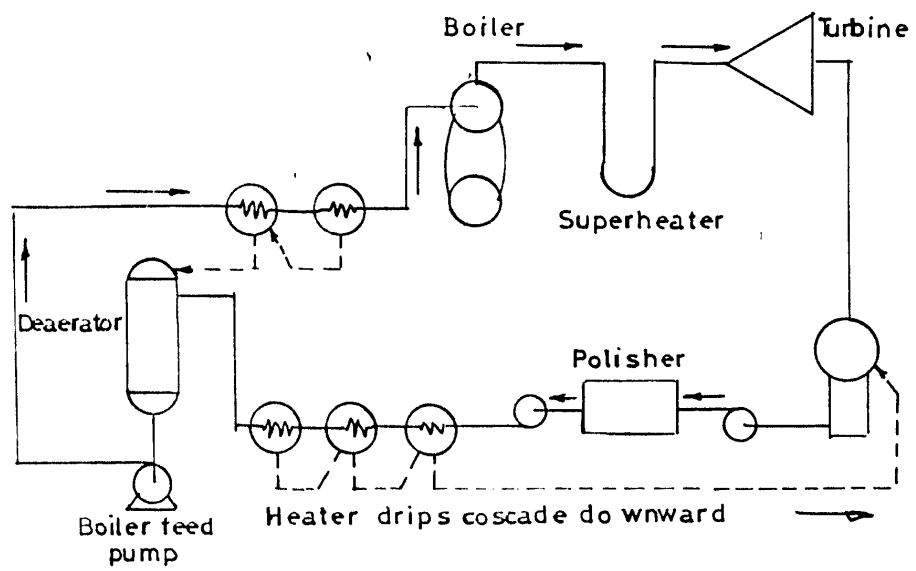
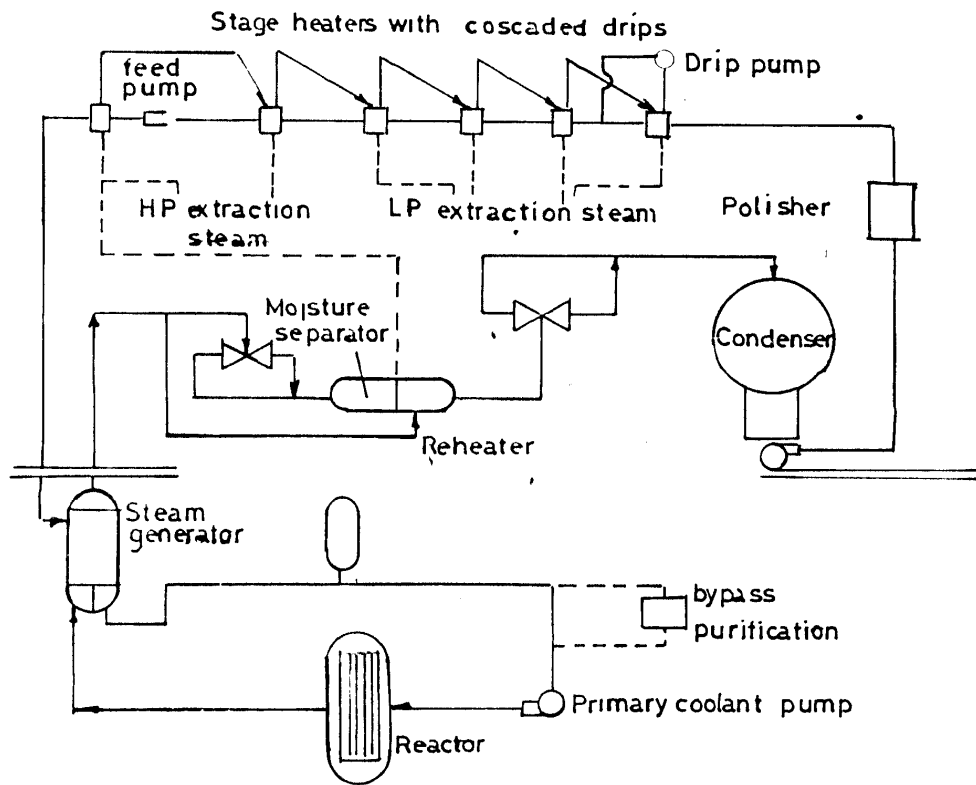
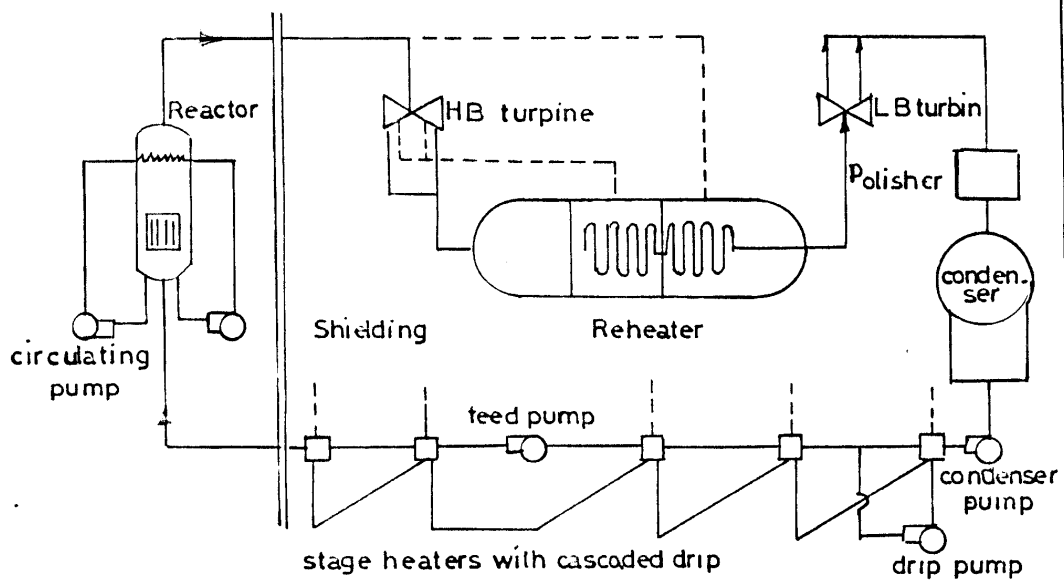


Fig.( 2)



Fig( 3 )



Fig( 4 )

## Acquaintance With IAEA Safeguards System

M.A. Sultan

Reactors Department, Inshass

---

### Objectives of Nuclear Safeguards

- Prevention of theft of Nuclear Material (U,Pu,Th)
- Detection of theft
- Recovery of stolen materials
- Response of threats of nuclear violence .

### **International Co-operation For Implementation Of Safeguards**

-Bilateral co-operation .This took place since the early fiftieth between the US and many countries to extend nuclear co-operation to them , based on the US Atomic Energy Act of 1954.

-Regional co-operation .An example is the co-operation between European Economic Community . The Euratom co-operation started in 1955 between six countries and later joined by the UK in 1973.

-International Co-operation : Proposal by President Eisenhower " ATOMS FOR PEACE "in 1953 . triggered this international cooperation.. It became successful in 1957 when the International Atomic Energy (IAEA) was created .

### **Development of IAEA Safeguards System**

- Started by a simple system of accountancy at the IAEA division of safeguards.
- In 1961 the first IAEA Safeguards Document was issued (INFCIRC/26). It concerns only reactors with power less than 100 MW thermal .
- In 1962 the IAEA became a third party to the US and Euratom .

2

In 1964 the IAEA Safeguards document ( INFCIRC /26/Add1) was issued to incorporate safeguarding of nuclear reactor with power more than 100 MW thermal .

-In 1965 the IAEA safeguards document INFCIRC/66 was issued as a modification to previous documents .

-In 1966, the IAEA safeguards document INFCIRC/66/Rev.1 was issued to include reprocessing plants under IAEA safeguards .

-In 1968 ,the IAEA safeguards document INFCIRC/66/Rev.2 was issued to include also conversion and fuel fabrication plants .

-In March 1970 the treaty on Non proliferation of nuclear weapons (NPT) entered into force after being signed by countries. The IAEA started implementing safeguards under NPT .

-It is important to note that the objective IAEA safeguards under NPT "is the timely detection of significant quantities of nuclear material..... and deterrence of such diversion through the risk of early detection ".

-In IAEA issued for the implementation of safeguards under NPT, the document (INFCIRC/153) under the name .

"the Structure and content of Agreements Between Agency and states in Connection with the treaty on

### **Requirements for Implementation of safeguards**

-Initiation of a National System of Accountancy in countries party to N.P.T Treaty.(par.3 of NPT).

Initiation of Physical protection and strict security System around nuclear facilities.

### **Methods for implementation of NPT safeguards**

- Containment.

- Surveillance

- Accountancy

"The Accountancy is defined as the activities carried out to establish the quantities of nuclear material present within defined environments and changes in there quantities taking place within defined periods of time.



# *Legal Basis Of NPT Accounting*

- INFCIRC 153
- Subsidiary Arrangements
- Code 10

## INFCIRC 153

'The Structure and Content of Agreements between the Agency and States Required in Connection with the Treaty on the Non-Proliferation of Nuclear Weapons'

This material is used as the basis for negotiating safeguards agreements under the NPT.

## Subsidiary Arrangements (Par. 39).

### - General part.

A set of technical and administrative procedures designed primarily to implement the safeguards procedures laid down in safeguards agreements.

### - Facility Attachment - a part of the Subsidiary Arrangements

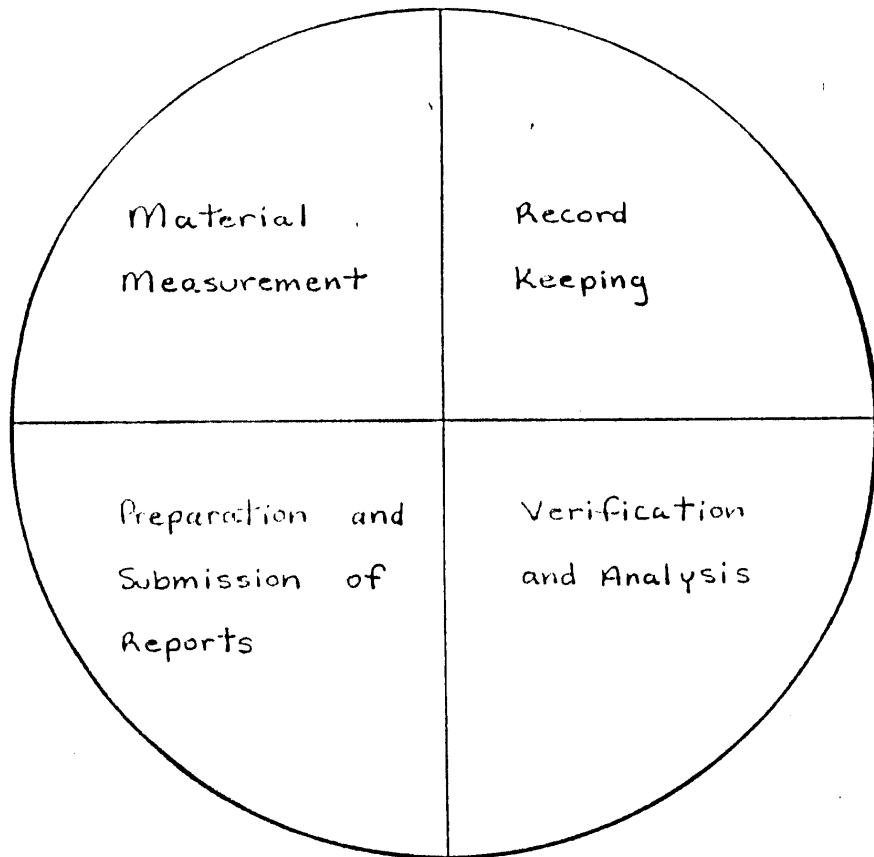
- Description of the facility
- Provisions for the submission of changes
- Accountancy measures for the facility
- etc

## Code 10

Detailed description of providing data to the Agency using forms designed to:

- Reflect all the relevant requirements of the Agency
- Lend themselves to data processing techniques

## NPT Accounting (in MBAs.)



## Records System

### 1) Accounting Records for MBAs

- All inventory changes
- All measurements at key measurement points for physical inventory taking.
- All adjustments and corrections associated with inventory changes. (book & physical inventories)

### 2) Operating Records

- Data from : calibrations, instruments, sampling, analysis.
- Actions taken for determination of physical inventory to ensure that they are correct.
- The cause of any accidental losses in nuclear materials.

## Required Reporting under NPT

### \* Inventory Change Report (ICR)

' Showing changes in the inventory of nuclear material . . . specifying identification and batch data for each batch of nuclear material, date of the change, the type of change and the sending and receiving MBR'

### \* Material Balance Report (MBR)

' Showing the material balance based on a physical inventory of nuclear material actually present in the MBR'

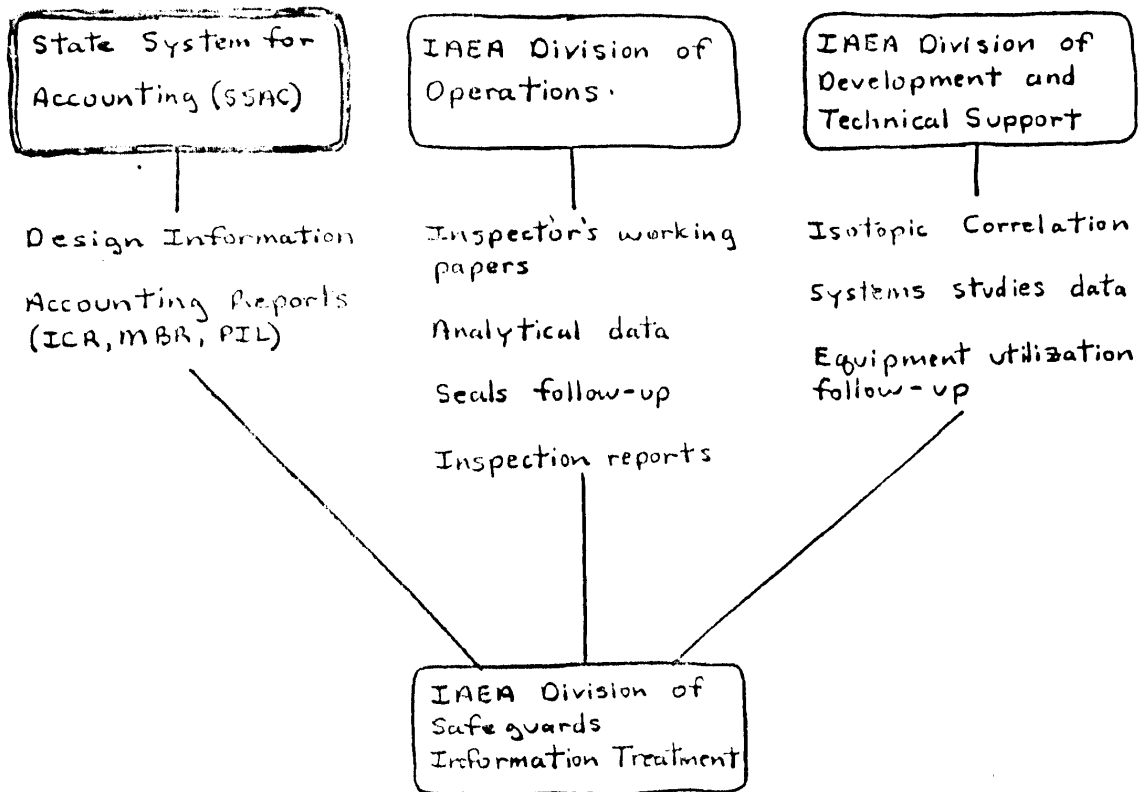
### \* Physical Inventory Listing (PIL)

' Listing of all batches and specifying material identification and batch data for each batch'

\* Design Information (Arts & Art 46)

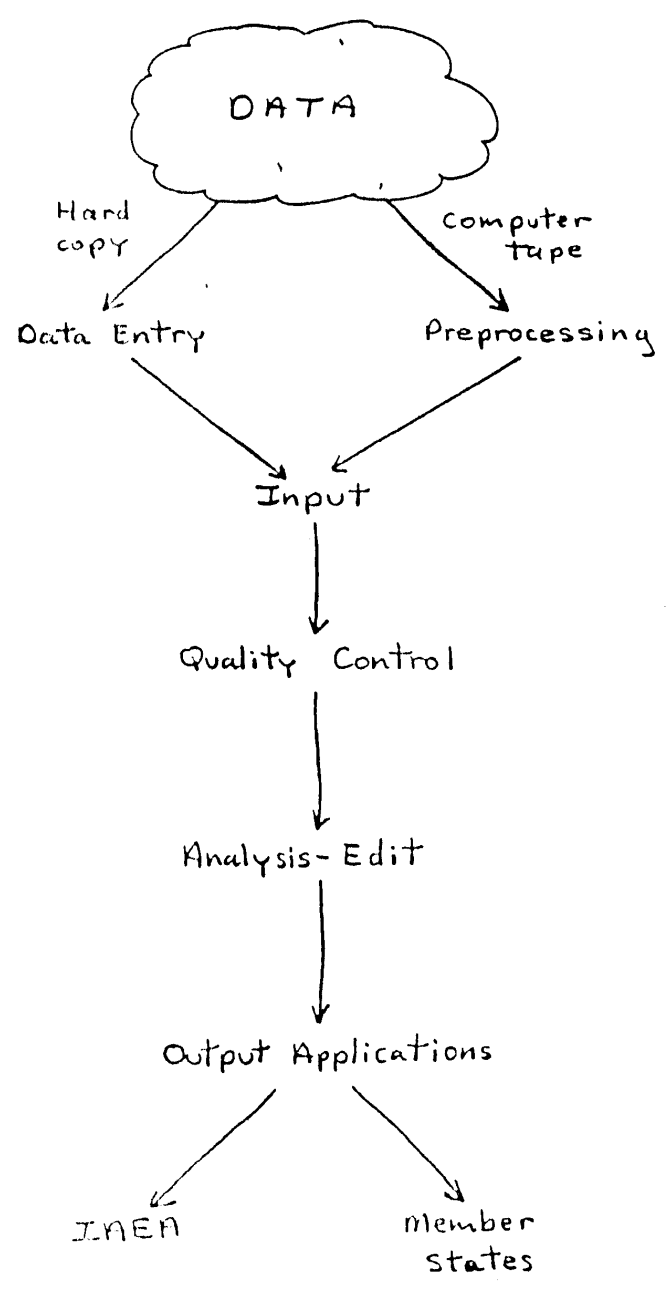
'Information concerning nuclear material subject to safeguards under the agreement and the features of facilities relevant to safeguarding such material'. It defines MBA & KMP.

## Sources of Information

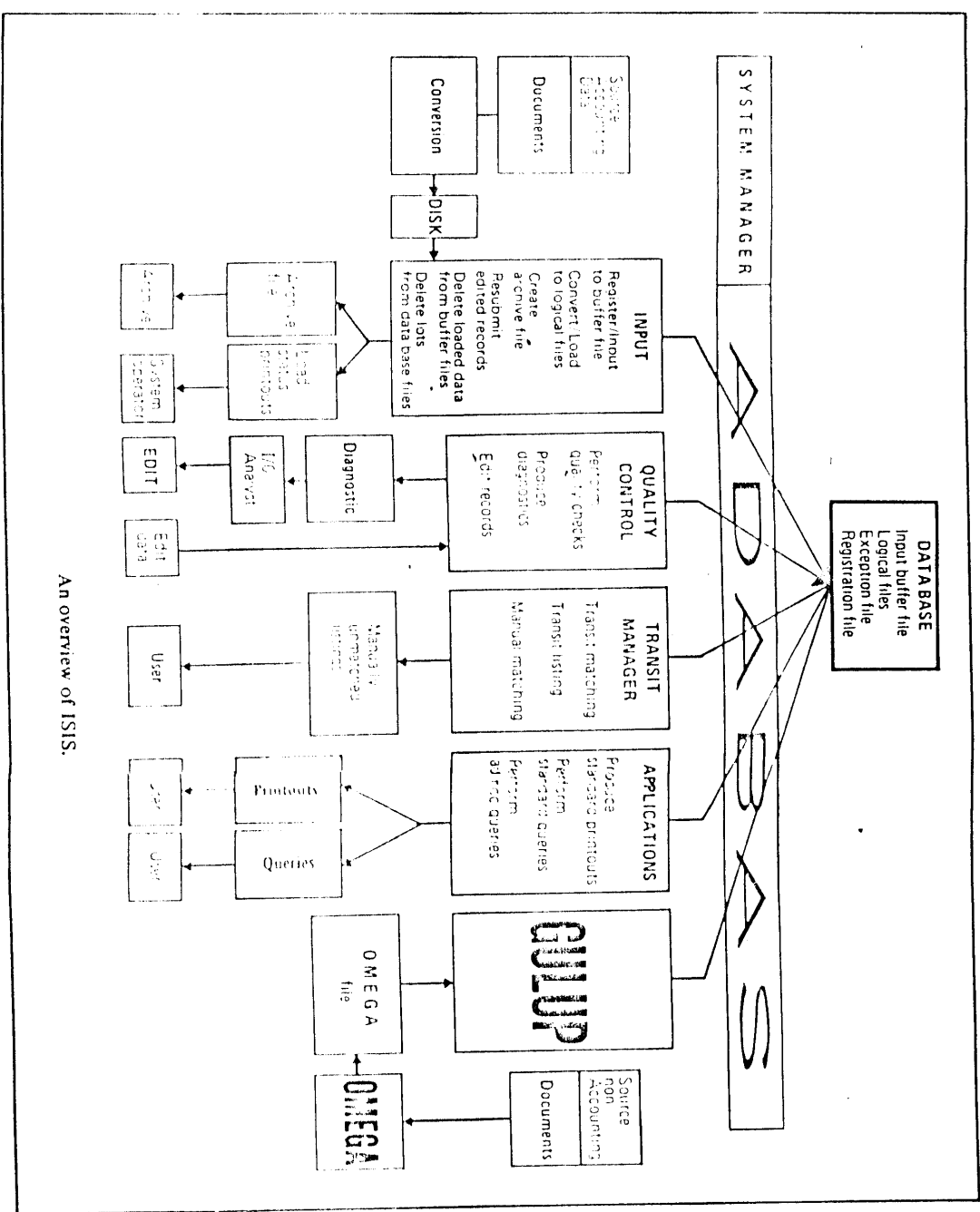


# International Safeguards Information System (ISIS)

## Processing of State Data







An overview of ISIS.

The IAEA conducts three types of inspection: ad hoc, routine, and special. The greater part of the inspection effort is made on routine inspections, which may include the following activities:

- Examining the records kept at a facility to establish the book inventory of nuclear material present and its flow through the facility;
- Comparing these records with shipping documents, facility operating records, and with the state's reports to the Agency to establish that shipments and receipts are consistent with each other and with the records of companion facilities;
- Verifying the stated nuclear material inventory, in many instances by statistical sampling and non-destructive analysis (NDA);
- Confirming that previously verified material remains undisturbed, by installing and servicing containment and surveillance devices.

# Experience Gained in Refurbishing of the ET-RR-1 Research Reactor in Egypt

M.S.Khattab F.H.Dimitri M.K.Shaat  
Reactor Department, Nuclear Research Centre  
Atomic Energy Authority, Cairo, Egypt.

## Abstract

The Egyptian first research reactor is a WWR type reactor that went critical in 1961. Around this reactor several labs have been created. Scientific research in different fields assisting reactor operation has been done. Through these activities, development of man power and training in the relevant fields have been established. This paper describes the in-service inspection program and the rehabilitation of the control, process measuring and radiation monitoring equipments, as well as the computerized safety logic and signaling systems. Current problems and future plan for improving the safety of systems are discussed.

## Introduction

Egypt has successfully carried out a program of rehabilitation to Inshass reactor, ET-RR-1. Through IAEA technical assistance projects as follows:  
Modernization of radiation monitoring equipments, EGY/09/15/1987.  
Modernization of process measuring system. EGY/04/28/1989 [1]  
Installation of Computerized Safety Logic and signaling systems, EGY/09/025/1993.  
The equipments of these projects were supplied from Hungary. Modernization of nuclear devices, safety and control instruments were early carried out in 1984. The equipments were supplied from Germany. [2].  
In-Service Inspection Program was arranged through the IAEA technical assistance project EGY/09/024/1989 to verify the state of reactor components particularly those which have influence on safety. The work was bounded by the equipments of the primary cooling system inside the pump room.  
The major inspection was carried out in December 1992 in collaboration with Petersburg Nuclear Physics Institute (PNPI). The work included reactor core, vessels, horizontal channels and spent fuel storage tank. Results revealed from this inspection are very important in deciding on the possibility of raising the power of the reactor.

### In-Service Inspection of ET-RR-1 Reactor

The ET-RR-1 reactor was designed and constructed basically with materials and components from Russia. By the time of design & construction there had been no sufficient experience to give reliable prediction on expected life time of the mechanical system of the reactor (tanks, valves, pumps, cooling system, etc...). In the meantime, during the life time of the reactor aggressive environments and operating conditions caused degradation of the materials and systems below their initial specifications.

This conformed what may be called the current reactor problems which are mainly associated with, [3], [4]:

- Pitting and crack corrosion near the weld joints of the ion exchange vessel, Fig. 1.
- Obsolescent valves of the drainage system.
- Obsolescent internal structure of the cooling tower.
- Limited capacity of the spent fuel storage tank, etc...

An In-Service Inspection (ISI) of the reactor internals mechanical parts was therefore, necessary to be carried out for speculation on these current problems.

The ISI Program was carried out on two stages; the first one was in collaboration with the IAEA in December 1989, Figs. 2-5 and the second one was the major inspection carried out in collaboration with Petersburg Nuclear Physics Institute (PNPI), in September, 1992, Figs. 6-9, [5].

The main Objectives of the ISI Program were:

- a- To verify the state of reactor components. This verification reveals and identifies the character of imperfections-manufacture or inservice imperfections; determines the form, localization, orientation, distribution and the individual or accumulated dimensions of the relevant imperfections.
- b- To evaluate the defects revealed on the basis of existing standards.
- c- To assess the significance of the existing defects for further operation of the reactor.
- d- To evaluate the ISI results as a first step towards postulation of acceptance criteria and suggestion of a program for further ISI activities.

The program of the ISI of ET-RR-1 reactor comprises the following:

- a- Plan of The ISI Program

The program comprises the following investigations:

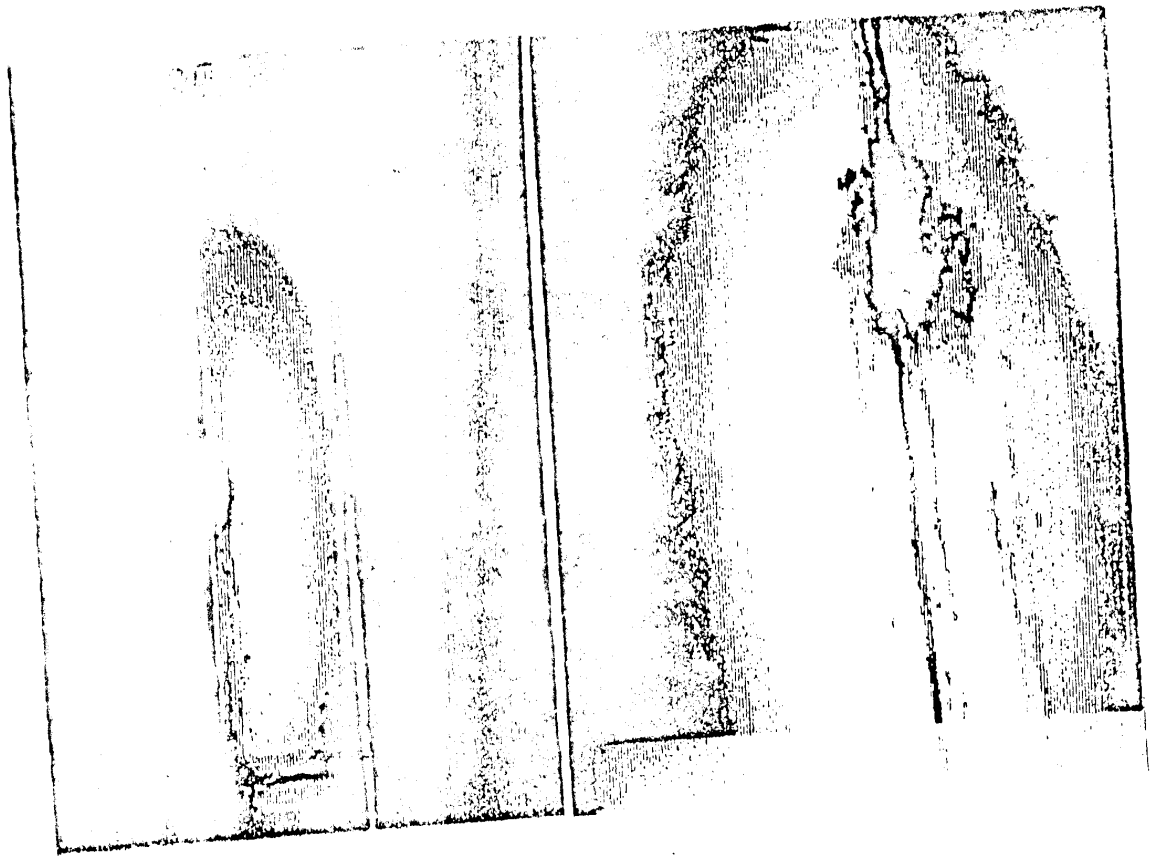
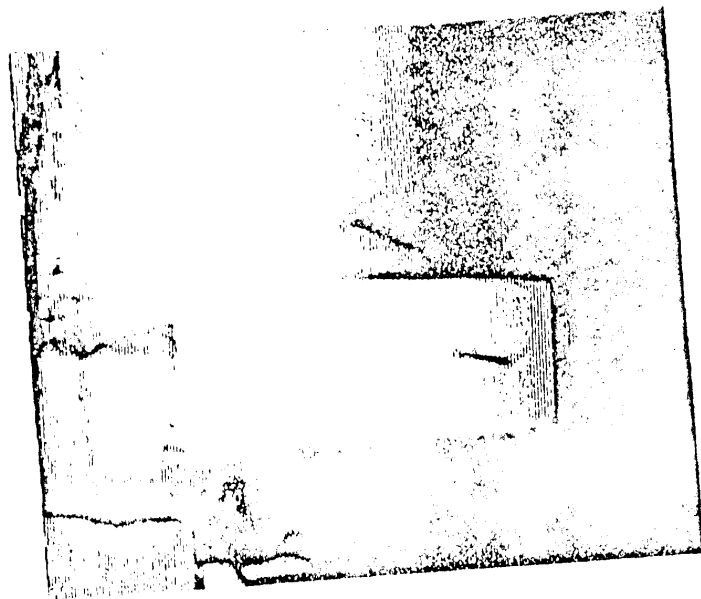


Fig.1 Pitting Corrosion



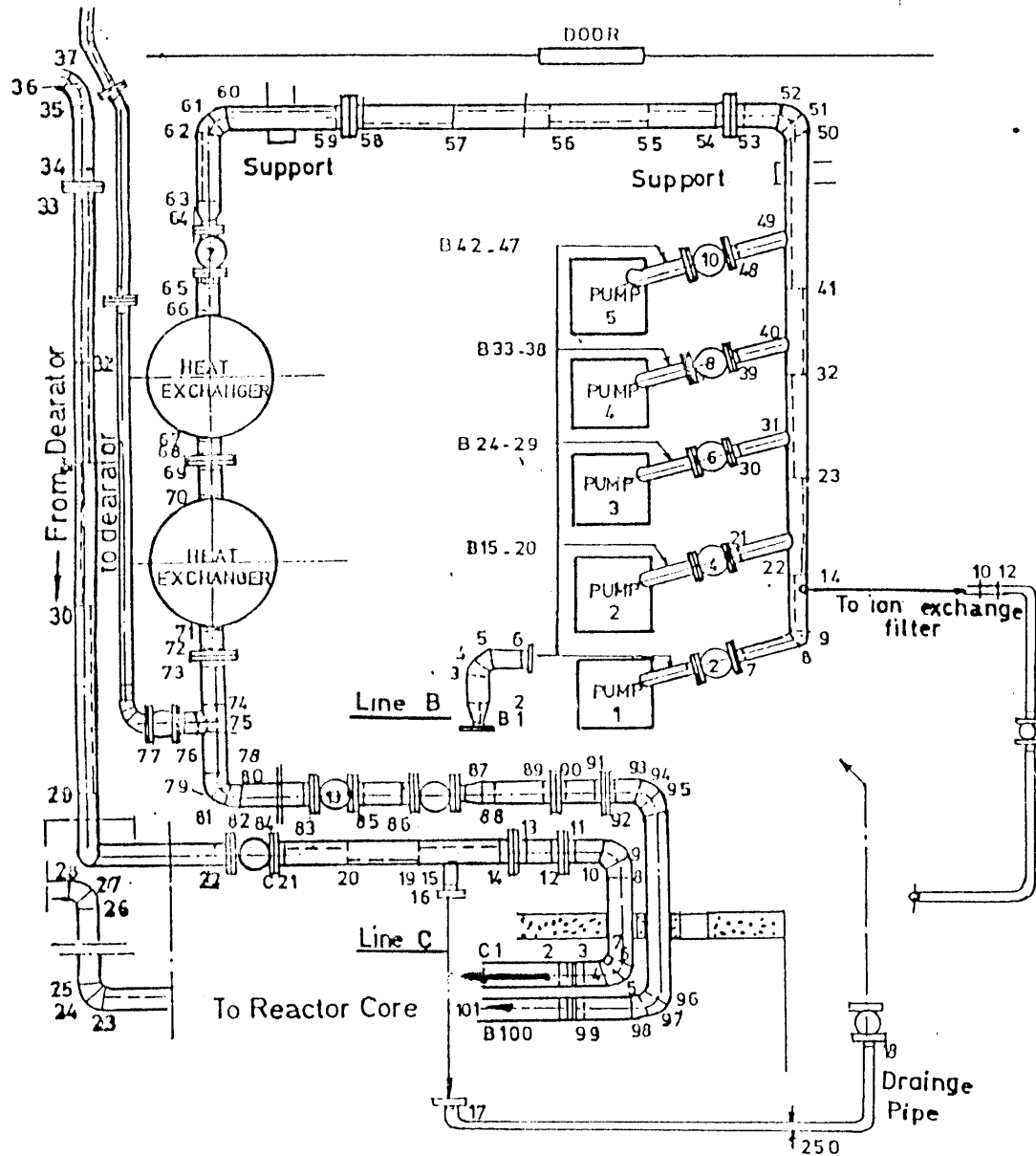
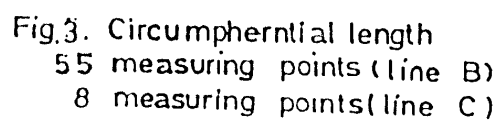


Fig.2. Circumferential and Longitudinal Welding Identifications  
in Reactor Primary cooling System  
Line B 101 Circumferential Welding  
( Pressure Side )  
Line C 37 Circumferential Welding



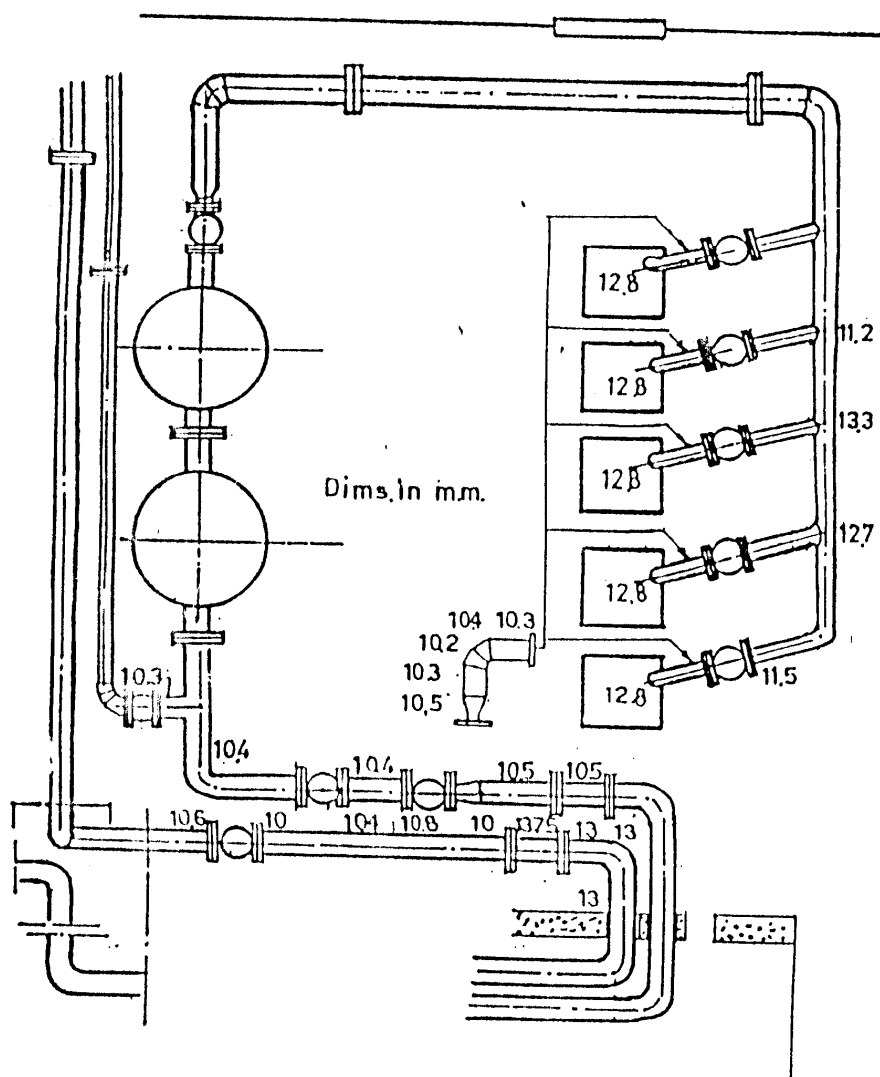


Fig.4 Thickness measurements  
 39 measuring points on Line B  
 9 measuring points on Line C



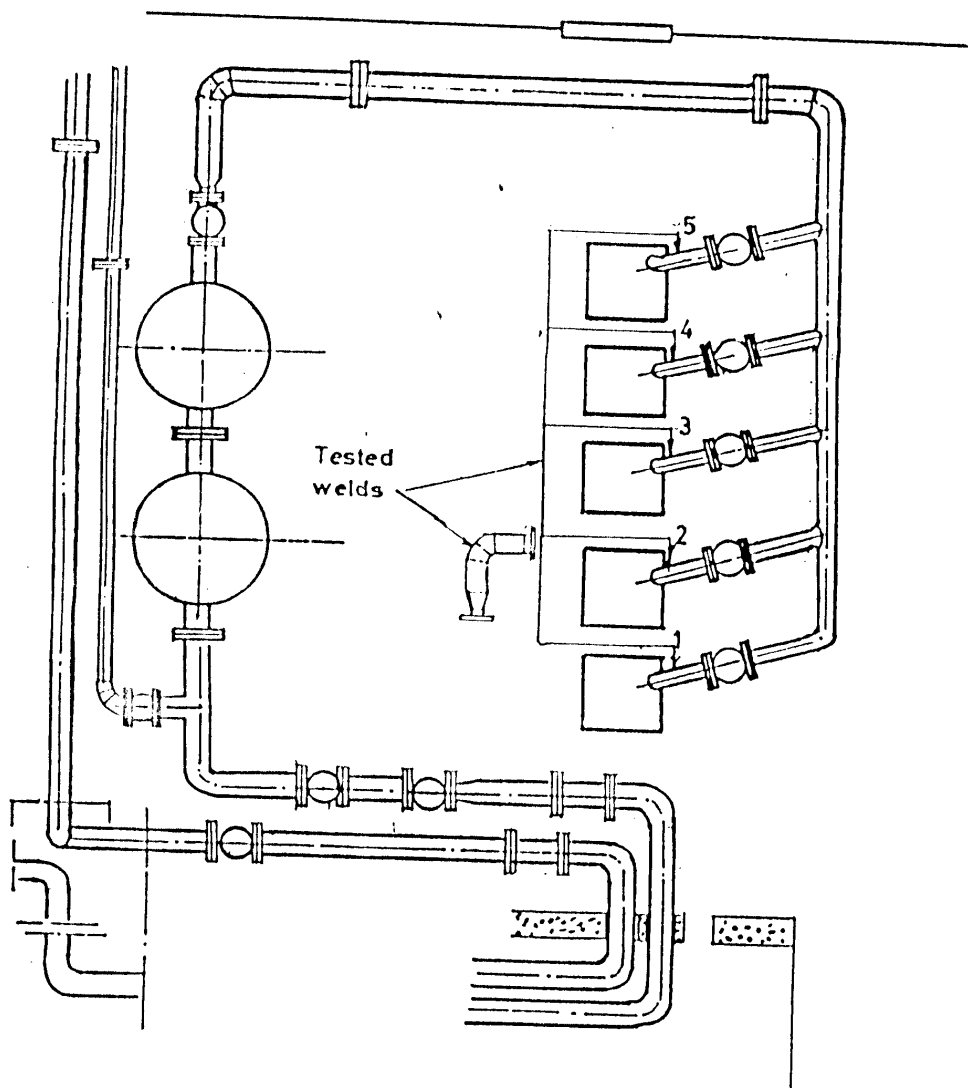


Fig.5 Liquid Penetrant Measuring Points

5 Measuring points

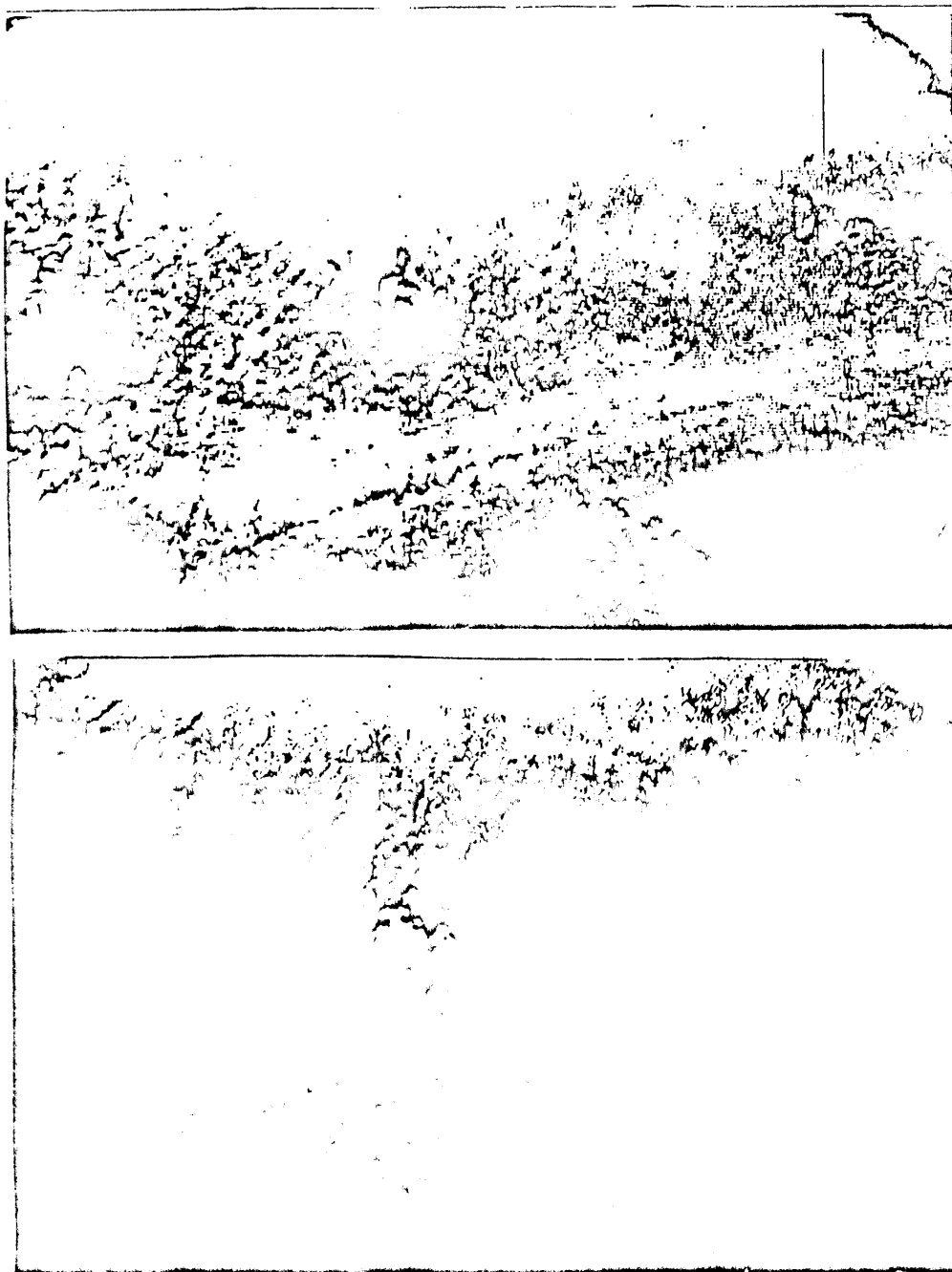


FIG. 6 Pit on the separator shell before and after conditioning  
the surface

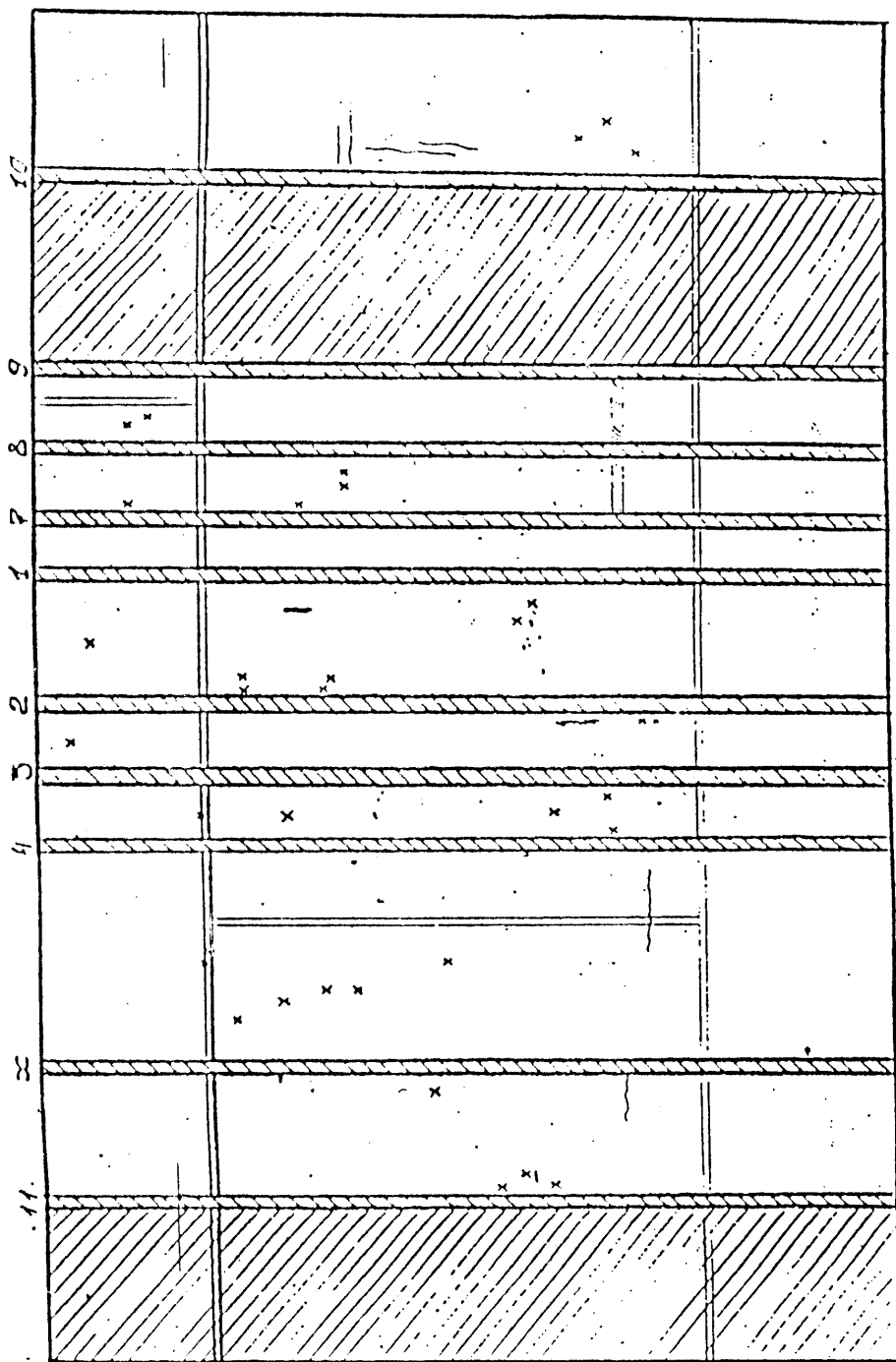


FIG. 7 Plane Projection of the Surface of the Separator



FIG 8 Weld between reactor tank and bottom (upper figure).  
Weld between separator and tank bottom.



FIG 9 Surface of metal in storage.

- In-Core Inspection as well as central and shield vessels surfaces.
- Horizontal Channels Inspection.
- Inspection of the Spent Fuel Storage Tank.
- Inspection of the Primary Cooling System Components.

#### b- Inspection Techniques

The inspection of reactor components was done using non-destructive methods. The inspection techniques are as follows:

##### Visual method

In this method the following equipments were used:

- Under water video camera system type TBO-1 for internal surfaces and welds inspection.
- Magnification optical device for horizontal channels and in-core inspection.
- Special Optical Rods for under water inspection.

##### Thickness measurements

Ultrasonic devices calibrated with standard specimens of reactor materials were used. Defects shape and thickness were determined by replica method.

Fluorescent Liquid Penetrant method For Welds examination.

Water Chemical Analysis.

#### Results of ISI

The results of ISI can be summarized as follows:

- Visual Inspection of Reactor Vessels by the under water video camera showed that Central and Shield Tanks as well as welds and core barrel are in good condition.
- No changes seemed to be happened in thickness measurements of reactor components by the ultrasonic devices referring to the original metal thickness.
- Welds examination by fluorescent Liquid Penetrant method showed satisfactory results.
- Spent fuel storage tank status is not satisfactory. There is no system for water purification or agitation. The tank has limited capacity and difficulties to open its drainage valve.
- The life time of the ion exchange vessel cannot be guaranteed even the corrosion areas have been repaired.
- Drainage valve system has to be changed.
- Reconstruction of the internal structure of the cooling tower is necessary.

## Renewal of Instrumentation and Control of ET-RR-1

Due to the aging of the Instrumentation and Control Systems (I&C) of the reactor and the lack of spare parts supply, it was decided at the end of the seventies to renew the whole I&C Systems. The renewal process was made in steps as follows:

### Nuclear Instrumentation

Through bilateral agreement with KFA Julich new nuclear instrumentation system was jointly designed in 1984. This system consists of :

- 3 Safety Channels
  - 3 Logarithmic Channels with period meter.
  - 1 Multirange Channel to measure the power in 8 decades.
- This channel is connected to a three point step controller for the automatic control system of the reactor.

### Radiation Monitoring System

Through an IAEA technical assistance project No. EGY/09/15, a system was supplied and installed by the Technical University of Budapest - Hungary. This system consists of 25 channels. The Silicon semiconductor detectors cover different ranges of radiation exposure from  $0-3 \times 10^4$   $\mu\text{Sv/h}$  in five steps. Another five channels utilize Geiger-Muller detectors as gamma indicators for measuring the activity concentration in the sampled air. Each channel has an alarm output (Sound and Light) with adjustable levels. Installation of this system was finished in March 1989. [6].

### Process Instrumentation

In Dec. 1989 a system for process instrumentation was installed. It was supplied from Hungary (Gamma Werk) through the IAEA technical assistance project No. EGY/04/28. The system consists of 30 channels to measure the process parameters, table 1. Based on the signal coming from the water level in the reactor central tank a replensher system was designed and introduced into the feed water supply system to open its valves automatically to supply the reactor with demineralized water if the level decreases below 580 cm. The charging system is useful to compensate water level between 600 cm and 580 cm. The system can also manually operated.

TABLE I TECHNICAL SPECIFICATION OF THE UPGRADING MEASURING  
SYSTEM OF INCHAS REACTOR

No.	Loop No.	Measuring circuits & func	Measuring range	Signal
1) Level Measurements				
LI002		Desinralized water tanks	0-200 cm	----
LIA002		Reactor central tank	0-700 cm	L500
LIA003		Reactor shield tank	0-700 cm	L500
LIA005		Spent fuel storage tank	0-500 cm	L300
LIA006		Level in deaerator	0-200 cm	L100
				H120
LIA041/2		Liquid waste storage tanks	0-800 cm	H700
2) Pressure Measurements				
PIA007		Pressure in primary circuit	0-3 bar	L2.2 LL2
PIA008		Depression in deaerator	-1+1 mbar	L-0.6
PIA009		Depression above reactor	-1+1 mbar	L-0.7
PIA010		Depression under reactor	-1.5+1.5 mbar	L-1.0
PIA011		Depression in pump room	-1.5+1.5 mbar	L-0.7
PIA012		Depression in spent fuel tank	-1.5+1.5 mbar	L-0.0
PIA013		Depression in hot cells	-1.5+1.5 mbar	L-0.7
PI018		Depression before ventilators	0-25 mbar	----
PIA043		Pressure in secondary circuit	0-7 bar	L5.0
3) Conductivity Measurements				
QI016		Conductivity in primary circuit	0-20 uS/cm	----
4) Flow Measurements				
FI017		Flow in ion exchange filter	0-16 m3/h	----
FIA019		Flow in deaerator	0-250 m3/h	L80
FIRA020		Flow in secondary circuit	0-400 m3/h	L315
FIRA021		Flow in primary circuit	0-1000 m3/h	L810 LL720
FIA022		Air flow in deaerator	0-160 m3/h	L70
5) Temperature Measurements				
TI023		Deaerator outlet temperature	0-60 C	----
TI024		Pump room air temperature	local	
TIRA025		Reactor outlet temperature	0-60 C	H40
TI026		Temp. in secondary circuit	0-40 C	----
TDIRA027		Temp.diff. in primary circuit	0-10 C	H2.4
TDIRA028		Temp.diff. in secondary circuit	0-20 C	H7.4
TI029		Temp. in cooling tower	0-40 C	----
TI030		Air temp. in corridor	local	
TA031		Pump bearing temp. (10 points)	0-100 C	----
L : Warning signal at low level    LL : Emergency signal H : Warning signal at high level				



## Computerized Safety & Logic System (CSLS)

The CSLS was supplied from Hungary (KFKI) through the IAEA technical assistance project No. EGY/09/025/1993. The new safety system is based on Programmable Logic Controllers (PLC) from EBERLE.

Free contacts from the different instrumentation and control system are connected to 3 identical PLC's through photocouplers. The shutdown and interlock signals from the 3 PLC's are connected in 2 out of 3 logic voters. A fourth PLC was used to generate signals or combination of signals to test the hardware and software of the 3 PLC. A display shows the status of the input and output signals to the operator with first alarm signal display and safety rod drop time.

### Signaling System

Through further cooperation with the Hungarian KFKI a signaling system was purchased to replace the old system. Installation of this system will take place in Dec. 1993. The signaling system is based on the same PLC type used for the CLCS. It has 80 free contact input to PLC's and displays for the warning and shutdown signals. Eighty relays are installed to duplicate the input signals to the data acquisition system. Two different tones are used; one for warning signals and the other for shutdown condition.

### Camera Monitoring System

In 1991 closed loop system consisting of 6 cameras were installed in the important places in reactor hall, control room and entrances to check personnel inside these areas. The operator can change the scanning time or fix one camera or bypass another one.

### New Operator Console

New Operator Console Fig. 10 was installed to simplify the man-machine interface. The middle part of the new console is the main part. It contains all the necessary keys and push buttons to move the control rods. The important parameters from the nuclear and process instrumentations are duplicated on this part. The CSLS are located to the right of the operator with all its push buttons and display lamps. The signaling system control push buttons and 30 important signals are located to the left of the operator. The monitor and control of the camera monitoring system occupies another part to the right of the operator. This part contains also 20 lines telephone communication system. The last part is reserved for the data acquisition system. It will contain 14 inch colored monitor with the keyboard.

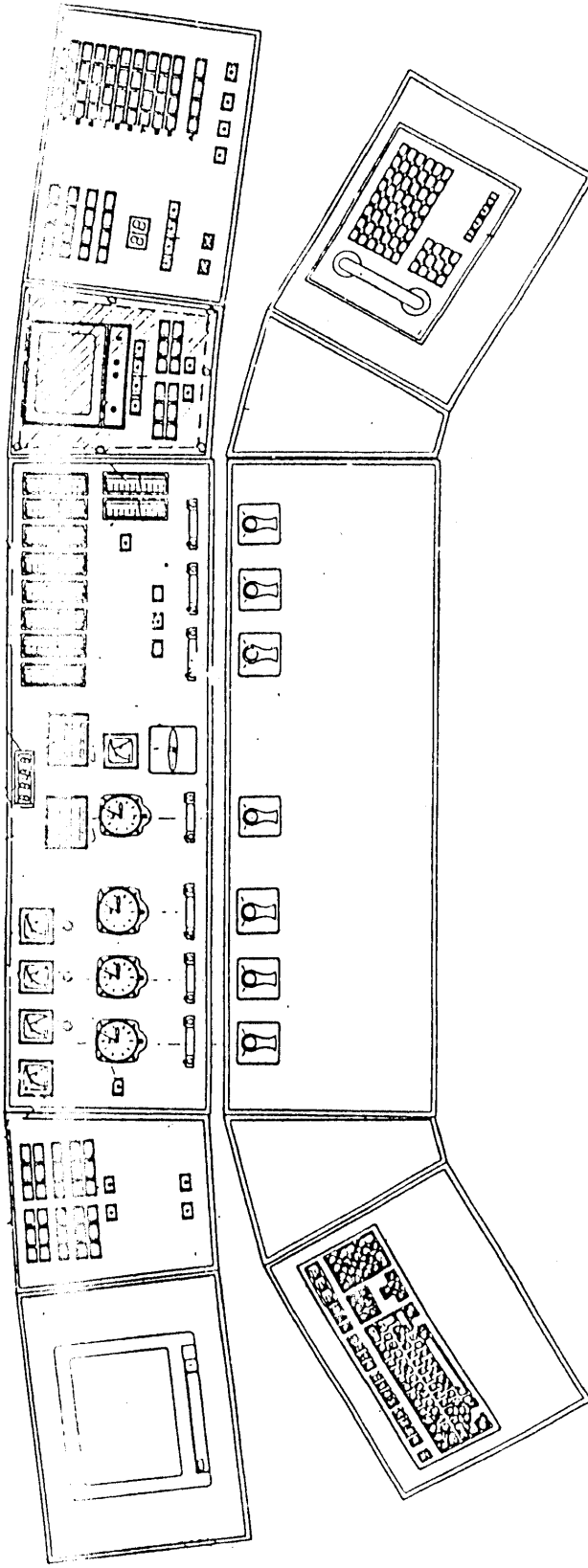


FIG 10 PROPOSED ARRANGEMENT OF THE INSTRUMENTS (TYP C)

## Future Plan of I&C Modernization

The following systems will be introduced into the reactor system to increase its safety and reliability of operation.

### 1- Data Acquisition System

A system with 48 analog and 128 digital inputs are designed to provide the data acquisition of every important measured and displayed analog and digital signal. The main tasks of this system are:

- Data Collection
- Calculation of some parameters from the collected data.
- Creation of Records and Log Book.
- Archivation and store of the input signals for future analysis purposes.
- Operator aid through schematic diagrams, charts and graphs.

### 2- Fission Chamber Assembly

It is foreseen to buy and install a fission chamber assembly to be added to the nuclear instrumentation. This will provide good monitoring of the reactor in the pre-start up to the power range.

### 3- Digital Reactivity Meter

A software program was developed to calculate the reactivity from the power signal of the multirange DC channel. Based on this program a digital reactivity meter is now under construction. It will be installed in the next year to help the operator to get the reactivity directly and automate the control and calibration procedures.

### 4- Compact Simulator

Although a PC based simulator was developed for training operators [7], it is hoped to build a hardware compact simulator for ET-RR-1 reactor to be used for more training capabilities and dynamic performance studies.

It is worth mentioning here that within the frame of developmental projects planned at the reactor a new storage for the spent fuel is foreseen. The accumulation of spent fuel from the reactor requires the preparation of additional storage area at the reactor facility. A dry storage for the EK-10 type spent fuel elements which has been stored for a long time in the present wet storage is one of the projects foreseen in the ET-RR-1 reactor. There could also be another additional storage area for spent fuel to be built in the part of the pump room of primary coolant where the present ion exchange filter exists.

### Conclusions

Successful rehabilitation processes have been carried out at the ET-RR-1 reactor. An in-service inspection was another project fulfilled at the reactor facility. The main objectives of these projects are to secure a safe and reliable operation of the reactor. It can be concluded that these processes and specially the positive results obtained from the in-service inspection program are quite satisfactory to make the raising of reactor power feasible.

### References

- [1] Dimitri F.H. and Khattab M. "Modernization of ET-RR-1 Measuring System" A.R.E.A.E.A./Int. Rep.-131, 1991.
- [2] Khattab M., Ahmed.E., Gaaffar M., Magid F. and Hamnad F. "Probabilistic Safety Analysis For ET-RR-1 Reactor. Safety Features and Qualitative Logical Analysis" A.R.E.A.E.A./Int. Rep.-128, 1990.
- [3] Khattab M. "Thirty Years Experience in ET-RR-1 Operation" A.R.E.A.E.A./Rep.-319, 1993.
- [4] Marwan M., Khattab M., Hanna A. "Water Treatment Process or nuclear Reactors" 5th Conf.Nucl.Sci.& Appl.Vol.1,1992
- [5] Khattab M., Shafy M., Konoplev K., Samodurva Yu., Orlov S. Didenko V.& Jackorev O. "In-Service Inspection of ET-RR-1 Reactor Vessels and Spent Fuel Tank" A.R.E.A.E.A./Rep.-320, 1993.
- [6] Khattab M. and Omar A. "Using Exsys To An Expert System For Fault Diagnosis of the Research Reactor of Egypt" AL-AZHAR Eng. Conf. Vol.14, 1989.
- [7] Sultan M., Khattab M., Dimitri F. " Digital-Analogue Simulation of ET-RR-1 Reactor For Dynamic Performance Studies and Training" Proceedings of the Eighth International Conference for Mechanical Power Engineering. Alexandria, Egypt, 1993, Vol. 3, pp. 167-177.

MOHAMED KHATTAB

REACTORS DEPT., NUCLEAR RESEARCH CENTER

# INTRODUCTION

ET-RR-1 is a 2 Mw research reactor with light water coolant, moderator and reflector. Average thermal neutron flux is  $1.0 \times 10^{13}$  n/cm<sup>2</sup> sec. Eight boron carbide control rods inside the core are used for safety and coarse control functions. One stainless steel rod is used for fine regulations. Fig. (1) shows Recirculating Cooling System of ET-RR-1. Figures (2) and (3) show the vertical and horizontal sections of the reactor respectively.

EK-15 type fuel rods are made of uranium dioxide dispersed in Mg matrix, 10% U-235 enrichment are clad in aluminum tubes, 10 mm outer diameter, 7 mm inner diameter and 600 mm length. The fuel bundle has 16 fuel elements, in a square array. Reactor core consists of 51 bundle positions.

Reactor comprises different systems which ensure its safety during normal operation and anticipated occurrences. The main reactor systems are:

- Primary and secondary reactor cooling circuits.
- Instrumentation and control (I&C)
- Ventilation
- Waste disposal
- Fuel handling and spent fuel storage
- Hot cells
- Water treatment facility

The reactor is used for isotope production as well as carrying out research work in the following fields:

1. Reactor physics and nuclear engineering.
2. Thermal safety experiments.
3. Neutron physics and neutron radiography
4. Neutron optics.
5. Solid state physics
6. Metallurgy and radiation damage.
7. Biology.

These research programs are carried out through experimental facilities such as thermal column, horizontal and vertical and biological channels.

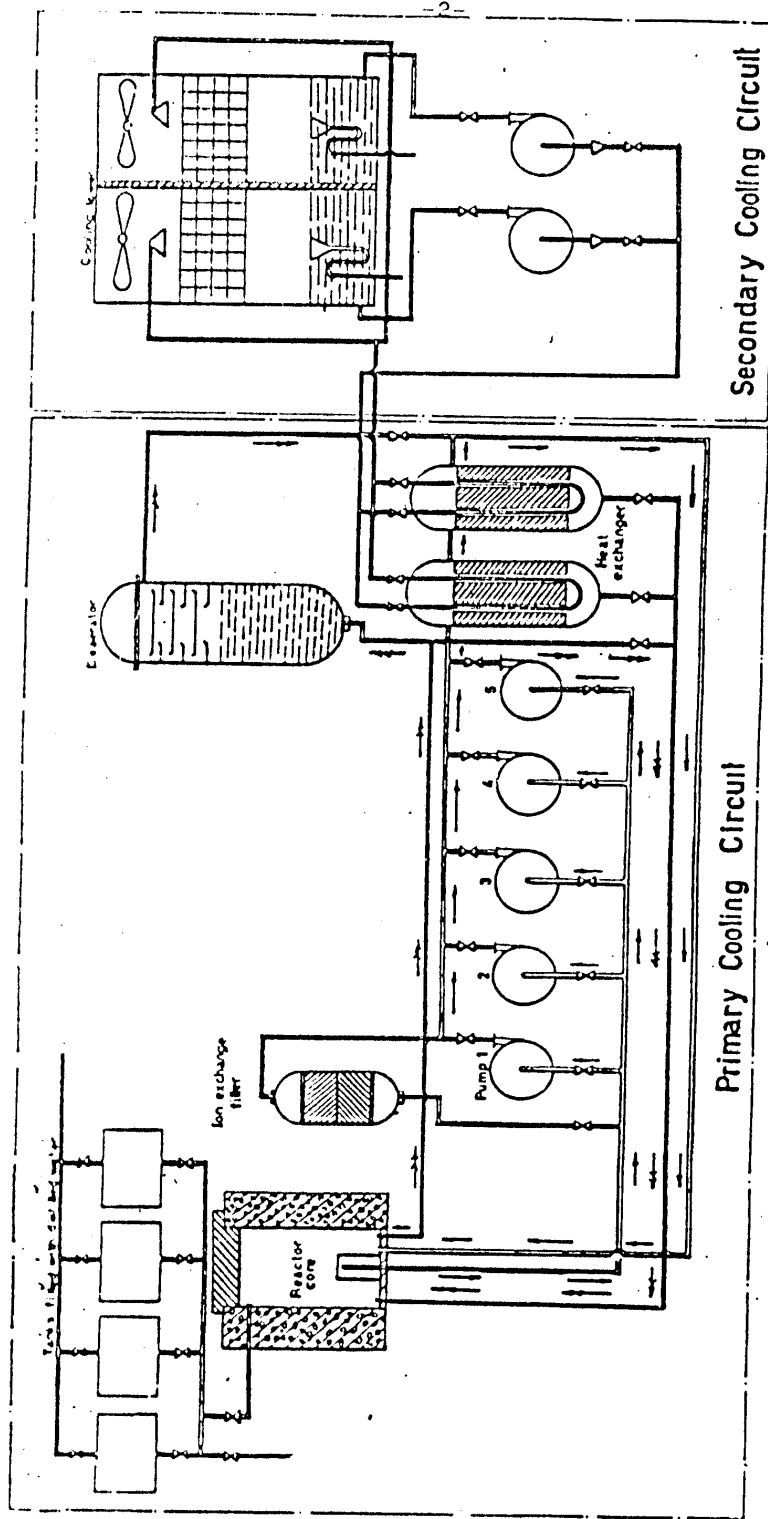


Fig.(1) Recirculating Coding System  
of ET-RR-1. Reactor

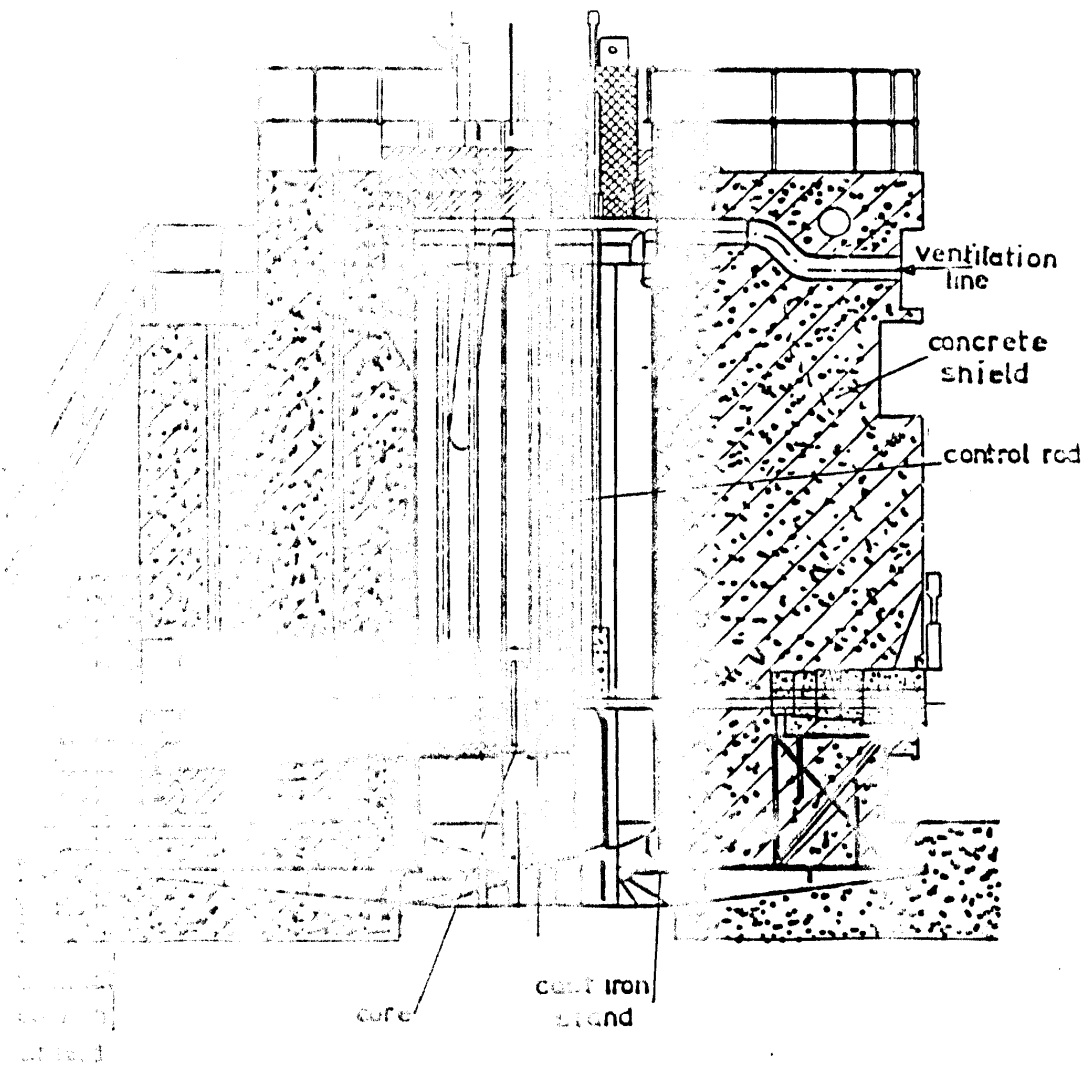


Fig.(c) Vertical Cross Section Of The Reactor

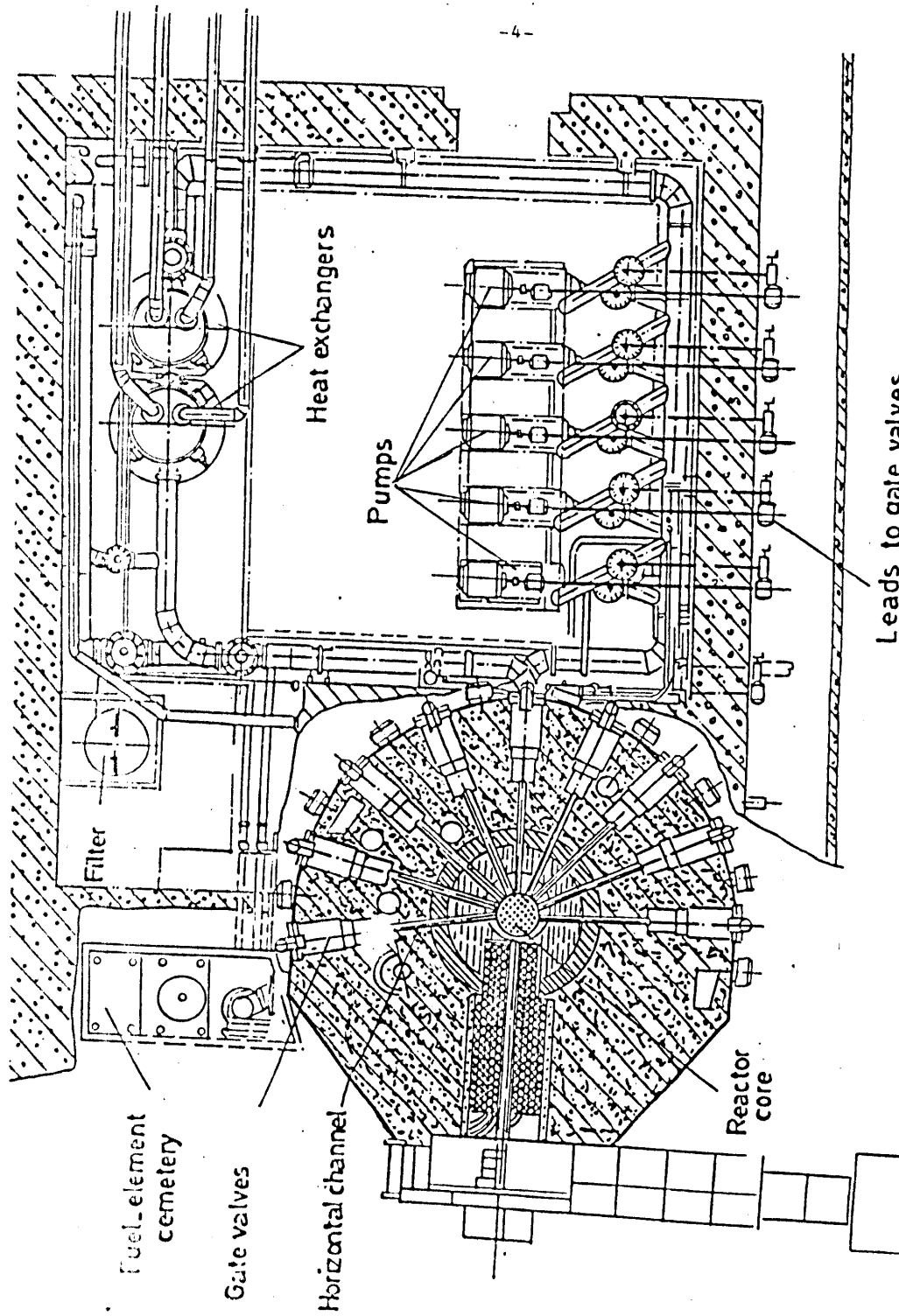


Fig. (3) Horizontal Cross Section Through The  
Reactor and Pump House .



## DESIGN SPECIFICATIONS of ET-RR-1

The reactor tank and spent fuel storage are constructed of Aluminum alloy type CAB-1. Cooling circuit, pumps, heat exchangers, and valves are manufactured from austenitic stainless steel type CT0.8x18H10T.

### *a-Central and Shield Reactor Tanks*

Figs. (2.a, b) illustrate geometrical construction of the reactor body. The central tank is cylindrical vessel 1130 mm inner diameter, 5920 mm height, and 12 mm thickness. The shield tank is cylindrical vessel 23000 mm inner diameter, 6900 mm height and 16 mm thickness. The vessels are welded to hemi-spherical dish bottom of thickness 20 mm. The top is shielded by non-pressurized rotating cover. Reactor supports as well as inlet and outlet pipes of primary circuit are welded to the tank bottom. The outlet pipe located under the core is designed as a mechanical filter. Coolant medium circulates to the central tank through the inlet pipe and baffle lattice. The coolant flows downwards through the core outlet pipe. The core barrel is eccentric at 560 mm apart from the central tank. The reactor body is shielded by heavy concrete.

### *b- Spent Fuel Storage Tank*

The spent fuel storage is a trapezoidal tank of 12 mm thickness. Water shield height is 4 m. The wall and bottom have external stiffing ribs. There is a cellular section installed on the bottom used for storing the spent fuel assemblies. Figs. (2.a, b) shows the construction of the spent fuel storage.

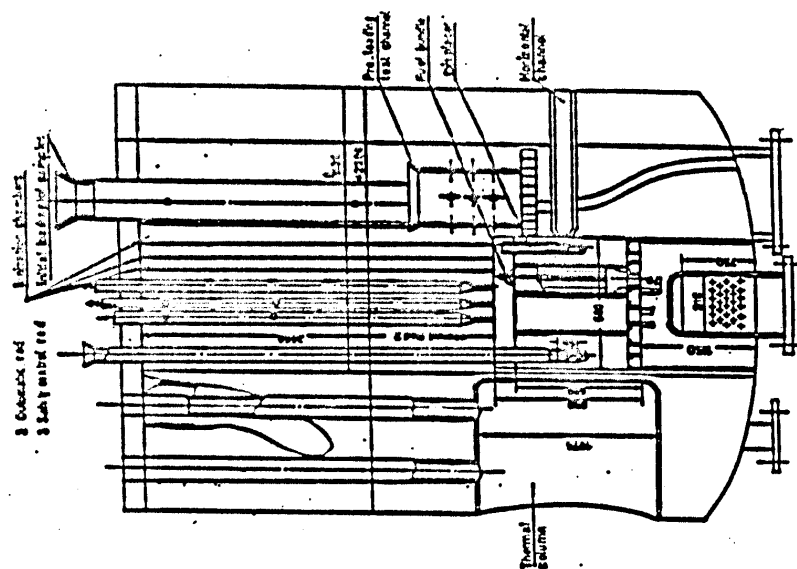
### *c- Feed Water Supply System (FWSS)*

Feed water supply system, Fig. (2) is composed of the following components {13}:

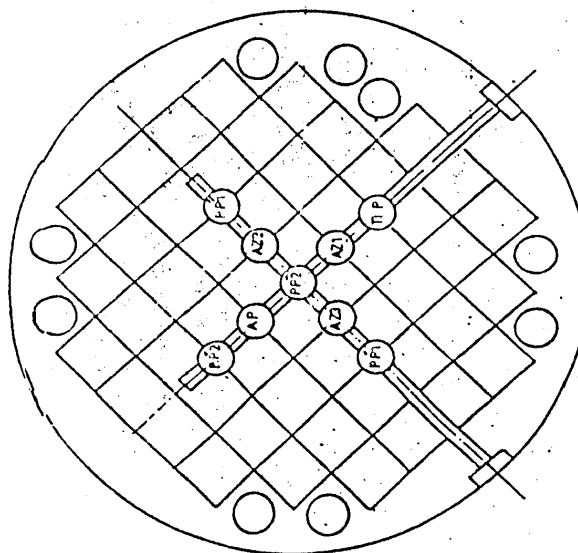
- Mixed bed deionizer unit of 15 m<sup>3</sup>/h
- Four tanks of capacity 40 m<sup>3</sup>

Feed water supply tanks (FWST) are made of stainless steel 1.0x18H9T sheets which have anti-corrosive properties. Their capacity are enough to fill reactor shield tank, central tank and primary cooling circuit.

The water is supplied from the deionizer to the FWST. The reactor shield tank is fed with the demineralized water. The central tank is fed from the shield tank through four openings located at the higher end of the central tank. Reactor primary cooling circuit is fed from the central tank. Spent fuel storage is fed from FWST directly. Water level in reactor vessels is maintained at its highest level at 6 m by automatic replensher device installed on the feed pipe to the shield tank. Overflow pipes define the upper limit of water level at 0.5 m below the cover inside the spent fuel storage and reactor vessels.



FIG(4.0) REACTOR CONSTRUCTION



First Shim Manual Rods PP1 and PP2  
 Second Shim Manual Rods PP2 and PP2  
 Safety Rods AZ1, AZ2 and AZ3  
 Automatic Regulating Rod AP  
 Precision Regulating Fine Rod PP

FIG(4.1) DISTRIBUTION OF THE CONTROL RODS IN THE ET-RR.1 REACTOR.

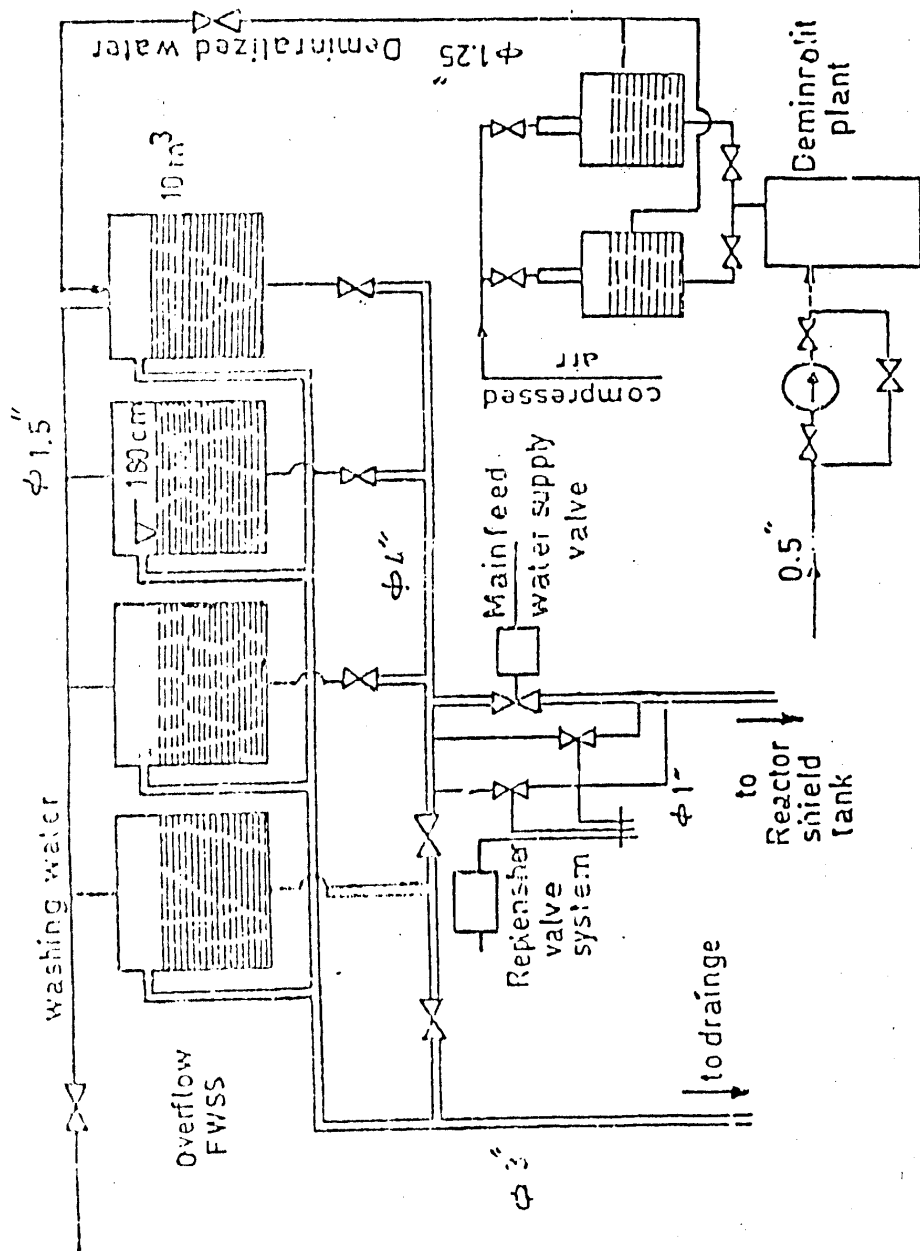


Fig.6.Reactor Feed Water Supply System  
( FWSS)

## REACTOR COOLING SYSTEM

Reactor cooling system consists of primary and secondary cooling circuits, Fig 1

### Primary Cooling Circuit (PCC)

The primary cooling circuit technological equipment are located in the basement floor at an elevation (-5 m) to satisfy the following purposes:

- Suitably access to any equipment for maintenance and repair purposes.
- Minimum hydraulic resistance of conduit pipes.
- Effective drainage and quick discharge of distillate in case of necessity.

The main components of PCC are:: five centrifugal pumps two heat exchangers, deaerator ion-exchange filter, and the necessary conduit pipes, valves and fittings. The five pumps and their pipe connections are mounted in parallel on a foundation frame. During normal operation, the nominal flow of the distillate is 860 m<sup>3</sup>/h. The temperature difference across the core is 2 °C. The coolant flows through the core downward to the suction side of the pumps, then it is discharged through conduit pipe to the heat exchangers. The total flow of distillate running into the primary circuit is determined by a flow meter which is set before the heat exchangers.

The pumps deliver distillate through the shell side of the heat exchangers which connected in series with the primary cooling circuit. the distillate upon emerging from the second heat exchangers is divided into two parallel streams.

The main stream (about 85%) is directed into the reactor core, and the second (about 15%) is directed to the deaerator. The amount of distillate running into the deaerator ( $130 \text{ m}^3/\text{h}$ ) is controlled by a gate valve and determined by a flow meter washer. It is connected to the primary circuit in series. The coolant is purged of detonating gases by rarefaction above the central tank and in the deaerator by air blowing. The ion-exchange filter is designed for purifying the distillate at a rate of  $10 \text{ m}^3/\text{h}$ . It is operated upon request depending on the quality of the coolant. It reduces the radioactive contamination of water. It is connected in parallel with the primary circuit. During reactor operation, the pump room is inaccessible, and is closed by hermetically sealed door.

#### Secondary Cooling Circuit (SCC)

The secondary cooling circuit cools down the primary circuit through the tube side of the heat exchangers. Temperature difference across the heat exchanger is about  $5^\circ\text{C}$ . Total flow rate discharged is  $350 \text{ m}^3/\text{h}$ . The water circulates by one pump through the heat exchangers and back to the cooling tower where it falls down in droplet form on wooden frames against upward stream of air. The air is directed upwards by means of two suction fans placed at the top of the cooling tower, Fig. 1. The cooled water is collected in the basement dwell of the cooling tower, to the suction side of the pump. The components of primary and secondary circuits is summarized in Table 1.












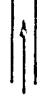
SYMBOL	PRIMARY COOLANT CIRCUIT AND DRAINAGE			SECONDARY COOLANT CIRCUIT		
		VALVE NO	TOTAL		VALVE NO	TOTAL
	MANUAL OPERATED VALVE	6,7,8,9,10,11,15 15A,16,18,19	11	MANUAL OPERATED VALVE		6
	MOTOR OPERATED VALVE	1,2,3,4,5,17	6	MOTOR OPERATED VALVE	21,22	2
	NORMALLY CLOSED VALVE	20,25,26,27,30	5	NORMALLY CLOSED VALVE	23,24	2
	MANUAL NORMALLY CLOSED VALVE	28,29,30	3+57 Drainage	PUMPS MANUAL NORMALLY CLOSED VALVE		3
	CENTRIFUGAL PUMP	I II III IV V $\frac{11111}{2/3}$	5	CENTRIFUGAL PUMP	$\frac{11}{1/2}$	2
	PRESSURE BREAKDOWN ORIFICE	Reactor flow, Degerator, Filter & Air flow to degerator.	4	PRESSURE BREAKDOWN ORIFICE		
	HEAT EXCHANGER	1460 tube 24 mm. diameter, 1 mm. thickness	2	370 U tube, 13 mm. diameter, 1.5 mm. thickness Cooling surface area 2X95 m <sup>2</sup>		
	LEVEL TRANSMITTER	Reactor central tank, Degerator, Storage Feed water tanks.	4	LEVEL TRANSMITTER		3
	TEMPERATURE TRANSMITTER	Outlet from reactor, Degenerator & 1/0 Diff. peering of pumps.	13	TEMPERAT. TRANSMITTER		2
	PRESSURE TRANSMITTER		1	PRESSURE TRANSMITTER		1
	FLOW TRANSMITTER		4	FLOW TRANSMITTER		1
	PIPE LINE 350 mm DIAM.			PIPE LINE 300mm DIAM.		

Table (1)

## REACTOR SYSTEMS MODIFICATION

1 -The Surface area of the outer concrete shield of the reactor body was covered by three adjacent layers of iron plates in 1967. The thickness of each plate was 15 mm. Machining on plates to form radial shape was done by heavy rolling machines. Horizontal channels shielding configuration as well as ventilation grids in concrete shield were accurately measured and properly appointed on the plates by a die then they were cutout by oxygen. The iron plates were welded vertically and horizontally at their edges and corners, Fig. (7). About 50 tons of iron plates were mounted around the concrete shield. The costs were about 10,000 LE. Project management and daily problems were the experience obtained during that time.

2 -Since reactor technology have been developed during the last decades, it was necessary to up-grade the ageing control, radiation, protection and measuring systems of ET-RR-1 to achieve safety requirements. A plan was carried out in three stages:

### First Stage

- Modernization of nuclear devices, safety and control instrumentation of the reactor through technical assistance from west germany, in 1984.
- Rabbit system irradiation facility through the IAEA technical assistance program in 1986.

### Second Stage

- Modernization of radiation measurement equipments with a new system from Hungary through IAEA contract No. (EGY/09/15) in 1987. The system contains 30 measuring points distributed in different areas in the reactor building to monitor the radiation levels.
- Installation of a TV monitoring system for continuous observations of working people.
- Installation of a new water treatment equipment to produce demineralized water according to the required quality. The system realizes economy of the exploited power, and reduces the time of demineralized water production.
- Renewal of the cooling tower by adding new steel and peach-pine wooden structures.

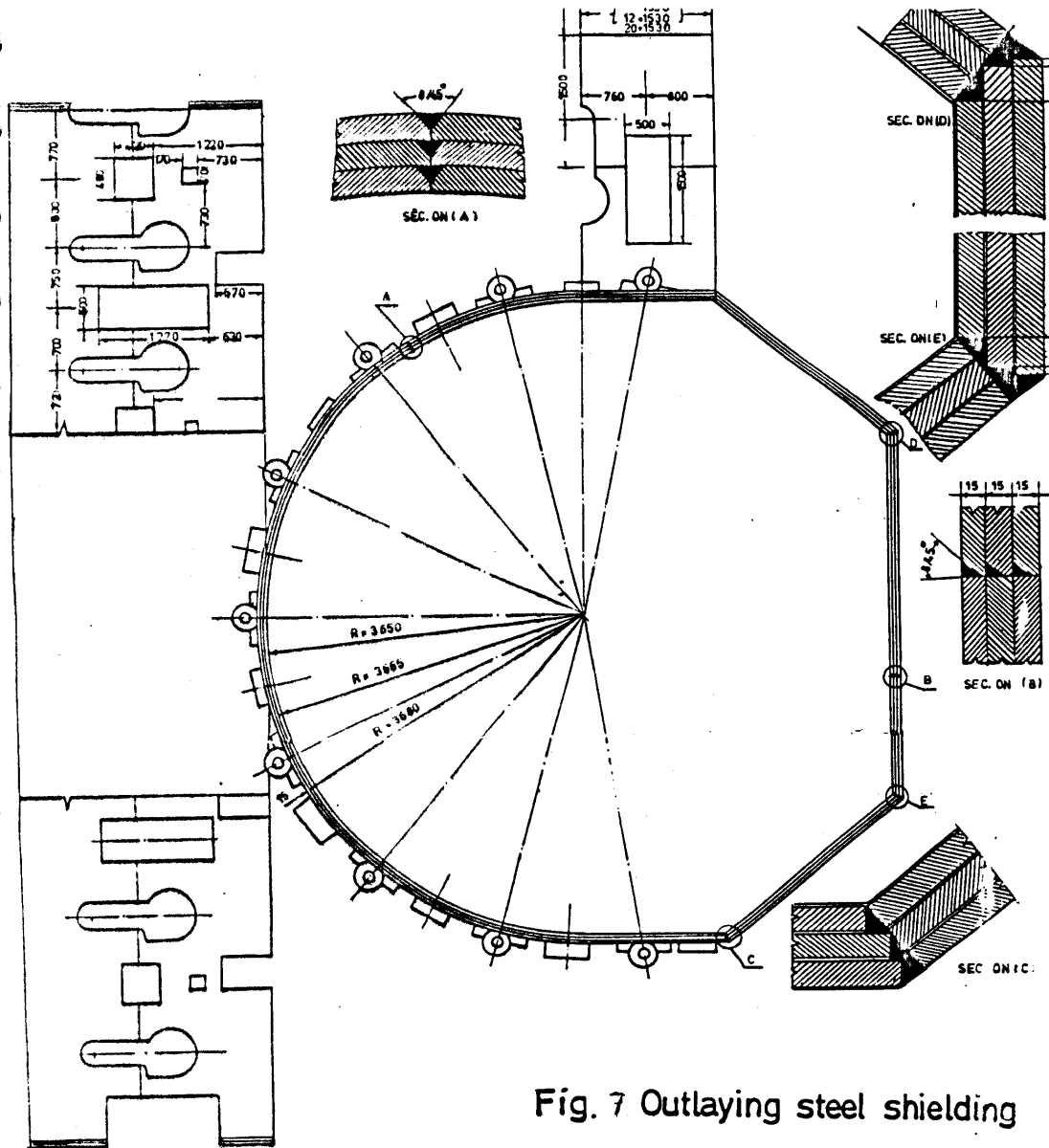
### Third Stage

- Modernization of ET-RR-1 measuring system. The system performs measurements of coolant flow rate, pressure, temperature and water level inside the reactor core. The project was carried out by the Y company in Hungary through the IAEA technical

TABLE I TECHNICAL SPECIFICATION OF THE UPGRADING MEASURING SYSTEM OF INCHAS REACTOR

No.	Loop No.	Measuring circuits & func	Measuring range	Signal
1) Level Measurements				
	LIA002	Deminalized water tanks	0-200 cm	----
	LIA002	Reactor central tank	0-700 cm	L500
	LIA003	Reactor shield tank	0-700 cm	L500
	LIA005	Spent fuel storage tank	0-500 cm	L300
	LIA006	Level in deaerator	0-200 cm	L100
	LIA041/2	Liquid waste storage tanks	0-800 cm	H120 H700
2) Pressure Measurements				
	PIA007	Pressure in primary circuit	0-3 bar	L2.2
	PIA008	Depression in deaerator	-1+1 mbar	LL2
	PIA009	Depression above reactor	-1+1 mbar	L-0.6
	PIA010	Depression under reactor	-1.5+1.5 mbar	L-0.7
	PIA011	Depression in pump room	-1.5+1.5 mbar	L-1.0
	PIA012	Depression in spent fuel tank	-1.5+1.5 mbar	L-0.7
	PIA013	Depression in hot cells	-1.5+1.5 mbar	L-0.7
	PIA018	Depression before ventilators	0-25 mbar	----
	PIA043	Pressure in secondary circuit	0-7 bar	L5.0
3) Conductivity Measurements				
	QI016	Conductivity in primary circuit	0-20 uS/cm	----
4) Flow Measurements				
	FI017	Flow in ion exchange filter	0-16 m3/h	----
	FIA019	Flow in deaerator	0-250 m3/h	L80
	FIRA020	Flow in secondary circuit	0-400 m3/h	L315
	FIRA021	Flow in primary circuit	0-1000 m3/h	L810
	FIA022	Air flow in deaerator	0-160 m3/h	LL720 L70
5) Temperature Measurements				
	TI023	Deaerator outlet temperature	0-60 C	----
	TI024	Pump room air temperature	local	----
	TIRA025	Reactor outlet temperature	0-60 C	H40
	TI026	Temp. in secondary circuit	0-40 C	----
	TDIRA027	Temp.diff. in primary circuit	0-10 C	H2.4
	TDIRA028	Temp.diff. in secondary circuit	0-20 C	H7.4
	TI029	Temp. in cooling tower	0-40 C	----
	TI030	Air temp. in corridor	local	----
	TR031	Pump bearing temp. (10 points)	0-100 C	----
L : Warning signal at low level      LL : Emergency signal				
H : Warning signal at high level				





assistance program (contract No. EGY/04/28) in 1989.

- Installation of an automatic compensation system for water level replacement inside the core.
- Installation of Computerized Safety Logic system, CSIS, (project EGY/09/025), which increases safe operation of reactor and enable continuous system check up.
- Data acquisition system, DACQUS.

#### IN- SERVICE INSPECTION PROGRAM (ISI)

Inspection of the ET-RR-1 main components were carried during the period from 26-8-1992 to 9-9-1992 for : reactor vessel, shielding vessel, part of the horizontal channels, spent fuel storage vessel and some parts of the primary circuit piping. The following equipments were used for inspection:-

- 1- Television video system comprises:
  - Closed circuit television camera with the cable.
  - Camera control unit.
  - Display.
  - Video cassette recorder.
- 2- Ultra device for measuring thickness.
- 3- Several aluminum pipes having 50 meter length and 60 kg weight approximately.

The results show that the reactor vessel surfaces are in good condition and the reactor can work safely [5].

#### CONCLUSIONS

- Data collection and record documentation should be maintained regularly.
- Creating adequate training and retraining programs.
- Maintenance program should be scheduled regularly to rigorous inspection and visual examination program.
- Surveillance and testing program should be applied.

For future development some proposals are given as follows :

- Providing the spent fuel storage with mobile purification and cooling system.
- Dismantling the dearator and using its place for mounting new ion exchange filters for the primary cooling water.
- Providing the hot cells with press machine for pressing the radio-active waste cans.
- Inserting manual gate valve (normally open) before the primary coolant pumps, replacing the sleeve of the suction pipe.
- Studying the problem of increasing the capacity of the spent fuel storage for any temporary core unloading in the future.

An idea of dry-storage for the complete burnt-up fuel assemblies (20 % burn-up) can be investigated. New rack may also be constructed above the existing rack of the spent fuel around its contour.

- Preparing the reactor system for upgrading its power.

#### REFERENCES

- 1 - M. Khattab, el , " Reactors Department Scientific Bulletin", 1961 - 1992.
- 2 - F.H. Dimitri , el, " Modernization of ET-RR-1 Measuring System ", A.R.E.A.E.A./Int. Rep.- 131. 1991.
- 3 - M. Khattab, el, " Probabilistic safety analysis for ET-RR-1 Reactor safety features and qualitative logical analysis" A.R.E.A.E.A. / Int. Rep.- 128, 1990.
- 4 - M.A. Marwan el, " Water treatment process for nuclear reactors" , 5 th. conference nuclear science and application, Vol. 1, 228 - 241 , 1992.
- 5 - M. Khattab, el, " In-Service Inspection Of ET-RR-1 Reactor Vessels and Spent Fuel Storage Tank" A.R.E.A.E.A./Rep.-320. 1993.

# **CALCULATION OF DECAY HEAT AFTER SHUTDOWN.**

***BY***

***Dr. Abdel Rahman A.El-Kafas***

**Reactors department, Nuclear Research Center, Atomic Energy Authority,  
Cairo, Egypt.**

## ***Abstract***

The reactor power after shutdown is an important parameter when concerning the design and installation of major engineering safety features and nuclear auxiliary systems of a power plant. So, a means for cooling the reactor core after shutdown must be provided in all reactors except those operating at very low power levels such as residual Heat Removal system. Study on ET-RR-1 have been carried out to determine its decay heat after shutdown by using data Acquisition system.

## *1- Introduction:*

After reactor shutdown, the reactor power does not immediately drop to zero but falls off rapidly according to a negative period eventually determined by the half-life of the longest lived delayed neutron group.

## *2- Sources of heat after shutdown*

The sources of heat after shutdown can be summerized as follwos:

- 1- The residual fission power.
- 2- Decay heat of fission products.
- 3- Decay heat of actinides.

### **2-1. The residual fission power.**

The residual fission power does not significantly affect the total power after shutdown as the reactor period is usually under accidental conditions and hence the fission induced power, which is the main contributor to the total power during power operation, falls rapidly to small fractions of its normal value directly after shutdown. However, the residual power can be calculated using the prompt jump approximation method for the solution of the point reactor kinetic equations. (1).

### **2-2. Decay heat of fission products.**

The decay heat of fission products is considered to form the main contribution to the reactor power after shutdown. after a few days of reactor operation, the  $\beta$ - and  $\gamma$ - radiation emitted from decaying fission products amount to about 7 percent of the total thermal power output of the reactor. When the reactor is shutdown, the accumulated fission products continue to decay and release energy within the reactor.

The fission product decay energy can be quite sizable in absolute terms and a means for cooling the reactor core after shutdown must be provided in all reactors except those operating at very low power levels. If this is not done, the temperature of the fuel may rise to a point where the integrity of the fuel is compromised and fission products are released.

After shutdown, a reactor therefore continues to generate power,  $p_s$  (at decreasing rate of course) a function of time. The amount of such power generation depends on :

- The level of power before shutdown,  $P_o$ .
- The length of time,  $\theta_o$ , it operated to such a level.

Many efforts have been exerted to determine exactly the time behavior of the fission product decay heat after shutdown. The rates of the volumetric thermal source strength after shutdown  $q_s'''$  to that before shutdown  $q_o'''$  could be taken as the same ratio of the respective power, i.e.

$$q_s''' / q_o''' = p_s / p_o \quad (1)$$

The ratio  $P_s/P_o$  is given for Uranium fuels as :

$$P_s/P_o = \left[ 0.1(\theta_s + 10)^{-0.2} - 0.087(\theta_s + 2 \times 10^7)^{-0.2} \right] - \left[ 0.1(\theta_s + \theta_o + 10)^{-0.2} - 0.087(\theta_s + \theta_o + 2 \times 10^7)^{-0.2} \right] \quad (2)$$

where  $\theta_s$  and  $\theta_o$  are in seconds.

A simplified formula could be obtained from eqn (2)

if : (a)  $\theta_s > 200$  sec. and  $\theta_o \geq 1$  year.

$$P_s/P_o = 0.095 \theta_s^{-0.26} \quad (3)$$

(b)  $\theta_s > 200$  sec. and  $\theta_o < 1$  year.

$$P_s/P_o = 0.095 \theta_s^{-0.26} \left[ 1 - (1 + \theta_o / \theta_s)^{-0.2} \right] \quad (4)$$

The total energy release as a function of time after shutdown,  $E_s$ , is obtained for  $\theta_o = \infty$

$$E_s = 0.095 \int_{\theta_o}^{\theta_s} P_o \theta_s^{-0.26} d\theta_s = 0.128 P_o \theta_s^{0.74} \text{ MW.hr} \quad (5)$$

### 2-3. Decay heat of actinides.

If a  $^{235}\text{U}$  fueled reactor contains substantial quantities of  $^{238}\text{U}$ , as many of these reactors do, the decay of  $^{239}\text{U}$  and  $^{239}\text{NP}$  formed by the absorption of neutrons in the  $^{238}\text{U}$ , that contribute appreciably during the first few days after reactor shutdown, must also be taken into account.

The decay-heat rate due to these two species can be estimated as follows :

$$^{239}\text{U} (23.5 \text{ min}) = 0.474 \text{ Mev/decay.}$$

$$^{239}\text{NP} (2.35 \text{ dat}) = 0.419 \text{ Mev/decay.}$$

For longer cooling times additional decay heat will be liberated by longer-lived actinides formed by the neutron capture in the fuel material, e.g.,  $^{237}\text{U}$ ,  $^{238}\text{PU}$ ,  $^{240}\text{PU}$ ,  $^{241}\text{PU}$ ,.... etc and by radionuclides formed by neutron reactions with fuel structural material, such as metal cladding.

The quantities of these actinides at the time of reactor shutdown can be calculated using the techniques described in ref. (2). Study on ET-RR-1 have been carried out to determine its decay heat after shutdown by using data Acquisition system.

### *References :*

- 1- John R-Lamarsh, "Introduction to Nuclear Reactor theory", Addison Weley publishing company, (1966).
- 2- Shure, K., "Decay heat and decay rate of actinides in highly neutron irradiated uranium initially of high  $^{238}\text{U}$  content. "Nucl. Sci. & Eng., 85(1), 1983.
- 3- A.A. ElKafas, "Analysis of Residual Heat Removal systems in NPPs", M.Sc., Alexandria University, Egypt, 1991.



**Approach to criticality and critical mass determination****E. A. Saad****Reactor Department , Nuclear Research Centre,  
Cairo, Egypt.****Introduction**

For applying the fission reaction to practical utilization of nuclear energy , the essential condition is that a self sustaining chain reaction could be obtained . Since at least two neutrons are released in each fission process which are capable of inducing the fission of other nuclei , and so on , so the requirement of self sustaining chain reaction can be met . However , account must be taken of the fact that the neutron produced in the fission process can take part in other non fission reactions . In addition , there can be a loss of neutrons from the system by leakage .

Therefore , if a chain reaction is to be maintained , the minimum condition is that for each neutron undergoing a fission to one nucleus there shall be produced on the average at least one neutron which causes fission to another nucleus. This condition can be expressed in terms of the multiplication factor defined as the ratio of the number of neutrons of any one generation to the number of corresponding neutrons of the immediately preceding generation . If this factor is equal to or slightly greater than unity , the chain reaction will be possible and the system is said to be critical . If it is less than unity , even by a very small amount , the chain reaction can not be maintained and the system is subcritical . If it is greater than unity , the system is supercritical and needs to be controlled. There fore .

Criticality is the situation in which self sustaining chain reaction can be maintained without external influence, and :

critical mass is the mass of fuel satisfying the critical condition that the effective multiplication factor  $K P = 1$  where  $K$  is the infinite multiplication factor , and  $P$  is the nonleakage probability.

The aim of this experiment is to approach criticality by introducing more and more fuel assemblies in the core and

getting the relation between the number of fuel assemblies in the core  $N$  ( fuel mass ) and the corresponding multiplication factor  $M$ . i.e  $M = f(N)$ .

A neutron source is introduced into the core , followed by introduction of few fuel assemblies and the neutron population is measured . This is followed by another addition until it is possible to make an extrapolation to predict the critical mass.

More fuel addition is made and after each addition it is possible to predict the critical mass with increased accuracy .

Equipment used :

neutron source -3 neutron detectors with associated counting systems .

Experimental procedure :-

1- Three detectors for measuring neutron population are placed at different places in the core and at different heights and are connected to the counting system .

The choice of the detector position is of great importance since it affects the shape of the criticality approach curve . They must be located in such a way to be sensitive to neutron multiplication .

Although the detectors will be put in different locations , three different curves will be obtained but they all extrapolate to the same value of critical mass.

2- A neutron source ( eg. Ra- Be ) is located at the bottom of the core in a position suitable for all detectors to be affected by any fuel added .

3- The corresponding number of counts is recorded. This number is considered as the source reading  $c_0$

4- Before fuel loading , control rods are withdrawn from reactor core

5- Fuel assemblies are added in steps , in each step the counting rate is recorded and the value  $M = c/c_0$  is obtained .

6- Manual control rods are inserted into the core up to the depth sufficient to compensate the increase in the multiplication factor obtained by loading the last fuel assemblies

7- New fuel is added , control rods are withdrawn , the counting rate is recorded and the new  $M$  is obtained

By adding more and more fuel, fission neutrons will increase and as  $N$  reaches the critical mass, the fission process continues spontaneously and  $C, M$  reach i. e.  $1/m$  reaches 0

8- A graph is plotted between  $N$  and  $1/M$ .

the curve is extrapolated to zero value of  $1/M$

to give a prediction of the critical mass.

9- These steps are repeated and in each new loading the extrapolation gives a new, more accurate value of the critical mass. When criticality is reached the  $1/M$  curve gives the exact critical mass.

The relation between  $c/c_0$  and  $1/M$  for ET-RR-1 reactor core is shown in Fig 1 where it gives a critical mass of 30 fuel assemblies.

This experiment can be done at the first start up of the reactor as well as at any time the fuel is taken out of the core for reasons of maintenance, inspection, refurbishment, ... etc).

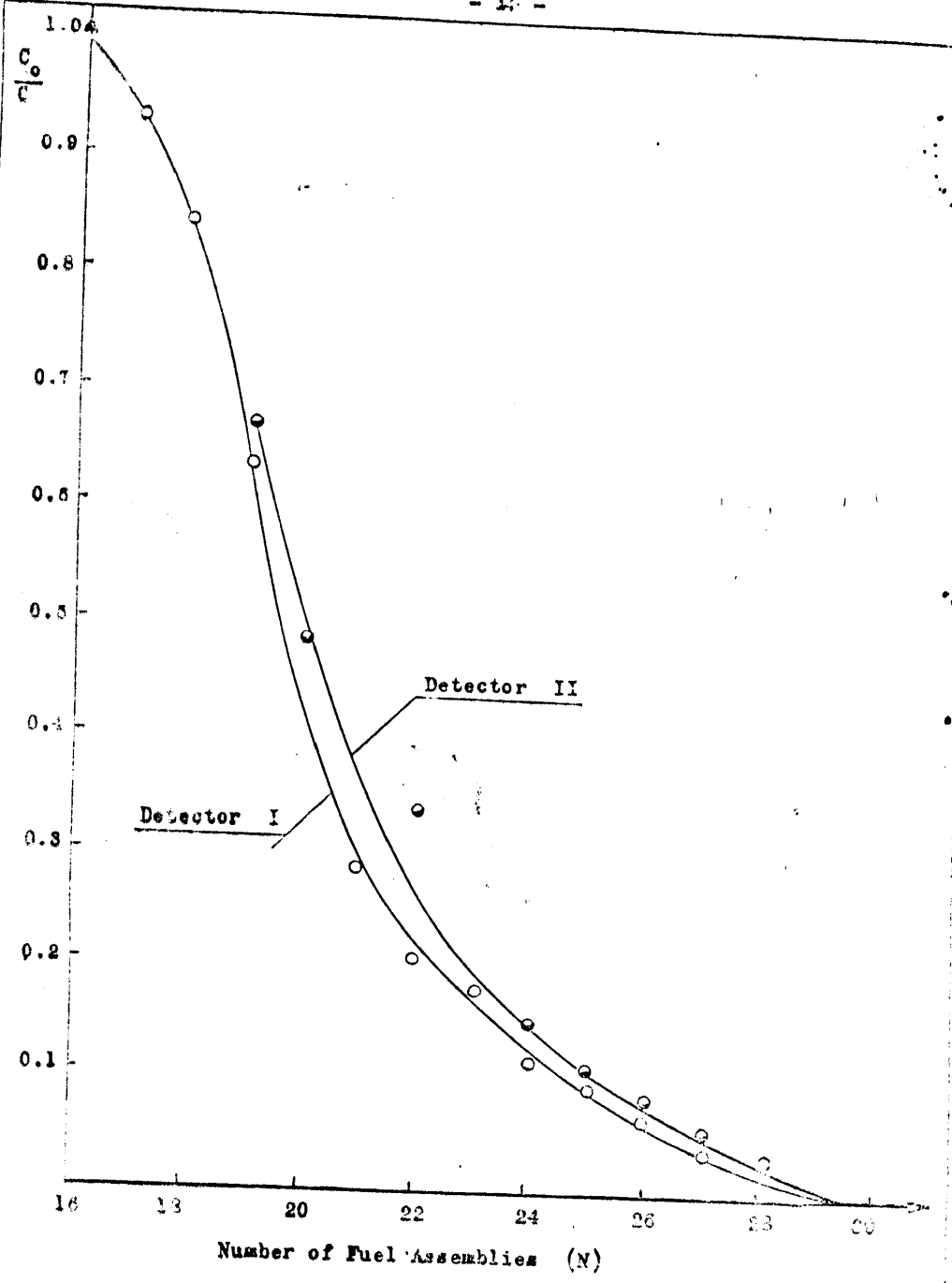


FIG. 1. Critical Approach Curves for Different Detectors.

M.A. GOMMA  
ATOMIC ENERGY AUTHORITY  
CAIRO - EGYPT

ON-SITE EMERGENCY

On-site response in the case of a radiological emergency may include a wide range of activities such as rescue operations, termination of accident propagation, mitigation of release of radioactivity to the environment, on-site sheltering and evacuation, preliminary hazards assessment, area and environmental monitoring, dosimetry and dose control, access control, and submittal of notifications and reports.

It would be impossible to efficiently handle a serious emergency situation where many of these activities have to be conducted under conditions of tension and pressure without the help of carefully laid plans for such situations.

In preparing plans for emergency situations the following points should be considered:

**Emergency Organization**

The roles of all employees should be preplanned and designated as far as possible. These roles should then be practised during exercises and drills, so that each person is well acquainted with his function. Alternates need to be designated for important roles. The emergency organization

should clearly show the lines of command and the authority of the key positions .

### **Emergency Activation**

In order to ensure prompt initiation of the emergency plan, it is important to have predetermined emergency classifications . Each class of emergency will have its own set of action levels and procedures . Action levels are reactor, or radiological parameters , which if exceeded , require that a particular class of emergency be declared .

### **Personnel Accounting**

A method of accounting for all personnel should be devised to ensure that no-one is inadvertently left inside an evacuated area .

### **Training and Drills**

All personnel should be trained in their emergency roles, and the plan should be exercised annually as part of the training . The objectives of these drills are to test the plan , and train the personnel .

### **Plans and Procedures**

An emergency plan which includes detailed procedures should be developed to cover all foreseeable aspects of research reactor emergencies . This plan and procedures should be reviewed annually and updated as necessary. Whenever possible, radiological emergency plans should be consistent with other emergency plans and require the same initial .

## Facilities and Equipment

### a) Control Centre

A control centre should be designated and equipped in preparation for the control and management of emergencies . In many instances this will be the reactor control room , but if so an alternate centre further away should also be prepared in case the control room is not tenable .

### (i) Communication Systems

It is necessary to ensure that sufficient local and offsite communications systems are available in an emergency . It is also important to write down and routinely exercise the activation and notification procedures to make certain that telephone numbers are still current .

### b) Alarm Systems

Distinctive, audible alarms are needed to indicate a reactor emergency . All personnel in the facility must be aware of the meaning of the alarms , and the actions required of them in the event of their . Ideally the alarms and the communications systems should be operable from the emergency control centre as well as the reactor control room .

## Emergency Procedures

### 1 - Chain of Commands Forms .

Post	Telephone	Address
Name :		
1) Chairman of the Research Insititute		
Deputy		
2) Chairman of the Reactor Division		
Vice-chairman		
3) Chairman of the Reactor Dept.		
Vice-chairman		
4) The Reactor Manger		
Deputy Reactor Manger		
5) Reactor Operator		
Deputy Reactor Operatar		
6) Head Reactor Phys. Dept.		
Deputy Head Reactor Phys. Dept.		
7) Head Rad. Prot. Dept .		
Deputy Head Rad. Prot. Dept		
8) Head Rad. Manitoring Grop.		
Deputy		



9) Head of Personnel Dosimetry Group  
Deputy

10) Head Reactor Safety Committee  
Deputy

11) Head Civil Defence Committee  
Deputy

12) Head of Isotope Production Dept.  
Deputy

## Emergency Procedures

### II - On Site Emergency Roam

#### 1) Personnel

Reactor

Physics

Rad. Protection

#### 2) Communication

#### 3) Equipment

## Emergency Procedures

### 1) Sheltering Procedures

#### • Sheltering Sites

#### 1) Shelter Site 1

Person

Communication

Equipment

#### 2) Shelter Site 2

Person

Communication

Equipment

#### 3) Shelter Site 3

## Emergency Procedures

### IV - Evacuation Procedures Forms

#### Responsible Person

Means of evacuation .

1- Bus No.

Direction

time

date

2 - Bus No.

Direction

time

date

## Emergency Procedures

### V - Radioprotective Procedures

Distribution of KI Tablets .

Responsible Person .

Name of Persons .

- 1.
- 2.
- 3.
- 4.
- 5.
- 6.
- 7.
- 8.
- 9.
- 10.
- 11.
- 12.
- 13.
- 14.

## Emergency Procedures

V2 - Control of access.

Position - I

1- Health Phys Group.

Chairman :

DEputy :

Name of Persons to leave	time	date
--------------------------	------	------

1.

2.

3.

4.

5.

Name of Persons to enter	time	date
--------------------------	------	------

1.

2.

3.

4.

5.

6.

## Emergency Procedures

### VII - Medical Monitoring

Responsible Person .

Name of Persons .

time

date

1.

2.

3.

4.

5.

6.

7.

8.

9.

10.

11.

## Emergency Procedures

### VIII - Dosimetric Monitoring Sheet

#### 1- External Monitoring .

##### Responsible Person

##### Persons .

Name

time

date

Dose.

1.

2.

3.

4.

5.

6.

7.

8.

#### 2- Internal Monitoring

##### Responsible Person

##### Persons

Name

time

date

Dose.

1.

2.

3.

4.

5.

6.

7.

8.



## **Emergency Procedures**

### **IX - Control of Food and Water Supply.**

**Responsible Person**

**Deputy**

**Actions**

## Emergency Procedures

### X- On Site Declaration of Emergency Situation .

- |                             |      |      |
|-----------------------------|------|------|
| 1. Reactor Operator         | time | date |
| approved by                 |      |      |
|                             |      |      |
| 2. Reactor Health Phys.     |      |      |
| approved by                 |      |      |
|                             |      |      |
| 3. Reactor Monger           |      |      |
| approved by                 |      |      |
|                             |      |      |
| 4. Reactor Safety Officer   |      |      |
| approved by                 |      |      |
|                             |      |      |
| 5. Reactor Dept.            |      |      |
| approved by                 |      |      |
|                             |      |      |
| 6. Reactor Division .       |      |      |
| approved by                 |      |      |
|                             |      |      |
| 7. Head Research Insititute |      |      |
| approved by                 |      |      |

## **Emergency Procedures**

### **XI - On Site off Site Emergency**

1. Head Research Institute
2. Head Nuclear Regulatory Centre
3. Head Atomic Energy Authority
4. Civil Defence Authority
5. Other Key Personnel
  - 1.
  - 2.
  - 3.

Lec. 14

## NUCLEAR FUEL MANAGEMENT

Prof Dr. M.L. Michael and R.A. Refaat,  
Reactors Department and Theoretical Physics Department  
Nuclear Research Centre - Atomic Energy Authority, Cairo,  
Egypt

### ABSTRACT

This lecture deals with the incore fuel management schemes beginning by batch loading, zone refuelling, scatter loading and ending by the checker board loading. The fuel grouping and region classification are discussed in detail. Also, a detail description of the shuffling algorithm is given.

## 1 Introduction

Nuclear fuel management has been defined as the management of nuclear fuel from the earliest stages of procurement through reprocessing and recycling in order to provide fuel for economical operation of the nuclear power plants. In general, nuclear fuel management is divided into two branches. The first is in-core nuclear fuel management and the second is out-of-core nuclear fuel management. Out of core fuel management involves uranium procurement, enrichment, fabrication, reprocessing, transportation, waste disposal and the scheduling of these activities. In-core fuel management involves parameters such as enrichment, loading pattern, lattice spacing, absorber management, mechanical integrity of fuel cladding and other aspects which directly affect the fuel while it is in the core. The incore fuel management is the objective of this lecture.

After the fuel assemblies are loaded into the reactor, it would normally take a long period (3 years in PWRs and 4-5 years in BWRs) before it is discharged. At each refueling only a fraction of the core is to be replaced. The fuel assemblies are shuffled to avoid power peak problems. Since the number of loading patterns that can be generated by a set of fuel assemblies varies in a factorial manner, it is very difficult, if not impossible, to search all the patterns and choose the best one. However, through proper planning and management, it is possible to achieve significant saving and notably reduce the energy cost.

The main problem is that for any given set of fuel assemblies it is required to optimize the reactor fuel loading for minimum

power peak ratio in case of PWR's at beginning of the core life. This optimization problem of fuel loading also takes into account that during the core cycle the power profile is ideal in the sense that the power peaking does not exceed certain limit.

**The following assumptions are considered:**

- (1) All fuel assemblies have fixed dimensions.
- (2) Optimization of radial power peaks based on twodimensional analysis results in optimization of total power peaks.
- (3) Total radial power peaking ratios are calculated from an assembly-averaged radial power multiplied by a local power peaking factor for each assembly.

For the complexities generated from the collective requirements of economics, neutronics, materials and plant availability, the complete optimization of a refueling scheme for the entire reactor life time is unlikely to take of simple formula or code. It takes the form of general method or technique which can be tailored to the performance criteria of the particular power plant under consideration.<sup>(2)</sup> Although the early fuel management programmes have the virtue of being relatively simple, they unfortunately do not yield the most efficient use of the fuel<sup>(3)</sup>. The earliest and most costly of this schemes is "batch loading", the reactor is often operated until the reactivity becomes low enough to warrant refueling, then the entire core is replaced by a fresh one. Because the shape of the flux is generally non-uniform, the fuel receives an unequal exposure which results in much of the discharged fuel being relatively fresh, and

therefore batch loading is expensive. With the "Zone Refueling" programmes, the core is divided into equivolume concentric zones of fuel elements. After the zone which contain the fuel of the highest burn-up is emptied, the other fuel elements are moved, inward, or outward, in a step-wise progression into adjacent zones. The fresh fuel is then introduced into the core. Unfortunately, with the zone refueling patterns, undesirable flux shapes arise in large power reactors because the higher average burn up cause large reactivity difference between new and old fuel in their respective zone. "Scatter loading" or "roundelay" schemes are similar to the zone refueling method in that a fixed fraction of the fuel is replaced at each refueling, but they are different because the "zones" are distributed throughout the core and are intimately mixed which allows increased burn-up without causing widespread undesirable power shapes.<sup>(4)</sup>

It is desirable to employ a cost functional as the objective in order to predict fuel management decisions. In many previous studies, a non cost type of the objective function is employed. Some commonly used non cost functions for in-core fuel management are maximization of burn-up, minimization of fresh reload fuel and maximization of cycle length for a given amount of new fuel.

Wall and Benceh<sup>(4)</sup> demonstrated how the dynamic programming could be used to solve this problem. This method minimize the unit power cost over the life of a single enrichment (three zone, 1000 MWe, PWR) by determining at each refueling stage the optimum combination of 28 possible combinations of replacing and shuffling of the three fuel zones. It was assumed

that the fuel composition at any time can be determined by the burn-up parameter alone. Predictions of the end fuel composition and distribution, the core lifetime, and power peak were made from least-squares polynomial functions of burn-up fitted to previous calculations performed by multi-dimensional codes. In this scheme, the method of placing the fresh and partially burnt fuels in relatively separated regions cause an undesirable power distribution, and that scatter loadings are better. Also the approach was time consuming and limited to solve only few region problems, consequently, it does not match with the task of creating large power reactors. Stover and Sesonske<sup>(5)</sup> attempted to maximize the discharge burnup as the objective function. The method was applied to optimize the scatterloading of a three-zone BWR with constraints on maximum power peaking, burnup and plant life. The volume fractions of each core zone to be replaced by fresh fuel at each refueling are the decisions determined from the optimization. Fuel shuffling operations are neglected and the method suffers from dimensionality limitations. Fagan and Sesonske<sup>(6)</sup> assumed that the operating parameters and constraints for individual fuel assemblies could be expressed by the burn up of the fuel assemblies. A constant fraction of the core must be replaced each cycle with fuel of constant enrichment and reactor operating characteristics were all fixed. The approach maximizes the core life at each reload point, thus obtaining a minimum fuel cycle coast. The nuclear model is still one dimensional and is unable to describe the azimuthal power distribution within the radial zones and is also time consuming. Naft and Sesonske<sup>(7)</sup> attempted to improve the previous technique by developing an accelerated direct search<sup>(8)</sup> which minimize the radial peaking power and reduces the



number of feasible shuffling patterns through the use of a set of logical shuffling rules. A simplified semianalytical function was formulated to calculate X-Y power distributions. The algorithm was successfully applied to a medium-sized PWR. The method depends on the degree of the complexities of the power distribution calculations which tend to increase the problem to the point of almost being impossible to be handled effectively. Stout and Robinson<sup>(15)</sup> developed a direct search method which employed a practical shuffling logic to optimize the power peaking ratio for a given set of fuel assemblies.

Independent logic was employed for each of the four zones within the core. Also independent logic was used to shuffle the highly reactive fuel. A two-dimensional simulated two-group coarse mesh diffusion theory model was used to calculate the power distribution after each shuffle. Although the effectiveness of the algorithm is dependent upon the initial guess of the loading pattern and more computing times were still required, the shuffling logic achieved a significant reduction on the number of patterns that need to be searched. This study is modified by developing an algorithm<sup>(9)</sup> with significant reduction of computing time and improved power profile at begin of life and throughout the cycle. P. Chan, Dastur<sup>(10)</sup>, attempted to develop the checker board fueling scheme to make possible a significant increase in the initial enrichment and hence burnup of the fuel that can be used in existing Candu reactors.

No hardware changes to the reactor are required. Mixed oxide fuel with a fissile content are used. Sufficient flux and power

shaping, especially along the fuel channel, can be achieved with the scheme to improve the worth of the reactivity devices in the presence of enriched fuel. J.S. Suh<sup>(11)</sup>, optimize of the reload core design to achieve the maximum cycle length with the given fuel quantities while satisfying the safety constraints.

## 2 Fuel Loading Scheme:

### 2.1. Loading patterns of flat power distribution and ideal fuel distribution:

It is highly desirable to have a flat power distribution across the core for the economic penalties, the coolant temperature, the material problems and fuel failure. The relative power distribution of the reactor is very sensitive to the fuel distribution. Varying enrichment radially across the core is the most convenient to achieve a near uniform power density distribution. Theoretically in a reflected reactor, it is possible to develop an arrangement of fissile material that will yield spatially uniform power density,  $P(r)$ . it is assumed that:

- (a) All reactor properties are uniform except fissile materials content (12, 13, 14)
- (b) The size of the reactor is assumed of order of 3 to 6 m in diameter or larger.

Figure (1) shows such an idealized fissile material,  $N(r)$ , and neutron flux distribution,  $\phi(r)$  based on a one-group, one

dimensional analysis. The shape indicates that more fissionable material is needed in the peripheral region to counter balance the leakage of thermal neutrons.

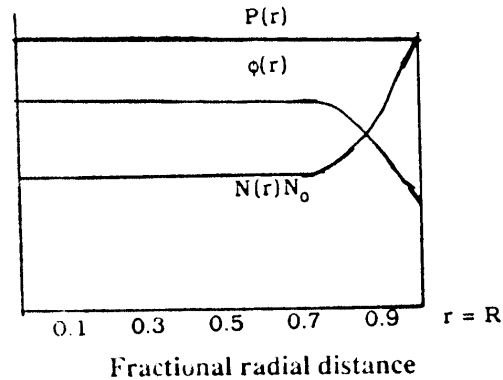


Figure (1) Flux and fissile material distribution for uniform power generation.<sup>(12)</sup>

The infinite multiplication factor,  $K_{\infty}(r)$ , represent the capability of the fuel assembly at location (r) as far as power peaking is concern. In the central region of the reactor, the fissile density correspond to  $K_{\infty} = 1.0$ . Near the periphery the fissile density increase by over a factor of two to maintain constant power. Most of this increase occur over a distance less than the thickness of a light water reactor fuel assembly (about 10% of the reactor core radius R).

\* A fissile material with distribution such as shown in figure (1) would be impractical to be designed and fabricated. Even if it were assembled, the reactor would not retain the proper fuel distribution with depletion. It does illustrate, however, that the reactor in which the weighted average infinite multiplication factor in the central region is unity (from  $r \approx 0$  to  $0.9 R$ ), surrounded by a relatively thin region of higher reactivity, will approach the ideal uniform power distribution. This is the general principle of the "out-in scatter loading" scheme used in many reactors nowadays. In the out-in scatter loading technique, fresh assemblies which have the highest fuel quality (highest infinite multiplication factor,  $K_{\infty}$ ) are loaded on the core periphery. The remaining assemblies are arranged in a central zone of very low buckling ( $K_{\infty} \approx 1$ ) in such a manner as to minimize local power peaking,  $P_L$ , effects.

### 3 Fuel Grouping and Region Classification:

To approach this ideal fuel distribution, the assemblies are arranged as fresh fuel (highest  $K_{\infty}$ ) on the core periphery and burnt fuel assemblies on the central region of the core which consist of once and twice burnt fuel assemblies. A reasonable arrangement of the two groups would be a checkboard pattern (figure 2). Actually, for large PWRs (600 to 1100 MWe), it is not possible to place all the new fuel assemblies on the core peripheral region of the reactor for a one third reload cycle. These excess fresh fuel assemblies are required to be placed in the interior core position to allow enough core excess reactivity to reach the end of subsequent cycle. This fresh fuel assemblies in the interior positions of the core cause large perturbations on

P (1.8)	P (2.8)	P (3.8)						
E (1.7)	O (2.7)	E (3.7)	P (4.7)	P (5.7)				
O (1.6)	E (2.6)	O (3.6)	E (4.6)	O (5.6)	P (6.6)			
E (1.5)	O (2.5)	E (3.5)	O (4.5)	E (5.5)	O (6.5)	P (7.5)		
O (1.4)	E (2.4)	O (3.4)	E (4.4)	O (5.4)	E (6.4)	P (7.4)		
E (1.3)	O (2.3)	E (3.3)	O (4.3)	E (5.3)	O (6.3)	E (7.3)	P (8.3)	
O (1.2)	E (2.2)	O (3.2)	E (4.2)	O (5.2)	E (6.2)	O (7.2)	P (8.2)	
E (1.1)	O (2.1)	E (3.1)	O (4.1)	E (5.1)	O (6.1)	E (7.1)	P (8.1)	

- X  
(I,J)
- X region identification
  - P periphery region "group one fuel assemblies"
  - O odd-parity interior region group two fuel assemblies"
  - E even-parity interior region "group three fuel assemblies".
- (I,J) Position identification.

Figure (2) Fuel arrangement for a typical one-quarter

local radial power peaking. The power peaks will almost always occur in these assemblies.

The method of grouping fuel assemblies is developed as follows:

- 1) Calculate the infinite multiplication factor  $K_{\infty}$  of each assembly.
- 2) Arrange all the assemblies with their  $K_{\infty}$  values in descending order.
- 3) The first (highest  $K_{\infty}$ ) assemblies are chosen as group one assemblies. They are usually fresh fuel assemblies which will be allowed to go into the zone "P" position (peripheral region). These assemblies are not permitted to be shuffled throughout shuffling iterations.
- 4) The following assemblies are chosen as group two assemblies. They will be allowed to be inserted into the zone "P" positions, odd parity interior region and will be allowed only to be shuffled with each other throughout the shuffling iterations.
- 5) The following assemblies is group three assemblies., they will be put in zone "E" position even parity. They will be shuffled with each other.
- 6) The remaining assemblies are the three-cycle burnt fuel assemblies, which have the lowest infinite multiplication factor. These assemblies are discharged.

#### 4. Shuffling Algorithm:

The shuffling rules allow for assemblies of the odd-parity interior region and even parity interior region to be shuffled. Stout and Robinson<sup>(15)</sup> had made studies to determine which fuel elements have to be exchanged for a loading with the minimum radial power peaking factor. From this studies certain trends were noticed from which two general rules were derived :

- (1) New fuel assemblies placed in the reactor interior cause large perturbation on the local radial power peaking. It is found that better results are obtained in shuffling iterations scheme if these elements are moved only one position at a time. Then new power calculations is made to determine the next movement rather than moving them directly from higher power area to a low power area.
- (2) The movement of any burnt fuel does not represent a large perturbation on the radial power distribution. Burnt fuel elements can be moved considerable distance from their position in one shuffle iteration to the next. Replacing a burnt fuel element in the vicinity of a radial power peak with one of less reactivity will always lower the power peak in this area and increase the relative power in the area where the more reactive fuel element is placed.

#### 4. The shuffling procedure is divided into two parts:

##### Part One:

Concerns the rearrangement of the high reactivity fuel elements inside group two.

**part Two:**

Deals with the rearrangement of the exposed fuel (of group two and group three) around the assembly which has the radial power peak.

These parts shuffle the fuel to a minimum power peak possible using the rules described in previous paragraph.

**4.1 Part One: Shuffling of High Reactivity Fuel Elements:**

This part of shuffling procedure arranges high reactivity fuel which may be placed in the interior of the core. As first step, it is necessary to check if the programme has exhausted all its shuffling possibilities by previous iterations or not. If it has, part two is called. If not radial power distribution is calculated and the maximum radial power element is determined and compared to the lowest radial power peak from previously shuffled loading patterns. If radial power peak is less than the previous one, this loading is recorded as the best for the programme. Then, all the iteration parameters are reinitialized because a new best loading has been found and the research begins for a new shuffling. The maximum power element which is not the central or the periphery is found.

The search is now made for a fuel element to be exchanged with the maximum power element if it occurs that the maximum radial power element is the central one or is located on the periphery, the highest power non-periphery assembly which is located adjacent to it will be moved. The search for the fuel element to be exchanged with maximum power element begins by finding the fuel element which has lowest power in the



vicinity of the non-periphery maximum power element. This element is called local minimum. If the position of the fuel element with maximum radial power is  $(I_{\max}, J_{\max})$  it was found that an area of  $(I_{\max} \pm 2, J_{\max} \pm 2)$  would be sufficient to determine the direction in which the element of maximum radial power would be moved. Figure (3) illustrates an example, in which the maximum power of 1.444 is position (4,4). Inside the search area of a local minimum (From  $I = 2$  to 6 and  $J = 2$  to 6) the lowest radial power is 0.758 at position (6,5) or (5,6). The program proceeds to determine, first, the parity of the maximum radial power fuel element, then, second, this fuel assembly is moved to a position of the same parity one position closer to the local minimum. If through this route one of the fuel elements to be shuffled was an element on the periphery, another assembly which is adjacent to the local minimum and closer to maximum element would be shuffled instead.

In this case, it can be allowed for the maximum element to be moved two positions closer to the local minimum, figure (4). Once the two elements to be exchanged in the shuffle have been determined, there will be two requirements:

(1) Insertion of an assembly with equal or higher reactivity in the position of the peak radial power than the one presently occupying the position will not improve the radial power peaking. Hence the program checks if the reactivity of the assembly which will be exchanged with radial power peak is less than that of the radial power peak or not. If not, this element is the logical choice to be moved. This element assigns temporarily the status of maximum power as indicated, figure (5), and return to search of a position to move this element. The procedure will

1.243	1.154	0.964						
1.034	.95	.93	1.065	.805				
1.021	1.39	.984	.943	.758 Loc. min.	.773			
1.052	1.06	1.439	.99	.864	.758 Loc. min.	.805		
.857	.98	1.069	1.444 Max.	.99	.943	1.065		
.844	.783	.957	1.069	1.439	.984	.93	.964	
.688	.769	.783	.98	1.06	1.39	.95	1.154	
.709	.688	.844	.857	1.052	1.021	1.034	1.243	

X radial power

Figure (3) Illustration example of the local minimum and shuffling of assemblies

1.25	1.21	1.05							
.99	1.06	1.09	1.14	.87					
1.26	1.01	1.36	.92	.86	.86				
.92	.95	.92	.97	.9	.85	.79 Loc. min.			
1.2	.84	.91	.94	.95	.91	1.05			
.89	.89	.89	.92	.91	1.38 Max	.92	.95		
1.36	.97	.88	.88	.97	1.01	1.02	1.14		
1.12	1.36	.9	1.25	.95	1.36	.96	1.2		

X radial power

Figure (4) Example for shuffling when the element to be exchanged with power peak is peripheral.



move this high reactivity assembly away from the actual maximum power assembly and reduce the radial power peaking factor in that area. An example of this situation is illustrated in Figure (5). Where the maximum radial power is 1.402 occurs at position (6,2) and local minimum of this position is 0.783 in position (8, 3), they hasn't the same parity. Then, the procedure designates an exchange of (6,2) and (7,3), but these element have same fuel type with zero exposure and no gain achieved with shuffling these two assemblies. Then the procedure will move the assembly in position (7,3) away from actual maximum power assembly. The procedure temporarily assigns the status of maximum power to 1.305 and searches for a move of this element. Its local minimum 0.724 in position (7,5) which hasn't the same parity. Then the procedure attempts to exchange (7,3) and (6, 4) and in this case, this particular shuffle lowered the radial power peak to 1.371 which occurred at position (2,4) so the shuffle was quite successful.

(2) There will be a requirement for the local reactivity, of those four assemblies immediately adjacent to the position of the assembly which will be exchanged with the maximum power assembly, that is to be sure that their reactivity summation will not be greater than those around the maximum power. This requirement can be expressed as:

$$G_{MIV} < H_{MIX}$$

where

$G_{MIV}$  = Summation of reactivities of four assemblies adjacent to the position of the assembly which will be exchanged with maximum power assembly, and

HMX = Summation of reactivities of the four assemblies adjacent to the position of maximum power assembly.

The most PWR's have the quarter centerlines symmetry bisecting fuel assemblies, then corresponding symmetrical positions on the axis share the same fuel assembly. Then if one of the two elements to be exchanged in a shuffle has  $I=1$  or  $J=1$ , the fuel in positions (I, J) and (J, I) can be exchanged with the other fuel element.

The previous procedure is the shuffle logic for "Part 1" used if the new radial power peak is lower than any previous loading pattern. If it is not, this will result in a rejection of the previous shuffle. But if the case that the new radial power peak appears in the reciprocal position of the power peak of the best loading, the procedure will shuffle this reciprocal position element in an

radial power peak of any shuffle iteration is greater than the radial power peak of the best loading and it is not in the reciprocal position, the shuffle is rejected and the best loading has been found. If it is the third or higher iteration, it will be attempt to shuffle the maximum power element.

This procedure continues until all possible moves of the maximum power element in the area  $I_{max} \pm 2$   $J_{max} \pm 2$  have been tried. This part 2 is called, to be used as a new set of logic in an attempt to lower, further, the radial power peak.

#### 4.2 Part 2: Shuffling of the Exposed Lower Reactivity Fuel

##### Elements:

To further reduce the radial power peak it will be necessary to rearrange the exposed lower reactivity fuel around the assembly of radial power peak. This doesn't mean that part 2 of the shuffling procedure is concerned only with the bounded area of the radial power peak but it moves less reactive fuel into the area which has the maximum radial power. It also moves more reactive fuel into the area which has low radial power factors.

## REFERENCES

1. S.H. Levine, "In-core Fuel Management, "IAEA, course on operational physics of power reactors, 3-28 March (1980).
2. Fuel Management Conference, "In-core fuel management: who should call the tune on fuel in reactor-utility or supplier" Nuclear Industry, 18,2, Feb., 1971, 10-17.
3. Samuel Glasstone and Alexander Sesonske, Nuclear reactor engineering, Van Nostrand Reinhold company, 1967.
4. I. Wall & H. Fenech, "the application of dynamic programming to fuel management optimization", Nuclear science and engineering, 22, 1965.
5. R. L. Stover and A. Sesonske, "Optimization of BWR fuel Management Using an Accelerated Exhaustive Search Algorithm", Journal of Nuclear Energy, 23, 1969.
6. J.R. Fagan & A. Sesonske, "Optimal Fuel Replacement in Reactivity Limited Systems," Journal of Nuclear Energy, 23, 1969.
7. B.N. Naft and A. Sesonske "PWR Optimal Fuel Management", Nuclear Technology, 14, 2, May 1972.
8. P.J. Fulford & A. Sesonske, "In-Core Fuel Management Optimization", Nuclear News, 13, 7, July 1970.
9. M.A. Elsherbiny "In-Core Nuclear Fuel Management in Pressurized Water Reactors", Ph.D. Thesis, 1983.
10. P.S.W. Chan and A.R. Dastur, "Checkerboard Fuelling. The key to advanced fuel cycles in existing CANDU reactors", Canadian Nuclear Society G. Annual Conference. Ottawa, on (Canada), 3-4 June, 1985.



11. J.S. Suh "Optimized automatic reload programs for PWR's using the haling power distribution". Thesis (Ph.D.), University Microfilms, P.O. Box 1764, Ann Arbor, MI48106, Pennsylvania State University, PA (USA).
12. Y.F. Chen, J.O. Mingle and N.D. Echhoff, "Optimal power profile fuel management," Ann. Nuc. Energy, 4, 1977, 407-415.
13. H.W. Graves, "Nuclear Fuel Management," John Wiley and sons Pub., 1979.
14. F. Winterberg", Special Nonuniform Fuel Distributions and Cooling Problems in Reactors, "Nuclear Data and Reactor Theory, Second, United Nations International Conference on The Peaceful Uses of Atomic Energy, Geneva, 16, 1958, 675-686.
15. R.B. Stout and A.H. Robinson, "Determination of Optimal Loading in PWR Using Dynamic Programming", Nuclear Technology, 20, November 1973, 86-102.